Author:
Crawley, Phoebe E

Title:
Investigating the role of EZH2 and PRC2 in WT1/BASP1-mediated gene regulation

Investigating the role of EZH2 and PRC2 in WT1/BASP1-mediated gene regulation

Phoebe Crawley

A dissertation submitted to the University of Bristol in accordance with the requirements for award of the degree of MSc by Research in the Faculty of Biomedical Sciences, School of Cellular & Molecular Medicine.

August 2021

Word count – 17,343

Table of Contents

I. ABSTRACT **3**

II. ACKNOWLEDGEMENTS **4**

III. AUTHOR'S DECLARATION **4**

IV. LIST OF FIGURES **5**

V. ABBREVIATIONS **6**

1. INTRODUCTION **8**

1.1 EPIGENETICS AND GENE REGULATION 8
1.2 WT1 8
1.2.1 WT1 gene and protein *9*
1.2.2 WT1 isoforms *10*
1.2.3 WT1 and cancer *10*
1.2.4 WT1 as an activator and a repressor *11*
1.3 BASP1 11
1.3.1 BASP1 gene and protein *12*
1.3.2 BASP1's co-suppressive properties *13*
1.3.3 BASP1 and cancer *13*
1.4 WT1/BASP1 COMPLEX 14
1.4.1 WT1/BASP1 recruitment of histone-modifying enzymes *15*
1.4.2 Other interactions of WT1 ..... *18*
1.5 EZH2 AND PRC2 18
1.5.1 PRC2 structure *19*
1.5.2 PRC2 and cancer *20*
1.6 THE PRC2 AND WT1/BASP1 COMPLEXES 21
1.7 AIMS AND HYPOTHESIS 22

2. MATERIALS AND METHODOLOGIES **23**

2.1 MATERIALS 23
2.1.1 General reagents *23*
2.1.2 Buffers and solutions *23*
2.1.3 Primers *24*
2.1.4 Antibodies *25*
2.1.5 siRNAs *26*
2.2 METHODOLOGIES 26
2.2.1 Cell culture *26*
2.2.2 Whole cell extract (WCE) preparation *26*
2.2.3 Immunoprecipitation *26*
2.2.4 Immunoblot *27*
2.2.5 Chromatin immunoprecipitation (ChIP) *27*
2.2.6 RNA interference *28*
2.2.7 Data analysis and statistical tests *29*

3. RESULTS **30**

3.1 ANALYSIS OF BASP1 AND PRC2 EXPRESSION IN K562 CELLS 30
3.2 OPTIMISATION OF THE CHIP PROTOCOL IN K562 CELLS 31
3.3 TRIMETHYLATION OF H3K27 IS ENRICHED DURING BASP1 EXPRESSION 32
3.4 PRC2 RECRUITMENT TO WT1-TARGET GENES IS BASP1-DEPENDENT 33
3.4.1 EZH2 is recruited to WT1-target gene promoters during BASP1 expression *33*
3.4.2 SUZ12 is recruited to WT1-target gene promoters during BASP1 expression *34*
3.5 PRC2 RECRUITMENT TO WT1-TARGET GENES IS LIPID-INDEPENDENT 36
3.5.1 EZH2 recruitment is independent of BASP1 lipidation *36*
3.5.2 SUZ12 recruitment is independent of BASP1 lipidation *38*
3.6 MCF7 CELLS ENDOGENOUSLY EXPRESS BASP1 AND EZH2 39

3.7 EZH2 MEDIATES BASP1-DEPENDENT TRANSCRIPTIONAL REPRESSION OF WT1 TARGET GENES 40
3.7.1 EZH2 siRNA 1 demonstrates a physiological role for EZH2 at WT1-target gene promoters 40
3.7.2 EZH2 siRNA 2 produced comparable results for EZH2 at WT1-target gene promoters 41
3.8 EZH2 MEDIATES H3K27ME3 DEPOSITION AT WT1-TARGET GENES 43
3.9 ANALYSIS OF POTENTIAL INTERACTION BETWEEN PRC2 COMPONENTS AND BASP1 45

4. DISCUSSION 47

4.1 CHARACTERISATION OF STABLE CELL LINES 47
4.2 BASP1 MEDIATES PRC2 RECRUITMENT TO WT1-TARGET GENE PROMOTERS. 47
4.3 BASP1-MEDIATED RECRUITMENT OF PRC2 IS INDEPENDENT OF BASP1-MYRISTOYLATION 48
4.3.1 Potential bivalency at WT1-target gene promoters 49
4.4 THE WT1/BASP1 COMPLEX AND PRC2 WORK SYNERGISTICALLY TO TRIMETHYLATE H3K27 50
4.4.1 Potential for a direct binding mechanism 51
4.4.2 Proposed alternative mechanisms of PRC2 recruitment 53
4.4.3 A possible mechanism for WT1/BASP1 complex coalescence with PRC2 at WT1-target genes 54
4.6 SIGNIFICANCE OF THIS STUDY AND ITS WIDER IMPACT 55
4.7 FUTURE DIRECTIONS 56
4.8 CONCLUSION 57

VI. REFERENCES 58

I. Abstract

The transcription factor WT1 is important in regulating physiological and pathological processes, including apoptosis, cell growth and cancer. BASP1 is a transcriptional co-suppressor of WT1; and together, these proteins constitute the WT1/BASP1 repressor complex. The WT1/BASP1 complex represses transcription by remodelling chromatin at the promoter region of WT1-target genes. Transcriptional repression by BASP1 requires its N-terminal myristoylation and a central role for lipids. Amongst other epigenetic modifications, the WT1/BASP1 complex deposits the repressive mark H3K27me3 on histone tails in the promoter region of WT1-target gene, yet the mechanism by which this occurs is undetermined. Previous experiments in the laboratory have indicated that EZH2 may play a role here. EZH2 is a core component of the polycomb repressor complex 2 (PRC2), alongside SUZ12 and EED. The PRC2 has been extensively linked to the deposition of H3K27me3 marks and inducing a transcriptionally repressive state at many target genes.

The current study used chromatin immunoprecipitation experiments to show a BASP1-dependent significant elevation in enrichment of EZH2 and SUZ12 at WT1-target gene promoters. Thus, this confirms that the intact PRC2 is recruited by WT1/BASP1 to WT1-target gene promoters. The recruitment of these two core PRC2 components was shown to be mediated independently of BASP1 myristoylation, suggesting that BASP1 directs transcriptional repression through both lipid-dependent and lipid-independent mechanisms.

Further experiments using RNA interference demonstrated a functionally relevant role for EZH2 in WT1-target gene repression. EZH2-targeted knockdown triggered an increase in *AREG* expression compared to the baseline level. The same dataset also suggested that both BASP1 and EZH2 work synergistically to invoke transcriptional repression, where no significant difference in *AREG* expression was observed during EZH2 knockdown compared to the combined knockdown of BASP1 and EZH2. Extended research integrating both RNA interference and ChIP techniques confirmed that trimethylation of H3K27 at WT1-target genes is EZH2-dependent, where knockdown of EZH2 led to a reduction in H3K27me3 enrichment at the *AREG* promoter.

Co-immunoprecipitation experiments failed to detect an interaction between BASP1 and the PRC2, and therefore it is proposed that the PRC2 is recruited to WT1-target genes following a BASP1-mediated alteration in the epigenetic landscape. Taken together, this study establishes a role for EZH2 and the intact PRC2 in BASP1-mediated deposition of H3K27me3 marks and BASP1-dependent transcriptional repression of WT1-target genes.

II. Acknowledgements

I would firstly like to thank my supervisor, Professor Stefan Roberts, for his constant support and guidance throughout the year. Stefan's help, feedback and mentoring has been incredibly invaluable, and he has helped build my scientific and experimental knowledge, which will be critical when moving onto my PhD and research-based career.

Additionally, I would like to thank Professor Anne Ridley, my academic mentor, for all her help and suggestions during our academic progress monitoring meetings. I found the meetings very useful, and Anne really helped with improving my scientific writing style.

Finally, I would like to thank Georgia Kingsley, my fellow Master's student, for all the help, support and entertainment over the course of the year. It has been a great environment to work in, despite the challenging year of COVID restrictions!

III. Author's Declaration

I declare that the work in this dissertation was carried out in accordance with the requirements of the University's *Regulations and Code of Practice for Research Degree Programmes* and that it has not been submitted for any other academic award. Except where indicated by specific reference in the text, the work is the candidate's own work. Work done in collaboration with, or with the assistance of others, is indicated as such. Any views expressed in the dissertations are those of the author.

Signed : Date :

IV. List of Figures

Figure 1. *Schematic structure of the WT1 protein*

Figure 2: *Schematic structure of the BASP1 protein.*

Figure 3. *Deposition and removal of the H3K9ac mark.*

Figure 4. *Chromatin remodelling by the WT1/BASP1 complex.*

Figure 5. *H3K27me3 recruitment at WT1-target gene promoters.*

Figure 6. *The structure of and interactions between the PRC2 factors.*

Figure 7. *EZH2 recruitment at WT1-target gene promoters.*

Figure 8. *Immunoblot analyses of whole cell extract with different antibodies.*

Figure 9. *BASP1 expression in K562 cells induces the removal of H3K9ac at the promoter of the WT1-target gene AREG.*

Figure 10. *BASP1 expression in K562 cells induces the recruitment of EZH2 at the promoter of the WT1-target genes AREG, ETS-1 and VDR*.

Figure 11. *BASP1 expression in K562 cells induces the recruitment of EZH2 at the promoter of the WT1-target genes AREG, ETS-1 and VDR*.

Figure 12. *ChIP analysis of SUZ12 enrichment at WT1-target gene promoters in K562 cells.*

Figure 13. *ChIP analysis of EZH2 enrichment at WT1-target gene promoters in mutant K562 cells.*

Figure 14. *ChIP analysis of SUZ12 enrichment at WT1-target gene promoters in mutant K562 cells.*

Figure 15. *Immunoblot analyses of whole cell extract in MCF7 cells.*

Figure 16. *Relative expression of WT1-target genes following RNA interference in MCF7 cells, with EZH2 siRNA 1.*

Figure 17. *Relative expression of WT1-target genes following RNA interference in MCF7 cells, with EZH2 siRNA 2.*

Figure 18. *Fold enrichment of H3K27me3 marks at WT1-target gene promoters during knockdown of BASP1/EZH2 in MCF7 cells.*

Figure 19. *Immunoblot analyses of SUZ12/EZH2 IP with BASP1/HA-tag probe in BASP1-K562 cells.*

Figure 20. *Two proposed mechanisms of PRC2 recruitment to the WT1/BASP1 complex.*

V. Abbreviations

AML	Acute myeloid leukaemia
APS	Ammonium persulfate
BASP1	Brain acid soluble protein 1
BRG1	Brahma related gene 1
CBP	CREB-binding protein
CBX	Chromobox family proteins
cDNA	Complementary deoxynucleic acid
ChIP	Chromatin immunoprecipitation
CRAC	Cholesterol recognition amino acid consensus
DMEM	Dulbecco's modified eagle medium
DMSO	Dimethyl sulfoxide
DTT	Dithiothreitol
ECACC	European Collection of Authenticated Cell Cultures
ECL	Enhanced chemiluminescence
EDTA	Ethylene diamine tetraacetic acid
EED	Embryonic ectoderm development
EGF-1	Epidermal growth factor
EMT	Epithelial mesenchymal transition
ERα	Oestrogen receptor alpha
EZH2	Enhancer of zeste homolog 2
FBS	Foetal bovine serum
HA-tag	Human influenza hemagglutinin tag
HDAC1	Histone deacetylase 1
Hepes	4-(2-hydroxyethyl)-1-piperazineethanesulfonic acid
IgG	Immunoglobulin
INM	Inner nuclear membrane
iPSCs	Induced pluripotent stem cells
JARID2	Jumonji and AT-Rich Interaction Domain Containing 2
kDa	Kilo Daltons
LLPS	Liquid-liquid phase separation
NLS	Nuclear localisation sequence
NMR	Nuclear magnetic resonance
NP-40	Nonident P40
mRNA	Messenger RNA
PBS	Phosphate-buffered saline
PcG	Polycomb group
PEST	Proline, Glutamic acid, Serine, Threonine

PIP2	Phosphatidylinositol 4,5-biphosphate
PK	Proteinase K
PKA	Protein kinase A
PKC	Protein kinase C
PMA	Phorbol 12-myristate 13-acetate
PML bodies	Promyelocytic Leukaemia Bodies
PRC1/2	Polycomb repressor complex 1/2
P/S	Penicillin streptomycin
qPCR	Quantitative polymerase chain reaction
RNA	Ribonucleic acid
RPMI	Rosewell Park Memorial Institute 1640
RTP	Room temperature and pressure
SDS	Sodium dodecyl sulfate
siRNA	Short-interfering RNA
SRPK1	Serine–arginine protein kinase 1
SRSF1	Serine–arginine splice factor 1
SUMO	Small ubiquitin-like modifier
SUZ12	Suppressor of zeste 12
TEMED	Tetramethylethylenediamine
Tris	Tris(hydroxymethyl)aminomethane
VEGF	Vascular epidermal growth factor
WCE	Whole cell extract
WT1	Wilms' tumour 1
YY1	Yin yang 1
± 17AA	Isoforms of WT1 Including or Excluding 17 Amino Acids
+/-KTS	Isoforms of WT1 Including or Excluding Lysine, Threonine and Serine 17 amino acid insert

1. Introduction

1.1 Epigenetics and gene regulation

Multiple mechanisms influence transcriptional control, with mounting evidence proving that gene expression is directly correlated to the accessibility of the DNA sequence to RNA polymerase enzymes and transcription factors (Almassalha et al., 2017). This is primarily regulated by the highly complex and inter-connected genomic organisation within the nucleus, which is influenced by mechanisms which extensively remodel chromatin, including DNA methylation, post-translational modifications of histone tails and nucleosome aggregation (Almassalha et al., 2017). These different processes fall under the umbrella-term 'epigenetic modifications' and are critical in directing correct cellular differentiation (Stypula-Cyrus et al., 2013; Wali et al., 2016).

Chromatin topology is either compact or accessible, and these are referred to as heterochromatin and euchromatin, respectively. In heterochromatin, DNA is tightly wound around histones making the gene inaccessible for transcription. The opposite is true of euchromatin; hence the gene is accessible for transcriptional processes and activation.

Histone-tail modifications include phosphorylation, methylation, acetylation, ubiquitination and SUMOylation; and which chromatin sites these occur at will influence whether they are archetypal of heterochromatin or euchromatin (Rechtsteiner et al., 2019). Chromatin remodelling is typically brought about via histone modifying enzymes at the protruding N-terminal tails of histones or by ATP-dependent chromatin remodelling complexes (Clapier et al., 2017). The resulting modifications can alter nucleosome density and chromatin compaction via conformational changes, which in turn may recruit downstream proteins and regulatory elements that control gene transcription (Liu et al., 2015).

1.2 WT1

The Wilms' Tumour 1 (WT1) gene encodes the WT1 transcription factor, which plays a major role in a wide range of cellular processes and has also been linked to cancer initiation and progression. It was first discovered as being involved in the paediatric renal cancer – Wilms' Tumour, due to its role in regulating kidney development during embryogenesis (Little and Wells, 1997). Since its discovery, scientific interest in the WT1 protein has grown as its function in physiological and pathological cellular processes has been established. Such processes include apoptosis, cell differentiation and cell growth (Toska and Roberts, 2014), as well as the progression of adult cancers (Qi et al., 2015). Overtime, WT1-target genes have been revealed, including growth factors and cell division regulators. These include, although are not exclusive to: *Bcl-2* (Mayo et al., 1999), *Bcl-xL* (Bansal et al., 2012), *BFL1* (Simpson et al., 2006), *cyclin D1* (Xu et al., 2013), *VEGF* (McCarty et al., 2011) and *c-myc* (Han et al., 2004). As a consequence of these far-ranging target genes, studies have shown that WT1-knockout is embryonically lethal in a murine model

due to cardiac defects (Kreidberg et al., 1993), as well as hypoplastic lungs (Cano et al., 2013), lack of spleen (Chau et al., 2011), absence of adrenal glands (Bandiera et al., 2013) and disruption of podocyte development (Dong et al., 2015). The importance of WT1 in development is also highlighted in Denys-Drash syndrome, in which a WT1-mutation within exon 8 or 9 leads to a disruption of DNA binding due to premature termination of WT1 translation (Guaragna et al., 2017). Thus, the majority of the WT1 zinc-finger DNA recognition domain is absent and therefore development is critically affected in these individuals (Guaragna et al., 2017).

1.2.1 WT1 gene and protein

The WT1 gene, first cloned in 1990, is situated on the short arm of chromosome 11 at position 13 (11p13) and consists of 10 exons, spanning 50kb (Call et al., 1990). The gene is highly conserved across all vertebrate species, including chicken, alligator, Xenopus laevis and zebrafish (Kent et al., 1995).

Overtime, a detailed structure of different portions of the WT1 protein has been uncovered using both X-ray crystallography and NMR spectroscopy (Stoll et al., 2007; Wang et al., 2018). Figure 1 illustrates how the WT1 protein possesses a proline/glutamine-rich domain at its N-terminus, which is important in self-association both *in vitro* and *in vivo* (Moffett et al., 1995) and RNA recognition, as displayed using structural modelling (Kennedy et al., 1996). Alongside this, the N-terminus also houses both a repression and activation domain between residues 84 and 124, and 181 and 250, respectively (Yang et al., 2007). These can act independently of each other to either repress or activate the transcription of target genes, dependent on the target gene promoter, cell type and cell cycle stage (Wang et al., 1995; Reddy et al., 1995). Functional analysis of the WT1 repression domain showed that a region of just ten amino acids is sufficient to suppress the activity of the WT1 activation domain, termed the suppression domain (Carpenter et al., 2004).

Four canonical Cys(2)His(2) zinc fingers exist at the C-terminus of WT1, which bind to GC-rich domains on DNA and RNA (Bardeesy and Pelletier, 1998) (Figure 1), such as the WTE motif (Nakagama et al., 1995) and EGF-1 consensus sequence (Englert et al., 1995). This interplay can occur via base-specific interactions of the second and fourth zinc finger domains deep in the major groove of the DNA (Stoll et al., 2007). Conversely, zinc finger 1 contributes to anchorage of WT1 to the target DNA or allows for interactions with RNA, depending on the particular WT1 isoform (Stoll et al., 2007).

Two major sites of phosphorylation exist within the WT1 protein structure. This is at serine 365, which can be phosphorylated by protein kinase A (PKA), and at serine 393 which is phosphorylated by protein kinase C (PKC) (Figure 1). Phosphorylation can reduce WT1's ability to bind to DNA and hence its transcriptional effects.

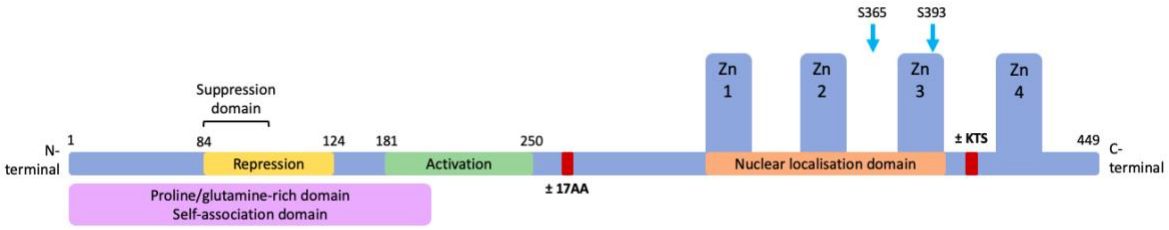

Figure 1. *Schematic structure of the WT1 protein.*
The residues (1-449) are indicated, with the repression and activation domains highlighted. The zinc finger domain, comprised of zinc fingers 1-4, is also labelled. The alternate splicing sites (±17AA and ±KTS) are shown in red, and the regions of phosphorylation by PKA and PKC are shown with the blue arrows.

1.2.2 WT1 isoforms

Whilst over 36 WT1 isoforms have been observed, the most common alternate splice sites are at exon 9, which frequently exhibits a lysine, threonine, serine (KTS) insert, and exon 5, where a 17 amino acid insert (17AA) is sometimes observed (Figure 1). These isoforms have been identified in a broad range of cell types.

The presence or absence of the KTS insert influences the ability of the WT1 protein to interact with DNA. WT1 forms that lack the KTS alternative splice (WT1 -KTS) act as a transcription factor (Bor, 2006), whereas, WT1 forms that contain the KTS alternative splice (WT1 +KTS) interact with RNA, which is crucial in olfactory development (Wagner et al., 2005). It is proposed that the location of the KTS insert at exon 9 causes displacement of the fourth zinc finger, decreasing the protein's DNA binding affinity (Ullmark et al., 2018). This idea is backed up through NMR analysis, which showed that WT1 +KTS isoforms have increased flexibility of the linker between zinc fingers 3 and 4, preventing zinc finger 4 from binding in the major groove of the DNA (Laity et al., 2000). Indeed, it was observed that both -KTS and +KTS isoforms are necessary physiologically, where knockout of either isoforms leads to severe developmental phenotypes (Hammes et al., 2001). Interestingly, no observable phenotypic changes are observed in ±17AA knockouts (Natoli et al., 2002). Despite this, imbalance of the isoforms is related to disease states. For example, overexpression of the WT1 -17AA -KTS mutant induces morphological changes in ovarian cancer cells, with enhanced migration and invasion *in vitro* compared to the wildtype TYK ovarian cancer cell type (Jomgeow et al., 2006). Thus, the equilibrium between these different isoforms is essential in maintaining physiological mechanisms.

1.2.3 WT1 and cancer

As previously mentioned, WT1 was first found to be a tumour-suppressor in the paediatric kidney cancer Wilms' Tumour. *In vitro* studies using the kidney-derived cell line RM1 showed WT1 expression reduced the number of colonies (McMaster et al., 1995). This is believed to be due to a WT1-mediated increase in the expression of genes encoding pro-apoptotic factor *Bak* (Morrison et al., 2005), alongside a downregulation of growth factor receptors including epidermal growth

factor receptor and the insulin receptor (Menke et al., 1997). Hence, a combination of these mechanisms leads to an overall increase in cell death, pointing towards the role of WT1 in tumour suppression.

Nevertheless, more recent research suggests that WT1 acts as an oncogenic factor in most adult cancers, where wildtype WT1 can upregulate drivers of the cell cycle and anti-apoptotic factors in many adult cancers. For example, WT1 overexpression was reported in 90% of breast cancer samples (Loeb et al., 2001) and has been associated with poor prognosis (Miyoshi et al., 2002). Moreover, these cases were linked to wildtype WT1 protein, rather than any mutant forms. Thus, this strongly indicates that wildtype WT1 acts an oncogenic factor in breast cancers (Oji et al., 2004). In accompaniment, studies have suggested that wildtype WT1 has a role in the development and progression of other solid tumours, such as lung (Oji et al., 2002) and colon adenocarcinomas (Oji et al., 2003); and meta-analysis showed that WT1 expression was correlated with poor prognosis in ovarian and endometrial cancers (Qi et al., 2015). Additionally, WT1 has been linked to non-solid tumours including acute myeloid leukaemia (AML) (Owen et al., 2010).

The role of WT1 in cancer is possibly underpinned by dysregulation of a co-suppressor, which would consequently lead to unregulated proliferation and cell cycling, allowing for maintenance of survival, as observed in AML cells (Karakas et al., 2002). As well as this, WT1 may initiate unfavourable splicing events, leading to the de-repression of the splice factor SRPK1. As a follow-on, SRPK1 causes upregulation of SRSF1, as observed *in vitro* in PC3 and K562 cell lines (Belali et al., 2020), altering VEGF splicing, and hence inducing vascularisation (Amin et al., 2011; Belali et al., 2020). These events allow for tumour growth and metastases.

1.2.4 WT1 as an activator and a repressor

WT1 was first discovered as a transcriptional activator, where it was shown to upregulate a host of genes associated with an active gene state, including *AREG*, a facilitator of kidney differentiation (Lee et al., 1999); *ETS-1*, a transcription factor involved in stem cell development, cell senescence and death, and tumorigenesis (Wagner et al., 2008); and *VDR*, a ligand-activated transcription factor (Lee and Pelletier, 2001). Nevertheless, further research isolated the co-repressor protein BASP1 at the WT1 suppression domain (Carpenter et al., 2004). This interaction was shown to be a driver of a transcriptionally repressive state; thus, implying that WT1 can switch from an active transcriptional regulator to a repressive one dependent on its binding partners.

1.3 BASP1

BASP1 was first isolated from rat and chicken brain, where it was discovered as a cytoplasmic membrane-bound protein in neuronal cells (Maekawa et al., 1993). Here, BASP1 accumulation

can alter plasma membrane structure and actin cytoskeleton organisation, leading to neuronal growth, motility and cell surface dynamics (Mosevitsky, 2005). Further studies have reported that BASP1 is also present in the nucleus (Carpenter et al., 2004). BASP1 contains a myristoyl group at glycine 2, allowing it to associate with membranes and phospholipids, and sequester nuclear lipids. Importantly, research has shown that BASP1 is recruited to WT1-target genes where it functions as a co-suppressor of WT1 (Toska et al., 2012).

1.3.1 BASP1 gene and protein

The BASP1 gene is located at chromosome position 5p15.1 and encodes for the 22.7kDa BASP1 protein. The structure of this protein is illustrated in Figure 2, with the important structural landmarks highlighted. This includes the myristoylated group at glycine-2, several transient phosphorylation sites, well-conserved PEST domains and a bipartite nuclear localisation sequence (Green et al., 2009; Toska et al., 2014).

It has been observed that myristic acid can acylate glycine-2 via N-myristoyltransferases by forming an acid-amide bond. This mechanism allows for BASP1 to sequester lipids, such as membrane phospholipids and the cortical cytoskeleton (Wiederkehr et al., 1997; Mosevitsky, 2005), including the phospholipid phosphatidylinositol 4,5-bisphosphate (PIP2) (Toska et al., 2012). Moreover, recent evidence indicates that BASP1 is not only a membrane-bound protein, with studies demonstrating that PKC can phosphorylate serine-6 on cytoplasmic BASP1, disrupting the electrostatic interaction between BASP1 and its membrane-bound lipids (Takasaki et al., 1999; Hartl et al., 2020).

Additionally, BASP1 also contains multiple phosphorylation sites which are targeted by PKC within its PEST domains (regions rich in proline, glutamine, serine and threonine). PEST domains are indicative of proteins with a high turnover rate, and thus the multiple phosphorylation sites within these suggests that phosphorylation may play a role in regulating BASP1 stability and turnover (Mosevitsky et al., 1997).

Also, BASP1 is a nuclear protein, where it is able to interact with nuclear lipids, via its myristoylated motif in order to associate with nuclear phospholipids (including nuclear PIP_2), and regulate gene expression (Carpenter et al., 2004; Goodfellow et al., 2011; Toska and Roberts, 2014). These genes include WT1-target genes where BASP1 functions as a co-suppressor; as shown experimentally when BASP1 was isolated through interaction with the repression domain of WT1 (Carpenter et al., 2004). BASP1 is also able to interact with cholesterol via its CRAC domain, which allows BASP1 to associate with cholesterol-rich domains within membranes and also aids in conferring transcriptional repression (Loats et al., 2021).

Nuclear BASP1 can be SUMOylated (Small Ubiquitin-like Modifiers are added) at lysine residues 78 and 83 (Green et al., 2009) (Figure 2), allowing the protein to relocate from the chromatin to the nuclear matrix, including redistribution to promyelocytic leukaemia (PML) bodies, which is densely packaged and enriched (van Steensel and Belmont, 2017). Thus, the subcellular localisation of

BASP1 seems to be important in regulation and may aid in understanding the differing function of WT1 in different cell types (Green et al., 2009).

Figure 2. *Schematic structure of the BASP1 protein.*
The residues (1-243) are labelled, as well as the PIP2 binding site which encompasses the myristoylated tail from G2. Phosphorylation sites are shown using a blue arrow and SUMOylation sites are shown using red arrows. Their respective specific sites are indicated above. NLS depicts the nuclear localisation sequence, and PEST regions are highlighted.

1.3.2 BASP1's co-suppressive properties

Although a nuclear function for BASP1 was first identified as a cofactor for WT1, BASP1 has since been found to interact with other transcription factors (Hartl et al., 2020). BASP1 has been reported to transcriptionally co-suppress the transcription factor yin-yang 1 (YY1), reducing smooth muscle cell proliferation and migration (Santiago et al., 2021). BASP1 also acts as a transcriptional co-suppressor against the oestrogen receptor α (ERα) (Marsh et al., 2017), which is a hormone receptor associated with enhanced proliferation in breast cancer (Paterni et al., 2014). In accompaniment, this interaction is enhanced by the addition of tamoxifen (Marsh et al., 2017) – a commonly used ERα-targeted therapeutic agent for breast cancer. Together, BASP1 and tamoxifen can enhance growth inhibition via its interaction with ERα.

1.3.3 BASP1 and cancer

Endogenous levels of BASP1 are protective against many adult cancers. *In vitro* studies show BASP1 inhibits Myc-induced oncogenesis (Hartl et al., 2009), in which data suggests that BASP1 interferes with the Myc/calmodulin interaction (Raffeiner et al., 2017). Elevated Myc levels counteract BASP1's actions as observed in human leukaemia cell types (Valovka et al., 2013), and hence it is plausible that a similar oncogenic mechanism occurs *in vivo*. Furthermore, experiments have shown that BASP1 is involved in numerous cancer-protective mechanisms, including mediating cell cycle arrest in G1 phase, induction of apoptosis and inhibition of the β-catenin pathway in gastric and thyroid cancer cell lines, thereby reducing cell migration (Guo et al., 2016; Li et al., 2020). BASP1's tumour suppressive role has been observed in an acute myeloid leukaemia positive cell line, which showed BASP1 inhibited proliferation and colony formation by inducing apoptosis and cell cycle arrest (Zhou et al., 2018). An *in vivo* study using murine models showed BASP1 levels are depleted in squamous cell carcinoma cases (Ponzio et al., 2017).

Therefore, several adult cancers are inherently linked to downregulation of BASP1. Downregulation of BASP1 could be brought about by either direct transcriptional repression, micro-RNA-guided downregulation or promoter methylation (Kaehler et al., 2015; Xu et al., 2015). The latter is a common mechanism of BASP1-silencing and is demonstrated in thyroid cancer cell lines and xenografts, where ectopic BASP1 expression was shown to inhibit growth (Guo et al., 2016).

1.4 WT1/BASP1 complex

The co-localisation of WT1 and BASP1 was first shown in a study which used purified BASP1 antibodies (Carpenter et al., 2004). This showed that the two proteins spatio-temporally co-localise within the nucleus of cells expressing both proteins. Further work using immunofluorescence and immunoblotting technology demonstrated the association of BASP1 at the WT1 suppression domain at the promoters of WT1-target genes (Carpenter et al., 2004), which has since been shown using a model cell line of podocyte differentiation (Green et al., 2009). Studies showed that this complex has physiological roles in cell fate and differentiation *in vitro*, including how BASP1 controls the differentiation pathway of K562 cells (Goodfellow et al., 2011).

K562 cells in either the presence or absence of BASP1 were treated with the phorbol ester, phorbol 12-myristate 13-acetate (PMA) (Goodfellow et al., 2011). PMA is an activator of PKC, which is associated with transcription of genes involved in cellular differentiation and growth (Griner and Kazanietz, 2007). Beta-tubulin staining displayed how PMA treatment of K562 cells in the absence of BASP1 brought about differentiation into rounded megakaryocytes (Goodfellow et al., 2011). Yet, BASP1 represses the genes responsible for differentiation into megakaryocytes, and thus, when in the presence of BASP1, PMA induced extensive arborisation, elongation and formation of processes, with the upregulation and expression of several genes involved in neutrite outgrowth and synapse formation (Goodfellow et al., 2011). This possibly stems from the upregulation of P2X5 receptors which is observed when BASP1 is present (Goodfellow et al., 2011); and allows the cells to respond to ATP and possess neuronal-like properties and morphology.

To accompany this finding, the effect of BASP1 on induced pluripotent stems cells (iPSCs) has been explored. It found that inhibition of BASP1 in iPSCs formed from the OSKM cocktail (*Oct4, Sox2, Klf4* and *c-Myc*) negated the need for Sox2 in this cocktail (Boland et al., 2009; Rusk, 2017; Blanchard et al., 2017). As a result, this cemented the idea that BASP1 is crucial in cell fate and must be downregulated before cellular reprogramming can commence (Boland et al., 2009). Beyond this, research identified that BASP1 represses the WT1-target gene *Lin28,* an RNA-binding protein linked to pluripotency (Cho et al., 2012). Alas, these findings demonstrated that WT1 and BASP1 interact mechanistically *in vitro*. However, research was essential to confirm that this mechanism is also important *in vivo.*

Tissue analysis has shown that co-expression of WT1 and BASP1 takes place at several critical sites of WT1 activity, including within the embryonic kidney, adult brain, lungs and testes (Mosevitsky and Silicheva, 2011), indicating that the co-localisation of these two proteins is physiologically relevant *in vivo*. A recent study using mouse models of diabetic neuropathy demonstrated how BASP1 promotes kidney podocyte apoptosis and activation of the p53 pathway by co-repressing WT1 (Zhang et al., 2021).

Another study showed a physiological role of the WT1/BASP1 complex in cell fate *in vivo*, as demonstrated using taste receptor cells isolated from mice (Gao et al., 2014; Gao et al., 2019). Originally, it was demonstrated that WT1 directs cell fate of taste receptor cells throughout the differentiation process by activating the *LEF1* and *PTCH1* genes, initiating the Wnt and Shh signalling pathways, respectively (Gao et al., 2014). The expression of these two genes is typically associated with progenitor cells, and hence, BASP1 must control differentiation levels by suppressing WT1. A follow-on study using immunohistochemistry conveyed how BASP1 expression increased towards the end of the differentiation process, leading to repression of certain genes. Thus, the WT1/BASP1 complex retains the taste cells in their differentiated state (Gao et al., 2019). Combined, these studies display a physiological role of the interaction between WT1 and BASP1 *in vivo.*

1.4.1 WT1/BASP1 recruitment of histone-modifying enzymes

Research has shown that WT1 binds to numerous factors besides BASP1. Both *in vivo* and *in vitro* work has demonstrated an interaction of WT1 with the co-activator CREB-binding protein (CBP) and its closely related paralog p300; termed together CBP/p300 (Wang et al., 2001). CBP was first shown to co-immunoprecipitate with WT1 in embryonic rat kidney cells (Wang et al., 2001). CBP/p300 are histone acetyltransferase enzymes which interact with WT1 to activate target genes by acetylating H3K9, with disruption shown to cause numerous developmental problems (Carré et al., 2018) (Figure 3A).

Further studies have demonstrated that BASP1 is recruited to WT1 to inhibit CBP-binding and thus, induce transcriptional repression (Toska et al., 2014). To constitute transcriptional repression, it was shown that the WT1/BASP1 complex deacetylated the active histone mark H3K9ac by recruiting the histone-modifying enzyme HDAC1 to form a large complex (Toska et al., 2012). The mechanism was observed to be lipid-dependent, and reliant on the binding of PIP_2 at BASP1's myristoylated tail (Toska et al., 2012). Furthermore, research has confirmed the necessity of prohibitin in this complex, which in-turn recruits BRG1, an ATP-dependent chromatin modifying enzyme (Toska et al., 2014) (Figure 3B). Thus, this complex works to induce transcriptional repression.

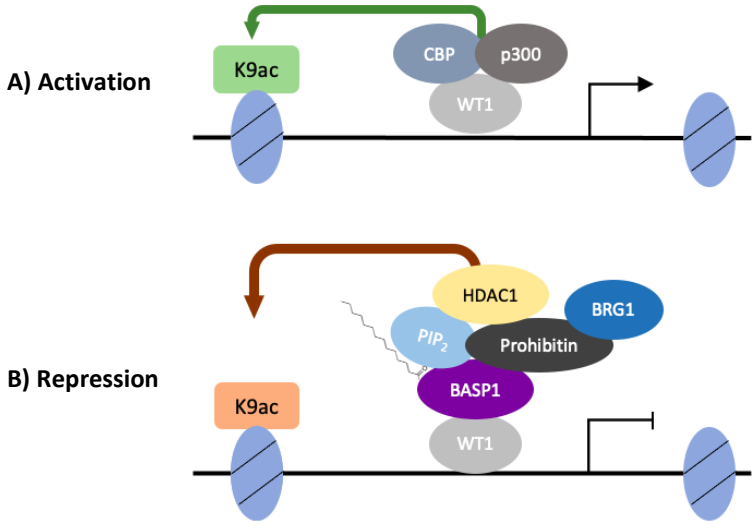

Figure 3. *Deposition and removal of the H3K9ac mark.*
A) The WT1 protein recruits CBP/p300 to the promoters of its target genes. This results in the deposition of an active acetyl mark at H3K9. Hence, transcription is initiated.
B) WT1 is also able to recruit BASP1 into a complex at promoters to induce transcriptional repression. BASP1 recruits histone-modifying factors into this complex, including PIP_2 which binds to the myristoyl group on BASP1. Thus, this interaction is lipid-dependent. Once PIP_2 is bound, a cascade of interactions ultimately brings HDAC1 into the complex, which deacetylates H3K9. This initiates steps towards repression of the gene.

Recent studies in the lab have uncovered further chromatin modifications which are made by the WT1/BASP1 complex. This includes the removal of the active histone mark H3K4me3, whilst also encompassing the deposition of repressive the histone marks, H3K9me3 and H3K27me3 (Figure 4) (Dey, 2019).

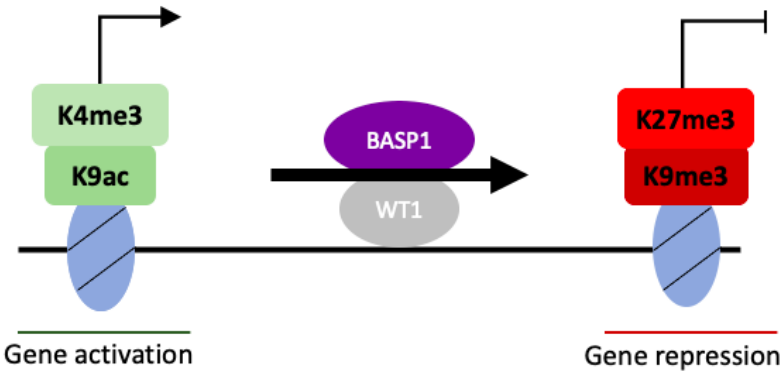

Figure 4. *Chromatin remodelling by the WT1/BASP1 complex.*
The WT1 and BASP1 proteins work together to direct transcriptional repression by removing the active histone marks H3K4me3 and H3K9ac (left), and instead depositing the repressive histone marks H3K27me3 and H3K9me3 (right).

The WT1/BASP1 complex was first shown to be important in the addition of repressive marks to chromatin in epicardial cells (Essafi et al., 2011). Here it was shown that WT1 recruits BASP1 to silence *Wnt4* by the addition of H3K27me3 marks (Essafi et al., 2011). The distribution of H3K27me3 marks allows the WT1/BASP1 complex to control epithelial-mesenchymal transition (EMT) and the generation of progenitor cardiovascular cells (Essafi et al., 2011). Recently, chromatin immunoprecipitation (ChIP) experiments have confirmed the relationship between H3K27me3 marks and BASP1, and these findings have shown how this is a lipid-independent mechanism, as the BASP1-G2A mutant, which lacks a myristylated tail, did not affect the addition of repressive marks (Figure 5) (Dey, 2019).

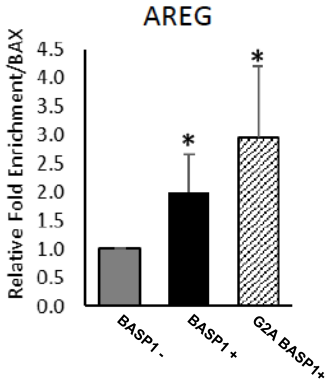

Figure 5. *H3K27me3 recruitment at WT1-target gene promoters.*
Previous work showed a significant increase in placement of the repressive histone mark H3K27me3 at the WT1-target gene promoter, *AREG*, in the presence of BASP1, independent of myristylation. Error bars represent the standard deviation of the mean, where n=7. *p<0.05 by Student's t-test comparing BASP1-positive K562 cells with BASP1-negative K562 cells. Data from Dey, 2019.

Interestingly, only factors which remove active marks are found to be lipid-dependent, whereas addition of repressive marks is independent of BASP1's myristoyl group (Dey, 2019). Recent work has found that BASP1 is also able to recruit cholesterol via its CRAC domain (Figure 2) during the removal of active mark H3K4me3 (Loats et al., 2021). These findings describe a role for nuclear lipids in transcriptional repression. Such lipids are present both within the inner nuclear membrane (INM) and throughout the nucleus. Recent work has shown that BASP1 binds to the nuclear envelope protein emerin in a myristoyl-dependent manner, raising the possibility that BASP1-mediated transcriptional repression might occur at the nuclear periphery (Dey, 2019). Indeed, there is mounting evidence that transcriptionally repressive heterochromatin is located at the nuclear periphery (Mir et al., 2019).

Previous work has shown that the G2A-BASP1 mutant is defective in inducing transcriptional repression (Toska et al., 2012). Instead, it has been shown that the lipid-dependent removal of

active marks is essential to drive transcriptional repression, whereas it is currently unclear whether lipid-independent deposition of repressive marks is critical in this process or whether removal of active marks is sufficient (Dey, 2019). It is therefore important to determine if the BASP1-mediated placement of H3K27me3 marks is required for transcriptional repression by the WT1-BASP1 complex.

Sites which contain both the active mark H3K4me3 and the repressive mark H3K27me3 are known as bivalent promoters, which are important in embryonic development (Voigt et al., 2013). This is currently an intense area of research; yet there is a lack of evidence surrounding the mechanism by which H3K27me3 marks are added in the presence of the active histone mark.

1.4.2 Other interactions of WT1

It has long been known that WT1 is co-localised with the tumour suppressor p53. Research in the developing kidney outlined that WT1 has a cooperative effect upon p53 by increasing stability and DNA binding activity of p53 (Maheswaran et al., 1993; Maheswaran et al., 1995). A recent study has unveiled that the interaction between WT1 and p53 is in fact mediated via BASP1, where BASP1 knockdown promotes downregulation of the p53 pathway via WT1, hence reducing apoptosis (Zhang et al., 2021). Research has delved into the effects of the WT1-p53 interaction clinically; with a recent study indicating the potential use of both p53 and WT1 as prognostic biomarkers in ovarian cancer (Carter et al., 2018).

1.5 EZH2 and PRC2

The deposition of trimethyl marks on H3K27 has been extensively linked to the action of the polycomb repressor complex 2 (PRC2) (Boros et al., 2014; Prokopuk et al., 2017; Lavarone et al., 2019), and thus, research has determined that this is an important complex in establishing and maintaining heterochromatin states.

The polycomb group (PcG) is a group of chromatin-modifying proteins which was originally discovered as an important regulator of *Drosophila* development, where it was noted that the proteins influence the spatio-temporal expression of the *Hox* genes (Deevy and Bracken, 2019). Orthologs of PcG genes have since been recognised in numerous species and have been associated with appropriate gene expression (Laugesen and Helin, 2014). PcG proteins are able to assemble into large protein complexes, typically the polycomb repressor complexes 1 and 2 (PRC1 and PRC2), which preferentially bind to CpG-rich domains (Laugesen et al., 2016).

Whilst the PRC1 catalyses the monoubiquitylation at lysine 119 of H2A to form H2AK119ub (Wang et al., 2004), the PRC2 acts as a methyltransferase complex, where it is essential in the monomethylation, dimethylation and trimethylation of H3K27 in a spatially-defined manner (Ferrari et al., 2014). The PRC2 is crucial in cell fate determination in embryonic stem cells and a PRC2 knockout is embryonically lethal (Pasini et al., 2007). An estimated 5-10% of histones are believed

to carry the H3K27me3 modification (Peters et al., 2003; Ferrari et al., 2014), which is an indicative mark of gene repression, as shown in research using mouse embryonic stem cells (Wiles and Selker, 2017). Conversely, H3K27me1 is believed to be associated with active enhancers (Barski et al., 2007). As a result, the PRC2 is critical in deciding which genes are expressed, making it vital in cell fate and differentiation.

1.5.1 PRC2 structure

The catalytic activity of the PRC2 is accounted for by the action of the SET domain of the core component EZH1/2 (enhancer of zeste homolog 1/2) (Wu et al., 2013). Other integral members of the PRC2 are suppressor of zeste 12 (SUZ12) and embryonic ectoderm development (EED). SUZ12 interacts with non-essential PRC2 accessory proteins, including AEBP2 and JARID2 (Jain et al., 2019). The complete function of these accessory proteins is currently being studied, although they seem to be involved in modulation of PRC2 recruitment and enzymatic activity (Højfeldt et al., 2019). On the other hand, a crystal structure of the active PRC2 showed that EED acts as a reader within the complex, where it is able to bind to H3K27me3 via its WD40 domain. This leads to a conformational change with numerous modulatory effects, including stabilising the PRC2 at its target whilst simultaneously increasing the complex's activity in the presence of the H3K27me3 mark by increasing EZH2 activity (Jiao and Liu, 2015; Lavarone et al., 2019).

The spatial arrangement of the PRC2 components was displayed using electron microscopy in conjunction with chemical cross-linking and mass spectroscopy data (Ciferri et al., 2012). This data aids our understanding of how the PRC2 regulates histone methylation. The SANT domains of EZH2 can couple enzymatic activity to histone-tail binding by interacting with SUZ12 and EED. EED-binding at one nucleosome positions the H3 tail from the subsequent nucleosome in close proximity to the EZH2 SET domain (Ciferri et al., 2012). This mechanism is indicative of a positive feedback loop, where upon H3K27 trimethylation, methylation of the neighbouring nucleosome is favoured. Hence, this allows the histone marks to spread across the chromatin in regions of spatial proximity (Oksuz et al., 2018). The points of interaction between the three core components of the PRC2 are outlined in Figure 6. It is important to note that the separate components of the PRC2 are highly unstable individually due to its vast interaction surface and hence, EZH2 activity and presence is likely to be accompanied with SUZ12 and EED (Pasini et al., 2007).

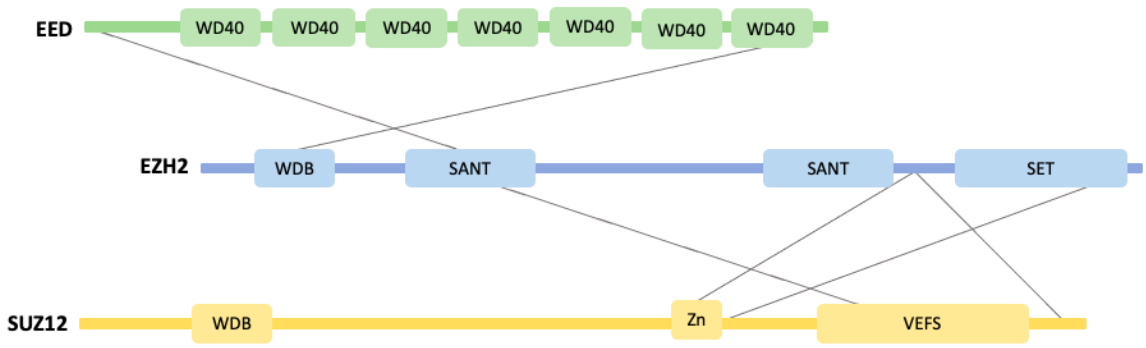

Figure 6. *The structure of and interactions between the PRC2 factors.*
The domains of the three core components of the PRC2 are outlined above, as well as the points of interaction between different PRC2 factors. This shows specifically which domains are able to interact, and thus how the PRC2 is biochemically formed.

There seems to be a dynamic interplay between PRC1 and PRC2 in order to reach transcriptional repression, in which H3K27 trimethylation by PRC2 facilitates PRC1 recruitment and H2AK119 monoubiquitylation (Blackledge et al., 2015); thus, mediating steps towards transcriptional repression. This recruitment is mediated by the CBX protein of PRC1, which recognises and docks to H3K27me3 marks with a high affinity (Blackledge et al., 2015). This mechanism has been termed the 'hierarchical recruitment model', nevertheless more recent studies have demonstrated that this inter-complex crosstalk may be bi-directional. Here, PRC1 histone ubiquitination is thought to recruit the PRC2 via the ubiquitin-interaction motif on the N-terminus of the accessory protein JARID2 (Cooper et al., 2016).

1.5.2 PRC2 and cancer

The deposition of trimethyl marks at H3K27 initiates steps towards repression via nuclear nano-architectural changes. Therefore, a mutation in EZH2 can alter the balance of H3K27me3 deposition and can cause chromatin to clump, change in size and undergo density distribution changes (Zink et al., 2004). All these alterations will impact gene expression, and consequently, many genes which would usually be repressed will instead be active.

As EZH2 holds the catalytic activity of the PRC2, a mutation causing a loss or gain of function of EZH2 is usually deemed the most detrimental to the working of the complex. However, a mutation in any core component can potentially lead to a conformational change and hence instability and inactivity of the PRC2. *In vivo* studies have shown that EZH2 dysregulation can be oncogenic, including in many solid cancers, but tumour suppressive in acute myeloid leukaemia and myelodysplastic syndromes. This is because EZH2 is able to function as both a transcriptional activator and repressor depending on the cell type and the type of methyl mark it deposits at H3K27.

Research has shown EZH2 upregulation can accelerate cell proliferation and survival in colorectal cancer, melanoma and breast cancer (Yamagishi and Uchimaru, 2017). Experimental evidence has shown that DZNep treatment, an EZH2 inhibitor, in a colorectal cancer cell line induces autophagy and apoptosis (Yao et al., 2016); whilst, EZH2 inhibition in cholangiocarcinoma cells arrests the cell cycle in G1, yet again reducing cell proliferation (Nakagawa et al., 2013).
As a result of these findings, EZH2 is frequently used clinically as a prognostic marker for cancers. This includes in epithelial ovarian cancer, where upregulation of EZH2 adds H3K27me3 marks in order to repress the *ARHI* tumour suppressor gene *in vitro* (Fu et al., 2015).

1.6 The PRC2 and WT1/BASP1 complexes

Previous work from our group using co-immunoprecipitation mass spectroscopy has shown that EZH2 may potentially interact with BASP1; raising the possibility that BASP1 deploys EZH2 to trimethylate H3K27 at WT1-target genes. However, further investigations are required to confirm this hypothesis. Recent ChIP experiments have demonstrated EZH2 recruitment to the promoters of WT1-target genes in a BASP1-dependent manner. This data is outlined in Figure 7, which shows a significant increase in EZH2 presence at the *AREG* promoter during BASP1 expression. Hence, this implies that EZH2 recruitment is BASP1-mediated; and inhibitor experiments have confirmed that EZH2 recruitment at WT1-target genes is not coincidental and instead possibly plays a critical role in the deposition of H3K27me3 to invoke transcriptional repression (Johnson, 2019). To accompany these findings, past studies have outlined how the recruitment of EZH2 to promoters is coupled with the other core components of the PRC2 for stability (Pasini et al., 2007).

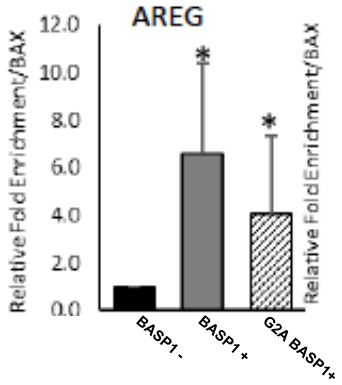

Figure 7. *EZH2 recruitment at WT1-target gene promoters.*
Previous work shows a significant increase in EZH2 recruitment to the WT1-target gene promoter, *AREG*, in the presence of BASP1. Significant recruitment is observed in G2A-K562 cells at the *AREG* promoter when compared to V-K562 levels – implying that the recruitment of EZH2 is lipid-independent. Error bars represent the standard deviation of the mean where n=10. *p<0.05 by Student's t test comparing BASP1-K562 or G2A-K562 with V-K562. Data from Dey, 2019.

1.7 Aims and hypothesis

This project seeks to extend our understanding of how BASP1 and PRC2 may interact to deposit H3K27me3 marks and influence WT1-target gene transcriptional states. Previous data collected in the laboratory has suggested an interaction between EZH2 and BASP1 following co-immunoprecipitation mass spectroscopy experiments, whilst also suggesting EZH2 is recruited to target gene promoters following chromatin immunoprecipitation experiments. By uncovering this physiological mechanism and improving knowledge of the potential WT1/BASP1/PRC2 complex; future studies can focus on understanding how this mechanism may be aberrant in cancer states. The study will use K562 cells; a common cell line extracted from a patient with chronic myelogenous leukaemia (Lozzio and Lozzio, 1975) and is frequently used in WT1/BASP1 research as they lack endogenous BASP1, whilst WT1 is still present. As a comparative tool, a K562 cell line derivative, termed BASP1-K562 cells, were transfected to stably express BASP1 (Goodfellow et al., 2011). Results from BASP1-K562 cells are typically compared to the vector control cell line Vector-K562 cells (V-K562s), and past affymetrix expression assays and ChIP experiments using BASP1-K562 cells showed that the BASP1-K562 cell line transcriptionally represses >90% of WT1-target genes compared to V-K562 cells (Goodfellow et al., 2011). Results in this study will be validated using MCF7 cells, a breast cancer cell line which endogenously expresses both BASP1 and WT1.

The first aim will investigate whether there is a significant fold enrichment of EZH2 at WT1-target gene promoters, by using a different EZH2 antibody to that used previously in the laboratory. Hence, this will further explore whether a significant increase in EZH2 recruitment occurs at the promoters of *AREG, ETS-1* and *VDR* during BASP1 expression. To accompany this, the recruitment of SUZ12 at these promoters will also be tested to explore whether the intact PRC2 is recruited. The study will explore whether recruitment of the PRC2 components is a lipid-independent process as past research has alluded to. In accompaniment, I will explore whether knockdown of EZH2 blocks BASP1-mediated repression, and whether this triggers a significant change in the placement of H3K27me3 marks at WT1-target gene promoters. Previous work in the laboratory has shown that EZH2 inhibitors block BASP1-mediated repression (Johnson, 2019). As a result of this, it will be interesting to determine if targeted knockdown of EZH2 will produce a similar transcriptional response, and hence confirm that EZH2 is critical in BASP1-mediated repression and the addition of H3K27me3 marks in a BASP1-mediated manner. The final aim will focus on whether there is an interaction between BASP1 and either EZH2 or SUZ12 in K562 cells. This will confirm whether the PRC2 is recruited directly into the WT1/BASP1 complex or instead that WT1/BASP1 promotes favourable conditions for PRC2 recruitment to the promoter.

2. Materials and methodologies

2.1 Materials

2.1.1 General reagents

Fisher Scientific: Ethanol, methanol, 4-(2-hydroxyethyl)-1-piperazineethanesulfonic acid (Hepes), sodium dodecyl sulfate (SDS), ammounium persulfate (APS), phosphate-buffered saline (PBS), bromophenol blue, ethylenediaminetetraacetic acid (EDTA), cDNA synthesis kit.

PanReac AppliChem: Tween, glycine, sodium deoxycholate, tris-base.

Sigma: Triton X-100, LiCl, glycerol, foetal bovine serum (FBS), acrylamide/bis gel mix (gel mix), trypsin.

Gibco: Rosewell Park Memorial Institute 1640 (RPMI) media, penicillin/streptomycin (P/S), L-glutamine, Dulbecco's Modified Eagle Medium (DMEM).

BioRad: SYRB green PCR mix, Clarity Western ECL Substrate.

Qiagen: RNeasy kit, PCR clean up kit, Hi-PerFect.

Others: G418 (Toku-E), $MgCl_2$ (Acros Organic), dithiothreitol (DTT) (Santa Cruz Biotechnology), protease inhibitor cocktail (Complete Mini), Rainbow Marker (Astiva). Formaldehyde and Nonident P40 (NP-40) (Merck). NaCl and KCl (VWR Chemicals). Tetramethylethylenediamine (Temed) and Dynabeads (Invitrogen).

2.1.2 Buffers and solutions

IP buffer: 20 mM Hepes pH 8, 100 mM KCl, 0.2 mM EDTA, 20% (v/v) glycerol, 0.5 mM DTT, 2.5 mM $MgCl_2$, 0.05% (v/v) NP40.

Lysis buffer: 25 mM Tris pH 7.4, 150 mM NaCl, 1% (v/v) NP40, 1 mM EDTA, 5% (v/v) glycerol, 1 mM DTT.

Resolving gel: 0.375 M Tris pH 8.8, 10% (v/v) gel mix, 0.1% (w/v) SDS, 0.25% (v/v) Temed, 0.25% (v/v) APS.

Stacking gel: 0.125 M Tris pH 6.8, 12.5% (v/v) gel mix, 0.1% (w/v) SDS, 0.375% (v/v) Temed, 0.375% (v/v) APS.

10X SDS-PAGE running buffer: 250 mM Tris, 1.9 M glycine, 35 mM SDS.

4X SDS sample loading dye: 200 mM Tris pH 6.8, 400 mM DTT, 8% SDS, 0.1% bromophenol blue.

Transfer buffer: 1X TrisGly, 10% (v/v) methanol.

Blocking buffer: 1X PBS, 0.1% (v/v) Tween, 5% (w/v) dried milk powder.

ChIP buffers:

ChIP buffer: 150 mM NaCl, 50 mM Tris pH 8, 5 mM EDTA, 0.5% (v/v) NP-40, 1% (v/v) Triton X-100.

High salt ChIP buffer: 500 mM NaCl, 50 mM Tris pH 8, 5 mM EDTA, 0.5% (v/v) NP-40, 1% (v/v) Triton X-100.

LiCl buffer: 10 mM Tris pH 8, 1 mM EDTA, 250 mM LiCl, 1% (v/v) NP-40, 1% (w/v) sodium deoxycholate.

TE buffer: 10 mM Tris pH 8, 1 mM EDTA.

Proteinase K buffer: 125 mM Tris-HCl pH 8, 10 mM EDTA, 150 mM NaCl, 1% (w/v) SDS.

2.1.3 Primers

Table 1. *ChIP primers*

Primer	**Forward**	**Reverse**	**Annealing temperature (ºC)**
18S	5'-GTAACCCGTTGAACCCCATT-3'	5'-CCATCCAATCGGTAGTAGCG-3'	60
AREG	5'-TTTAAGTTCCACTTCCTCTCA-3'	5'-GGTGTGCGAACGTCTGTA-3'	60
ETS-1	5'-CCTAAAGAGGAGGGGAGAGC-3'	5'-AGGGGAAGTTGGCACTTTG-3'	60
VDR	5'-CAACCTGGCTCAGGCGTCC-3'	5'-GCCAGGAGCTCCGTTGGC-3'	60

Table 2: *RT-PCR primers*

Primer	Forward	Reverse	Annealing temperature (ºC)
GAPDH	5'-TGCACCACCAACTGCTTAGC -3'	5'-GGCATGGACTGTGGTCATG AG -3'	60
AREG	5'-GGCTGCTAATGCAATTTTTGAT AA -3'	5'-TGGAAGCAGTAACATGCAA ATGTC -3'	60
ETS-1	5'- CTGACCCTGGAGACTTTGAC -3'	5'- TTCCTCTGCACTTCCTCA -3'	60
VDR	5'-AAACTTGCTACCATCCCGTACG T -3'	5'-ATGGTGAGAGTCGGCTTGA GAT -3'	60

Primer stocks of forward and reverse oligonucleotides were prepared at a concentration of 10μM.

2.1.4 Antibodies

Table 3. *Western blot, IP and ChIP antibodies.*

Antibody	Species	Source	Dilution for immunoblotting
BASP1	Rabbit	Pacific Immunology, California	1:2000
HA-tag	Mouse	Cell Signalling #23675	1:1000
EZH2	Rabbit	Abcam #ab186006	1:1000
SUZ12	Mouse	Invitrogen #MA5-11188	1:1000
β-tubulin	Rabbit	Abcam #ab6046	1:10000
Anti-mouse HRP	Goat	Jackson ImmunoResearch Laboratories	1:10000
Anti-rabbit HRP	Goat	Jackson ImmunoResearch Laboratories	1:10000
H3K27me3	Mouse	Abcam #ab6002	
Normal IgG	Mouse	Cell Signalling #27298	
Normal IgG	Rabbit	Merck #3543076	

2.1.5 siRNAs

Table 4. *siRNA proteins used during RNA interference experiments*

siRNA	**Source**
Control	Thermo Fisher #SIC001
BASP1	Sigma #EHU121851
EZH2 #1	Sigma #EHU073481
EZH2 #2	Santa Cruz Biotechnology Inc #sc-35312

2.2 Methodologies

2.2.1 Cell culture

K562 cells

K562 cells (ECACC) were previously stably transfected with pcDNA3 plasmids (Goodfellow et al., 2011). Cells were cultured at 37ºC, 5% CO_2 in RPMI culture medium with 10% (v/v) FBS, 1% (v/v) P/S, 1% (v/v) L-glutamine and 1 mg/mL G418.

MCF7 cells

MCF7 cells (ECACC) were cultured in DMEM culture medium with 10% (v/v) FBS, 1% (v/v) P/S and 1% (v/v) L-glutamine; at 37ºC, 5% CO_2. Trypsin was used to passage adherent cells.

2.2.2 Whole cell extract (WCE) preparation

40 million cells were harvested by centrifugation at 1000g for 10 minutes and washed twice with PBS. The pellet was resuspended in 2X packed cell volume of lysis buffer with 1X protease inhibitor. This was incubated at 4ºC for 20 minutes with frequent pipetting. The WCE was centrifuged at 13000g for 10 minutes, and the supernatant was kept.

2.2.3 Immunoprecipitation

Dynabeads Protein G (30 mg/mL) were washed twice with IP buffer. The beads were stored at 4ºC in IP buffer at the original bead volume. Samples were precleared using 10% WCE and 0.5% IP beads in IP buffer. This was rotated for an hour at 4ºC, and the supernatant kept. 1 µg antibody was added to 100 µL precleared WCE and rotated for 2 hours at 4ºC. 5 µL IP beads were added and this was rotated at 4ºC for an hour. The beads were washed three times for 10 minutes in ice-cold IP buffer and resuspended in 20 µL 1X SDS sample loading dye. 10 µL samples were loaded onto an immunoblot, alongside control antibodies and input WCEs.

2.2.4 Immunoblot

Gels were prepared from 10% (w/v) resolving gel and 4.5% (w/v) stacking gel. Following polymerisation, samples were heated at 95^{o}C for 5 minutes and loaded onto the gel. Gels were placed in SDS-PAGE running buffer and resolved at 150V, which was increased to 200V once samples hit the resolving gel.

Once the dye front approached the bottom of the gel, gels were removed from the cassette and washed in transfer buffer. Proteins were transferred onto a methanol-activated immobilon-P membrane (Merck) soaked in methanol and sandwiched between Western blotting filter paper previously soaked in transfer buffer. Transfers took place in a semi-dry transfer cell (BIORAD) at 25V for 45 minutes.

Membranes were blocked for 20 minutes in ~15 mL blocking buffer and rocked at 4^{o}C overnight with appropriate antibody in blocking buffer at a dilution concentration outlined in Table 3.

The membrane was washed four times with ~15 mL blocking buffer for 5 minutes each time. The membrane was rocked at room temperature with the specified concentration of HRP-secondary antibody diluted in blocking buffer (Table 3) for an hour. The membrane was washed four more times as before and covered in Clarity Western ECL Substrate (BIORAD). It was exposed using GenHunter PerfectFilm autoradiography film.

2.2.5 Chromatin immunoprecipitation (ChIP)

ChIP beads preparation

Dynabeads Protein G (30 mg/mL) were suspended in ChIP buffer at a concentration of 50%. After magnetising, the supernatant was removed, and the beads were resuspended in 1 mL ChIP buffer and 1% sheared salmon sperm DNA. This was rotated at 4^{o}C for one hour. The beads were magnetised and washed four times in ChIP buffer. The beads were stored at 4^{o}C in ChIP buffer at the original bead volume.

Harvesting cells and cross-linking

Ten million V-K562 and BASP1-K562 cells were harvested, resuspended in 1 mL PBS and incubated with 40 µL 37% formaldehyde at room temperature for 15 minutes. Cross-linking was quenched with 141 µL of 1 M glycine, which was left to stand for 5 minutes before centrifuging at 1500g for 5 minutes. The cells were resuspended in 1 mL ChIP buffer with 1% (v/v) protease inhibitor cocktail.

Sonication

Sonication was performed using a QSonica Q125 Sonicator at 50% amplitude for 10 seconds followed by cooling on ice. This was repeated 12 times, and then the chromatin was centrifuged at 13000g for 10 minutes. 5 µL ChIP beads were added, and this was rotated at 4^{o}C for an hour.

Chromatin immunoprecipitation

1 µg antibody was incubated with 1 mL ChIP buffer and 5 µL ChIP beads at 4ºC for four hours. These were washed with ChIP buffer, resuspended in 450 µL of the precleared chromatin, and left to rotate at 4ºC overnight.

Beads were washed with ChIP buffer and left on ice for 5 minutes. This step was repeated with high salt ChIP buffer, LiCl buffer and TE buffer; and finally resuspended in 100 µL proteinase K buffer and incubated at 65ºC overnight.

DNA isolation

1 µL of 2 mg/mL Proteinase K was added to the beads and this was incubated for three hours at 55ºC. Samples were centrifuged at 13,000g for a minute. The supernatant was retained, and DNA was isolated using the Qiaquick PCR purification kit (QIAGEN) according to the manufacturer's instructions. DNA was eluted in 100 µL nuclease-free water. The eluted DNA was prepared for q-PCR with 5 µL SYBR green PCR mix, 2 µL nuclease-free water and 1 µL primer mix (from a 10µM stock)(Table 1). Settings and temperatures for the q-PCR are outlined in Table 5. Melt curves were plotted at 0.5ºC increments between 65ºC and 95ºC.

Table 5. *q-PCR settings.*

Step	**Temperature (ºC)**	**Time (s)**	
Initial denaturation	95	180	
Denaturation	95	10	40 cycles
Annealing	60	10	
Extension	72	10	
Final extension	72	30	

2.2.6 RNA interference

Transfection

MCF7 cells were transfected with the respective siRNAs (Table 4) and set up as followed: 2X dose control siRNA; 1X dose BASP1 siRNA, 1X dose control siRNA; 1X dose EZH2 siRNA, 1X dose control siRNA; 1X dose BASP1 siRNA, 1X dose EZH2 siRNA. Here, one dose is equal to 0.05 nmol when diluted in RNase free water. After suspension, these were incubated at RTP for 3 minutes. 12 µL HiPerFect transfection reagent was added and incubated at RTP for 10 minutes. The transfection solution was suspended in 0.5 mL fresh DMEM media and added to the appropriate MCF7 cells for 48 hours.

RNA preparation

RNA was prepared using the Qiagen RNeasy kit instructions, according to the manufacturer's instructions. The RNA samples were diluted in 50 µL nuclease-free water and were either used in cDNA synthesis or stored at -20^{o}C.

cDNA synthesis

Each reaction was set up as followed, using the cDNA synthesis kit (Thermo Fisher):

9 µL water
1 µL oligo DT primer
1 µL random primer
2 µL RNA sample
4 µL 5X reaction buffer
2 µL 10 mM dNTP mix
1 µL M-MuLV RT

These reactions were then placed at 25^{o}C for 10 minutes, 42^{o}C for 30 minutes and finally 80^{o}C for 5 minutes. The cDNA was eluted in 50 µL nuclease-free water and prepared for q-PCR alongside 5 µL SYBR green PCR mix, 2 µL nuclease-free water and 1 µL primer mix (Table 2). Settings and temperatures for the q-PCR are outlined in Table 5. Melt curves were plotted at 0.5^{o}C increments between 65^{o}C and 95^{o}C.

2.2.7 Data analysis and statistical tests

For ChIP and RNA interference data, average CT-values were calculated, and fold enrichment was normalised against the control antibody. Unpaired Student's t-tests were performed on at least three independent ChIP experiments using GraphPad. One-way ANOVAs with Tukey's post-hoc test were used on three independent RNAi experiments using SPSS Statistics. Graphs were created using Microsoft Excel.

3. Results

3.1 Analysis of BASP1 and PRC2 expression in K562 cells

K562 cells lack endogenous BASP1 but contain endogenous WT1 and thus this characteristic has been exploited in our laboratory. The K562 cells used in the current study were originally generated by transfection with vectors to influence BASP1 expression (Goodfellow et al., 2011). Vector control K562 cells (V-K562s) were previously stably transfected with an empty pcDNA3 plasmid. On the other hand, BASP1-K562 cells have been previously transfected with a pcDNA3 plasmid driving BASP1 expression, tagged with C-terminal human influenza hemagglutinin (HA-tag). G2A-K562 cells were transfected with a pcDNA3 plasmid driving expression of a mutant BASP1 derivative containing a substitution of glycine at position 2 with alanine. This substitution prevents the N-terminal myristoylation of BASP1 (Toska et al., 2012). Expression of BASP1 and BASP1-G2A was confirmed through immunoblot analysis, where BASP1 presence is shown in BASP1-K562 and G2A-K562 whole cell extract compared to V-K562 whole cell extract input (Figure 8A).

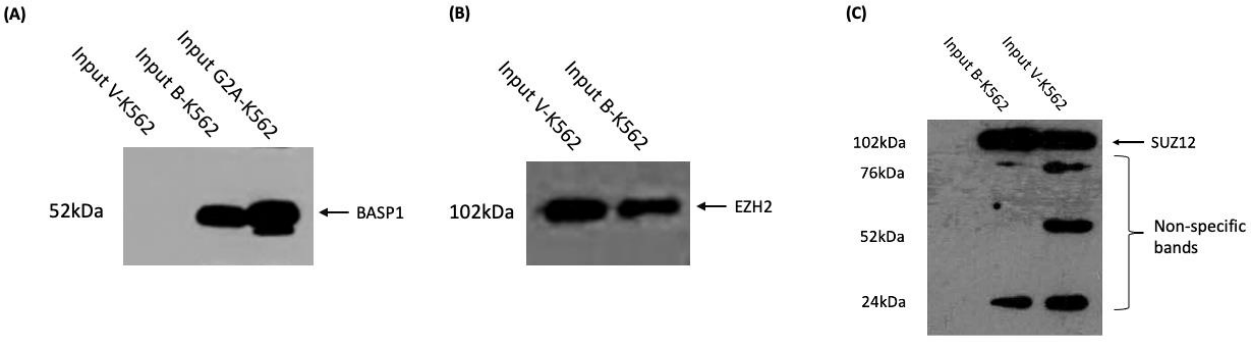

Figure 8. *Immunoblot analyses of whole cell extract with different antibodies.*
A) A Western blot experiment was performed with V-K562, BASP1-K562 and G2A-K562 whole cell extract and probed with BASP1 antibody. The data showed a band at 52kDa in BASP1-K562 cells and G2A-K562 cells, and an absence of this band in V-K562 cells.
B) BASP1-K562 and V-K562 whole cell extract was probed with EZH2 antibody. Bands were observed at 102kDa.
C) BASP1-K562 and V-K562 whole cell extract was probed with SUZ12 antibody. Bands were observed at 102kDa.

Figure 8A shows a whole cell extract immunoblot probed with BASP1. Here, a single band migrating at 52kDa was observed in the BASP1-K562 lane, whereas no band was observed in the V-K562 lane. This band corresponds to the expected molecular weight of BASP1, and thus these findings are consistent with the expected level of BASP1 in the respective cell type. The same is true in the G2A-K562 cell line lane, in which a strong band is observed at 52kDa corresponding to BASP1-G2A.

Immunoblotting V-K562 and B-K562 whole cell extracts with either EZH2 or SUZ12 antibody showed clear EZH2 and SUZ12 expression in both V-K562 and BASP1-K562 cell types (Figures 8B and 8C). Both Figure 8B and 8C show bands at 102kDa, which is consistent with the expected molecular weight of both EZH2 and SUZ12. In accompaniment, these results suggest that both antibodies are suitable for immunoblots and may be used to probe the membrane during immunoprecipitation experiments. Despite this, it is important to note a slight difference in EZH2 levels between V-K562 cells and BASP1-K562 cells. This result was not reproducible, with the difference here possibly attributed to an uneven whole cell extract concentration between the two cell line samples. In addition, attention should be drawn to the non-specific immunoreactive band in Figure 8C, running slightly above 52kDa in the input V-K562 lane. Although this should not interfere with any SUZ12 blots, it is necessary to acknowledge this immunoreactive band due to its similarity in size to BASP1.

3.2 Optimisation of the ChIP protocol in K562 cells

Several previous studies from the lab have demonstrated that BASP1 induces the removal of H3K9ac marks at the promoters of WT1-target genes (Toska et al., 2012; Loats et al., 2021). A H3K9ac ChIP was performed as a positive control to ensure that the ChIP assay was working optimally. V-K562 cells (which contain WT1 but not BASP1) and BASP1-K562 cells (which contain both WT1 and BASP1) were subjected to ChIP analysis with either a control antibody (IgG) or H3K9ac antibody. Following DNA purification, presence of the H3K9ac mark was analysed using quantitative-PCR (qPCR). The promoter region of the WT1-target gene *AREG* was amplified using the corresponding primers, and results were normalised against the control promoter region of the *18S* ribosomal gene. H3K9ac is an active histone mark, and as a result it is expected that its levels are higher in the absence of BASP1.

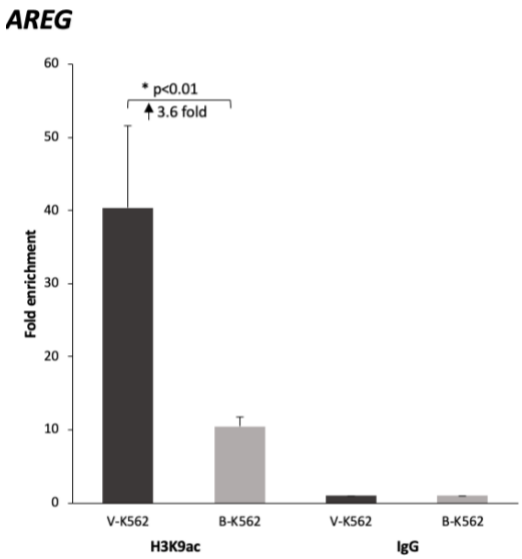

Figure 9. *BASP1 expression in K562 cells induces the removal of H3K9ac at the promoter of the WT1-target gene AREG.*
ChIP experiments were performed with V-K562 and BASP1-K562 cells using H3K9ac antibody normalised against control IgG antibody. The data showed H3K9ac enrichment in V-K562 cells at the promoter of the WT1-target gene, *AREG*, when compared to the promoter of the control gene, *18S*. Error bars are the standard deviation, where n=3. P-values were obtained from an unpaired Student's t-test, where * means p<0.05. P-values were p=0.01 for *AREG*.

Figure 9 displays a 3.6-fold increase in the active H3K9ac mark in V-K562 cells (40.38 ± 11.21) compared to the K562 cells that express BASP1 (10.4 ± 1.32) (n=3; unpaired Student's T-test, p=0.01). Hence, this datum confirmed previous results providing confidence that the ChIP experiments were working optimally.

3.3 Trimethylation of H3K27 is enriched during BASP1 expression

As mentioned previously, BASP1 has been shown to direct the trimethylation of H3K27, a repressive histone modification. It was therefore important to confirm a BASP1-dependent increase of H3K27me3 mark placement on histone tails at the promoters of WT1-target genes.

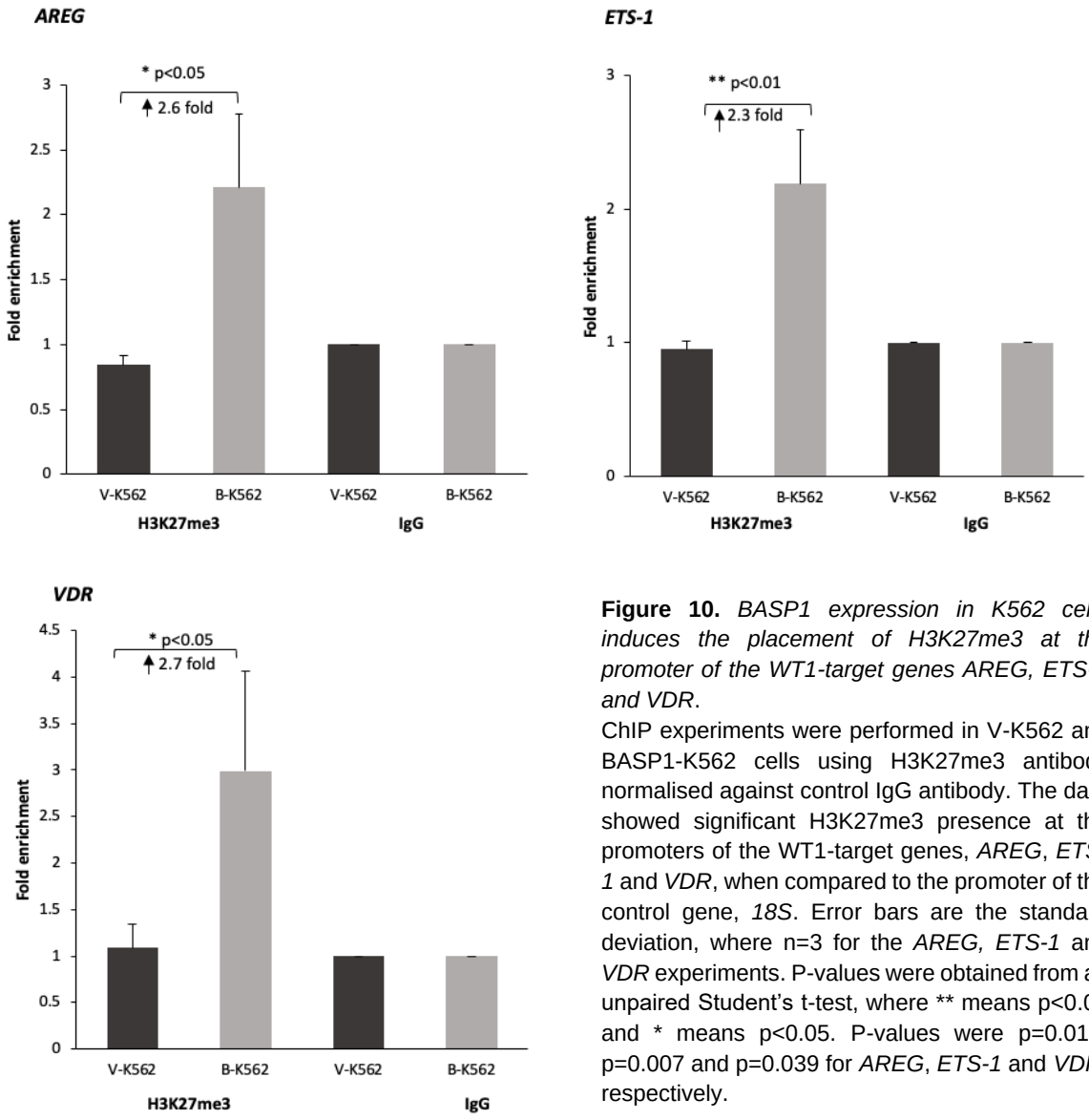

Figure 10. *BASP1 expression in K562 cells induces the placement of H3K27me3 at the promoter of the WT1-target genes AREG, ETS-1 and VDR*.
ChIP experiments were performed in V-K562 and BASP1-K562 cells using H3K27me3 antibody normalised against control IgG antibody. The data showed significant H3K27me3 presence at the promoters of the WT1-target genes, *AREG*, *ETS-1* and *VDR*, when compared to the promoter of the control gene, *18S*. Error bars are the standard deviation, where n=3 for the *AREG, ETS-1* and *VDR* experiments. P-values were obtained from an unpaired Student's t-test, where ** means p<0.01 and * means p<0.05. P-values were p=0.014, p=0.007 and p=0.039 for *AREG*, *ETS-1* and *VDR*, respectively.

An increase in the deposition of H3K27me3 marks at the promoter of the WT1-target genes *AREG, ETS-1* and *VDR* was observed in the presence of BASP1, as displayed in Figure 10. Here, data depicted a 2.6-fold increase in H3K27me3 enrichment in BASP1-K562 cells (2.21 ± 0.56) (unpaired t-test; p=0.014; n=3) at the *AREG* promoter compared to V-K562 cells (0.84 ± 0.07). The same was true at the *ETS-1* promoter which showed a 2.3-fold increase in BASP1-K562 cells (2.19 ± 0.41) (unpaired t-test; p=0.007; n=3) compared to V-K562s (0.95 ± 0.06). Consistent with these findings, the *VDR* promoter showed a 2.7-fold enrichment of H3K27me3 deposition in BASP1-K562 cells (2.99 ± 1.08) (unpaired t-test; p=0.008; n=3) compared to V-K562s (1.09 ± 0.25). These data display a correlation between H3K27me3 deposition and BASP1 expression in K562 cells.

3.4 PRC2 recruitment to WT1-target genes is BASP1-dependent

3.4.1 EZH2 is recruited to WT1-target gene promoters during BASP1 expression

Recent results from the laboratory demonstrated that BASP1 induces the recruitment of EZH2 to the promoter region of WT1-target genes (Dey, 2019). To confirm these findings, a different EZH2 antibody was used against the core catalytic component of the PRC2. Consistent with the previous data, BASP1 induced the recruitment of EZH2 to the promoter region of WT1-target genes when compared to the control IgG (Figure 11).

A significant 2.2-fold increase in EZH2 recruitment at the *AREG* promoter in the BASP1-K562 cell line (1.84 ± 0.35) compared to EZH2 presence at the same promoter in V-K562 cells (0.85 ± 0.13) (unpaired t-test; p=0.002; n=4) was observed. The same is true at the *ETS-1* promoter, where a 7.5-fold increase in EZH2 recruitment was found in the presence of BASP1 (1.83 ± 0.52) when compared to V-K562s (0.24 ± 0.52) (unpaired t-test; p=0.008; n=3). Finally, this trend was demonstrated at the *VDR* promoter, where BASP1-K562 cells (1.39 ± 0.27) saw increased enrichment of EZH2 compared to V-K562 cells (0.59 ± 0.19) (unpaired t-test; p=0.013; n=3). Taken together, these results indicate that BASP1 is involved in the recruitment of EZH2 to the promoters of WT1-target genes, suggesting a mechanism for the addition of the repressive mark H3K27me3 onto histone tails.

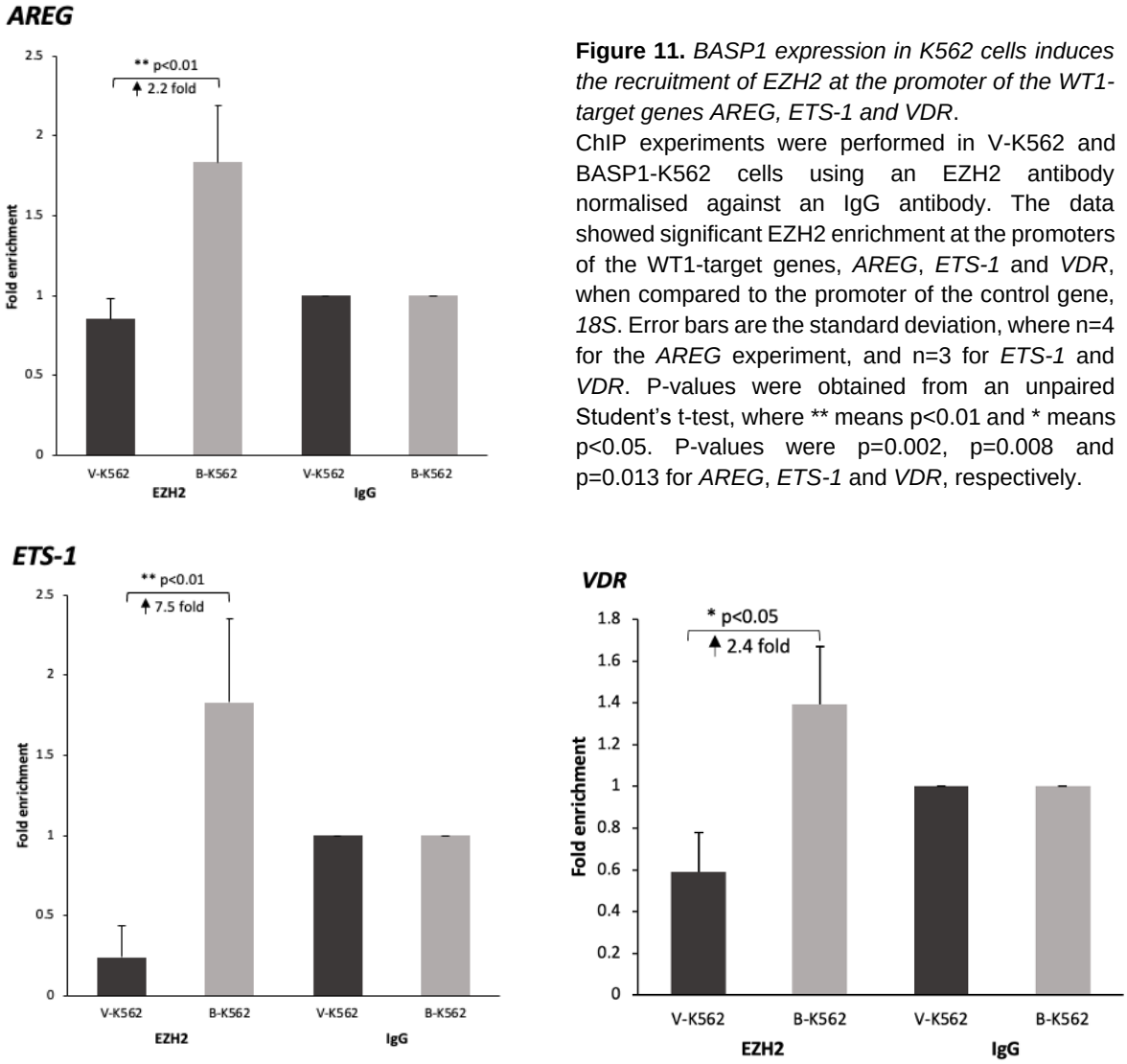

Figure 11. *BASP1 expression in K562 cells induces the recruitment of EZH2 at the promoter of the WT1-target genes AREG, ETS-1 and VDR*.
ChIP experiments were performed in V-K562 and BASP1-K562 cells using an EZH2 antibody normalised against an IgG antibody. The data showed significant EZH2 enrichment at the promoters of the WT1-target genes, *AREG*, *ETS-1* and *VDR*, when compared to the promoter of the control gene, *18S*. Error bars are the standard deviation, where n=4 for the *AREG* experiment, and n=3 for *ETS-1* and *VDR*. P-values were obtained from an unpaired Student's t-test, where ** means p<0.01 and * means p<0.05. P-values were p=0.002, p=0.008 and p=0.013 for *AREG*, *ETS-1* and *VDR*, respectively.

3.4.2 SUZ12 is recruited to WT1-target gene promoters during BASP1 expression

Previous studies have determined that EZH2 functions in concert with the other PRC2 core components – SUZ12 and EED (Li et al., 2019); and hence without these two proteins, EZH2 is unable to perform its role in deposition of the repressive trimethyl mark at H3K27. The potential recruitment of SUZ12 to WT1-target gene promoters alongside EZH2 was investigated using ChIP experiments. Figure 12 shows the significant relative fold enrichment of SUZ12 at *AREG*, *ETS-1* and *VDR* gene promoters in BASP1-K562 cells, compared to control V-K562 cells. This trend was evident at the *AREG* promoter, where BASP1-K562 cells (2.56 ± 0.64) saw a 1.9-fold enrichment of SUZ12 over V-K562 cells (1.36 ± 0.54) (unpaired t-test; p=0.01; n=5); the *ETS-1* promoter, where BASP1-K562 cells (1.79 ± 0.60) saw a 3.6-fold increase compared to V-K562s (0.50 ± 0.17) (unpaired t-test; p=0.02; n=3) and the *VDR* promoter, where a 2.3-fold increase in SUZ12 levels

was observed in BASP1-K562 cells (1.58 ± 0.21) compared to V-K562s (0.70 ± 0.22) (unpaired t-test; p=0.008; n=3).

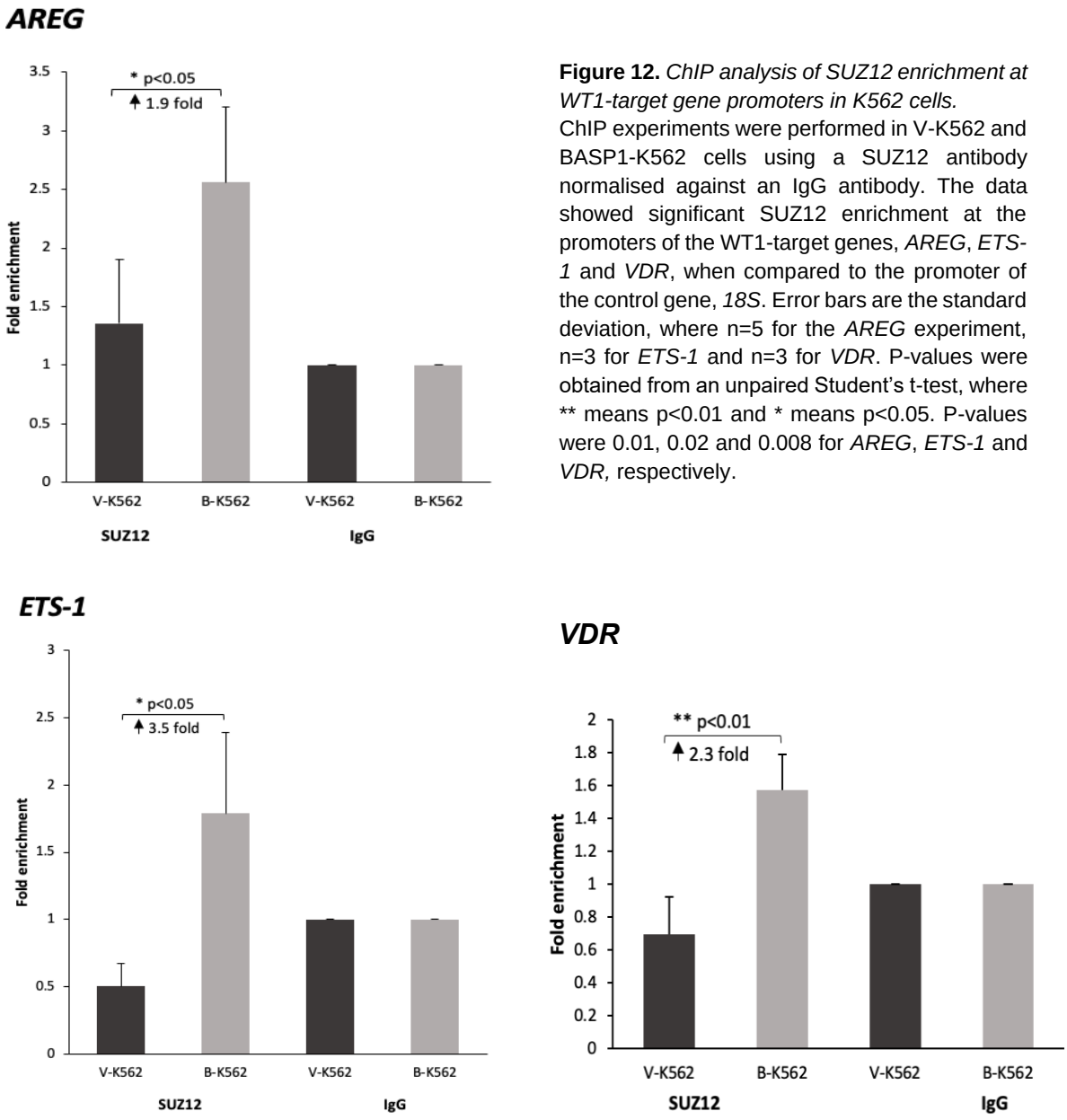

Figure 12. *ChIP analysis of SUZ12 enrichment at WT1-target gene promoters in K562 cells.*
ChIP experiments were performed in V-K562 and BASP1-K562 cells using a SUZ12 antibody normalised against an IgG antibody. The data showed significant SUZ12 enrichment at the promoters of the WT1-target genes, *AREG*, *ETS-1* and *VDR*, when compared to the promoter of the control gene, *18S*. Error bars are the standard deviation, where n=5 for the *AREG* experiment, n=3 for *ETS-1* and n=3 for *VDR*. P-values were obtained from an unpaired Student's t-test, where ** means p<0.01 and * means p<0.05. P-values were 0.01, 0.02 and 0.008 for *AREG*, *ETS-1* and *VDR,* respectively.

Taken together, the data in Figures 11 and 12 demonstrate that BASP1 is involved in the recruitment of both EZH2 and SUZ12 to WT1-target gene promoters. The data suggest that the intact PRC2 is recruited into the WT1/BASP1 complex to deposit trimethyl marks at H3K27 and thus, induce transcriptional repression. Whilst ChIP experiments are very useful in determining the presence of certain factors and complexes at target gene promoters, they are unable to distinguish direct interactions; and hence, it is unclear from this data whether BASP1 is able to bind to either EZH2 or SUZ12 in order to recruit them and induce gene repression, or whether this is an indirect mechanism. The data also leaves questions surrounding whether the PRC2 presence at promoters

of WT1-target genes is required for transcriptional repression, or whether its presence is coincidental.

3.5 PRC2 recruitment to WT1-target genes is lipid-independent

3.5.1 EZH2 recruitment is independent of BASP1 lipidation

Previous studies in the laboratory determined that the BASP1-mediated deposition of repressive marks, including H3K27me3, occurs in a lipid-independent manner (Dey, 2019). The current study used an EZH2 antibody to investigate whether EZH2 recruitment also occurs in a BASP1 lipidation-independent mechanism.

Figure 13 shows a significant fold enrichment of EZH2 recruitment at the WT1-target gene promoters *AREG*, *ETS-1* and *VDR* in both BASP1-K562 and G2A-K562 cells, compared to in V-K562 cells. Thus, implying that BASP1 recruits EZH2 independent of BASP1 lipidation. This trend was detected at the *AREG* promoter, where BASP1-K562s (8.37 ± 0.51) saw a 12.2-fold enrichment of EZH2 presence over V-K562s (0.68 ± 0.88) (unpaired t-test; p=0.0002; n=3); as well as G2A-K562s (2.69 ± 0.46), which saw a 3.9-fold enrichment of EZH2 recruitment over V-K562s (unpaired t-test; p=0.025; n=3). The same trend was observed at the *ETS-1* promoter, where BASP1-K562 cells (5.37 ± 1.14) saw a 6.0-fold increase compared to V-K562s (0.90 ± 0.41) (unpaired t-test; p=0.003; n=3); as well as G2A-K562s (4.84 ± 1.94), which saw a 5.4-fold enrichment of EZH2 recruitment over V-K562s (unpaired t-test; p=0.023; n=3). Also, this trend was demonstrated at the *VDR* promoter, where a 4.4-fold increase in EZH2 recruitment were observed in BASP1-K562 cells (3.66 ± 0.73) compared to V-K562s (0.83 ± 0.50) (unpaired t-test; p=0.0095; n=3). In accompaniment, G2A-K562 cells (1.90 ± 0.16) saw a 2.3-fold enrichment of EZH2 recruitment over V-K562s (unpaired t-test; p=0.025; n=3).

Although BASP1-G2A mutants recruit EZH2 over the background at the *AREG* and *VDR* promoters, the enrichment is reduced when compared to the wildtype BASP1 levels displayed in Figure 13.

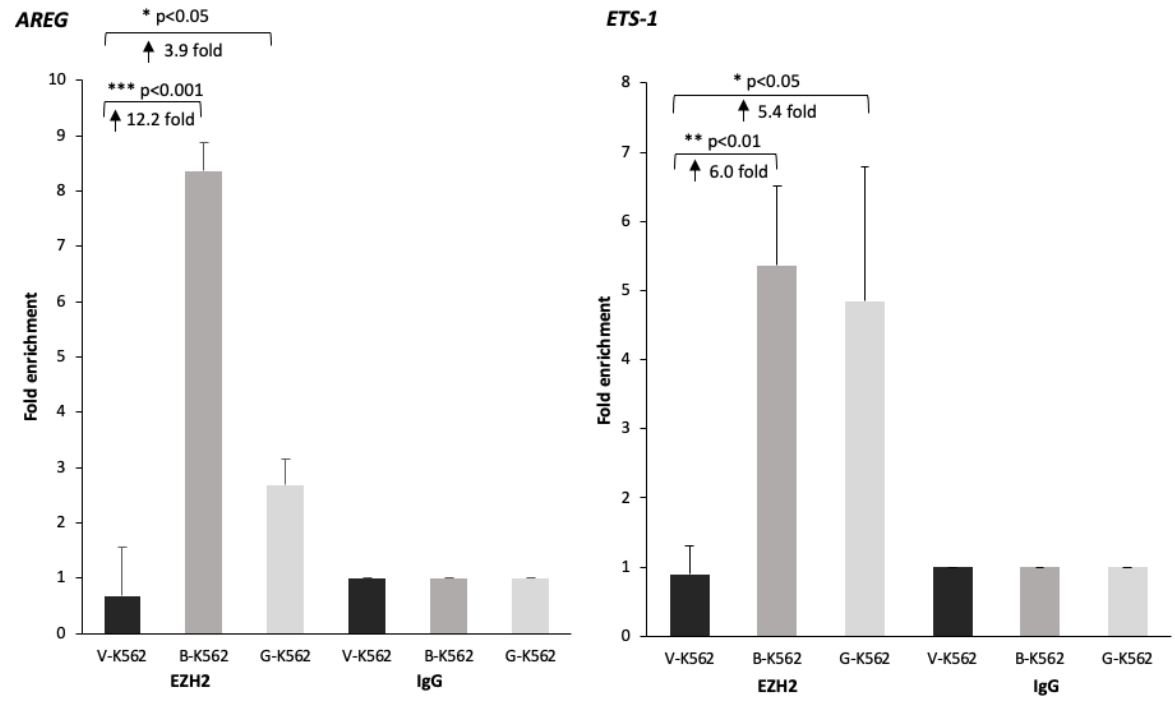

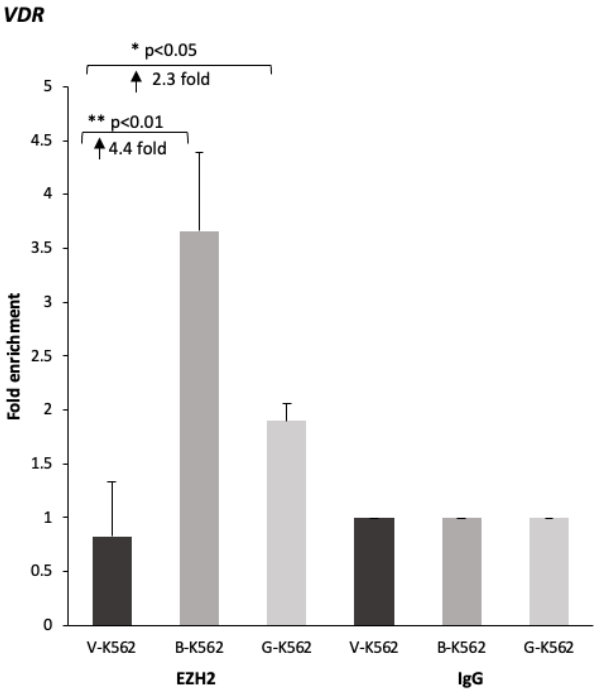

Figure 13. *ChIP analysis of EZH2 enrichment at WT1-target gene promoters in mutant K562 cells.* ChIP experiments were performed in V-K562, BASP1-K562 and G2A-K562 cells using an EZH2 antibody normalised against an IgG antibody. The data showed significant EZH2 enrichment at the promoters of the WT1-target genes, *AREG*, *ETS-1* and *VDR*, when compared to the promoter of the control gene, *18S*. Error bars are the standard deviation, where n=3 for experiments at all three promoters. P-values were obtained from an unpaired Student's t-test, where *** means p<0.001, ** means p<0.01 and * means p<0.05. P-values were 0.0002, 0.0030 and 0.0095 for *AREG*, *ETS-1* and *VDR,* respectively, when compared from BASP1-K562 results to V-K562 values. Additionally, P-values were 0.025, 0.023 and 0.025 for *AREG*, *ETS-1* and *VDR,* respectively, when compared from G2A-K562 results to V-K562 values.

3.5.2 SUZ12 recruitment is independent of BASP1 lipidation

Previous work had not investigated whether the recruitment of SUZ12 and thus the intact PRC2 is also a lipid-independent mechanism. Figure 14 shows significant relative fold enrichment of SUZ12 at *AREG*, *ETS-1* and *VDR* gene promoters in both BASP1-K562 and G2A-K562 cells, compared to in V-K562 cells. The results demonstrate that BASP1 recruits SUZ12 independent of the myristoyl group at glycine-2 on BASP1. This trend was detected at the *AREG* promoter, where BASP1-K562s (1.82 ± 0.35) saw a 1.9-fold enrichment of SUZ12 presence over V-K562s (0.29 ± 0.13) (unpaired t-test; p=0.0002; n=5); as well as G2A-K562s (3.26 ± 0.71), which saw a 11.4-fold enrichment of SUZ12 recruitment over V-K562s (unpaired t-test; p=0.0002; n=5). The same trend was observed at the *ETS-1* promoter, where BASP1-K562 cells (2.23 ± 0.29) saw a 4.8-fold increase compared to V-K562s (0.46 ± 0.25) (unpaired t-test; p=0.0001; n=5); as well as G2A-

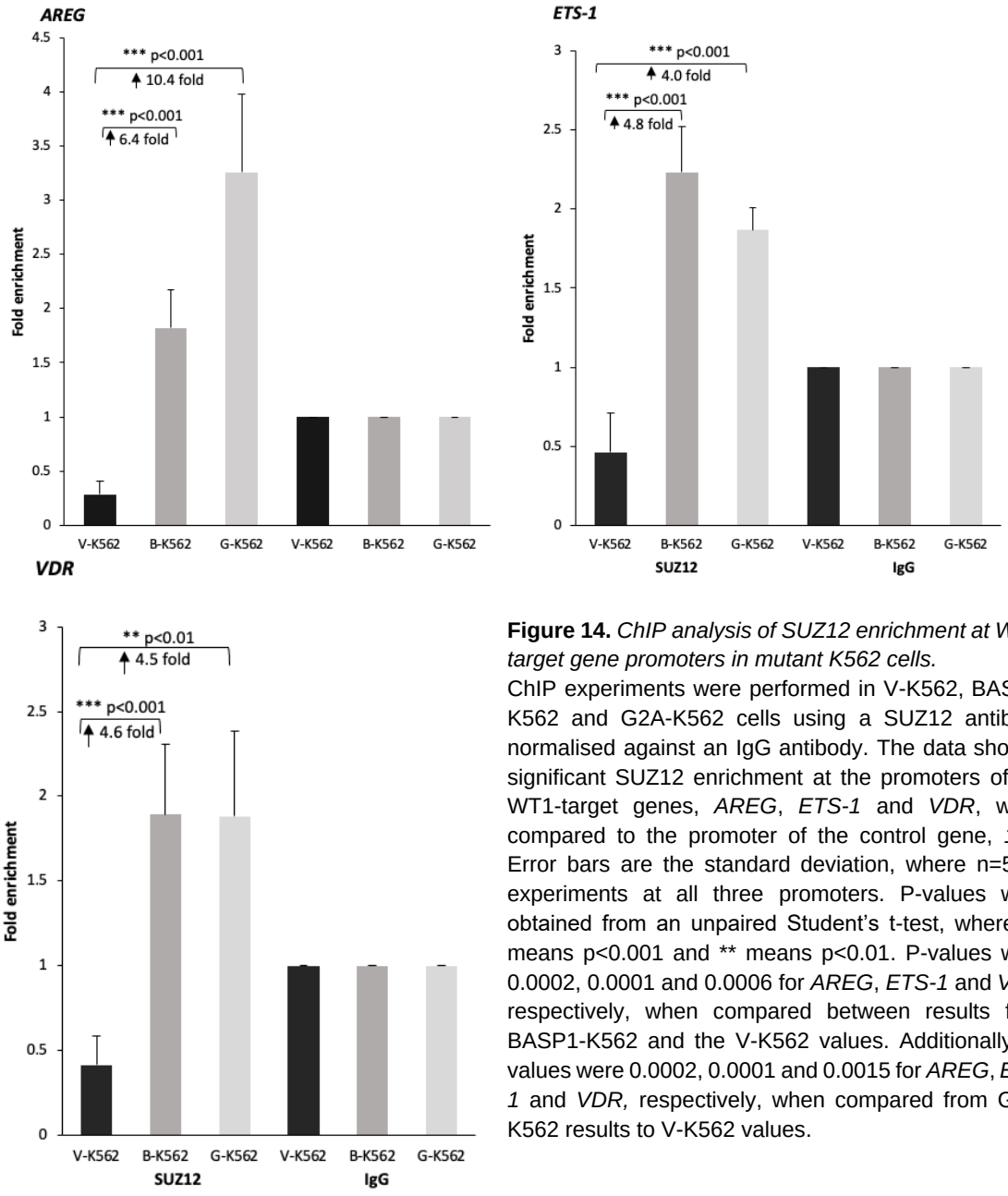

Figure 14. *ChIP analysis of SUZ12 enrichment at WT1-target gene promoters in mutant K562 cells.*
ChIP experiments were performed in V-K562, BASP1-K562 and G2A-K562 cells using a SUZ12 antibody normalised against an IgG antibody. The data showed significant SUZ12 enrichment at the promoters of the WT1-target genes, *AREG*, *ETS-1* and *VDR*, when compared to the promoter of the control gene, *18S*. Error bars are the standard deviation, where n=5 for experiments at all three promoters. P-values were obtained from an unpaired Student's t-test, where *** means p<0.001 and ** means p<0.01. P-values were 0.0002, 0.0001 and 0.0006 for *AREG*, *ETS-1* and *VDR,* respectively, when compared between results from BASP1-K562 and the V-K562 values. Additionally, P-values were 0.0002, 0.0001 and 0.0015 for *AREG*, *ETS-1* and *VDR,* respectively, when compared from G2A-K562 results to V-K562 values.

K562s (4.04 ± 0.14), which saw a 4.0-fold enrichment of SUZ12 recruitment over V-K562s (unpaired t-test; p=0.0001; n=5). Finally, this trend was also demonstrated at the *VDR* promoter, where a 4.6-fold increase in SUZ12 recruitment were observed in BASP1-K562 cells (1.89 ± 0.41) compared to V-K562s (0.42 ± 0.17) (unpaired t-test; p=0.0006; n=5). In accompaniment, G2A-K562 cells (1.88 ± 0.50) saw a 4.5-fold enrichment of SUZ12 recruitment over V-K562s (unpaired t-test; p=0.0015; n=5). These findings further suggested that the myristoyl group on BASP1 is not necessary for the recruitment of the PRC2 components and hence, deposition of repressive histone marks at the WT1-target gene promoters investigated.

3.6 MCF7 cells endogenously express BASP1 and EZH2

MCF7 cells were used to validate previous results and extend the study, as they allowed for a robust comparison between the ectopically BASP1-expressing K562 cells and the endogenously BASP1-expressing MCF7 cells.

MCF7 cells endogenously express both BASP1 and EZH2 proteins, as confirmed using Western blotting (Figure 15). Figure 15A demonstrates a strong band migrating at 52kDa in the whole cell extract from both cell lines consistent with the migration of BASP1. Figure 15A shows a higher level of BASP1 in BASP1-K562 cells, which is as expected considering that the protein expression is engineered within this cell line, as opposed to endogenous expression of BASP1 in the MCF7 cells.

In contrast, EZH2 levels are observed to be similar in both cell lines, with a band migrating at 102kDa in both cell lines, consistent with the molecular weight of EZH2. This is expected as the EZH2 protein is endogenously expressed in both BASP1-K562 cells and MCF7 cells. Such results were important to confirm before embarking on RNA interference experiments.

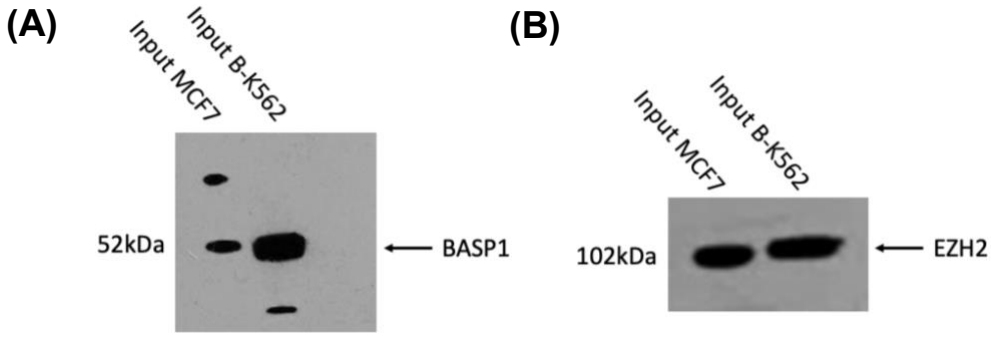

Figure 15. *Immunoblot analyses of whole cell extract in MCF7 cells.*
A) A Western blot experiment was performed with BASP1-K562 and MCF7 whole cell extract and probed with BASP1 antibody. The data showed bands at 52kDa in both cell lines.
B) BASP1-K562 and MCF7 whole cell extract was probed with EZH2 antibody. Bands were observed at 102kDa, as observed in both cell lines.

3.7 EZH2 mediates BASP1-dependent transcriptional repression of WT1 target genes

The physiological role of EZH2 at WT1-target gene promoters was investigated using RNA interference analysis. MCF7 cells were transiently transfected individually or with combinations of a control siRNA, siRNA targeting BASP1 or siRNA targeting EZH2. Forty-eight hours later, total RNA was isolated and cDNA was prepared. qPCR was used to analyse the relative expression of the WT1-target genes *AREG* and *VDR* during the knockdown of EZH2 and BASP1 compared to *GAPDH* control levels. In parallel, whole cell extracts were prepared and used in immunoblots to determine the levels of BASP1 and EZH2.

3.7.1 EZH2 siRNA 1 demonstrates a physiological role for EZH2 at WT1-target gene promoters

A significant increase in WT1-target gene expression during knockdown of both BASP1 and EZH2 was observed in MCF7 cells. This suggests a functionally relevant role of EZH2 at both WT1-target gene promoters, *AREG* and *VDR*.

Figure 16 shows a significant increase in relative expression of *AREG* and *VDR* during knockdown of either or both EZH2 and BASP1, where the control knockdown is normalised to a relative expression of 1. Knockdown of endogenous BASP1 in MCF7 cells led to increased expression of the WT1-target genes *AREG* (3.1-fold ± 0.54) (one-way ANOVA with Tukey's test; p=0.001; n=3) and *VDR* (3.1-fold ± 0.80) (one-way ANOVA with Tukey's test; p=0.003; n=3) compared to the control siRNA. Transfection of siRNA targeting EZH2 similarly increased *AREG* (3.8-fold ± 0.34) (one-way ANOVA with Tukey's test; p=0.001; n=3) and *VDR* (3.2-fold ± 0.20) (one-way ANOVA with Tukey's test; p=0.004; n=3) mRNA. Thus, both BASP1 and EZH2 act as transcriptional repressors of *AREG* and *VDR* in MCF7 cells. When MCF7 cells were transfected with a combination of EZH2 and BASP1 siRNAs, there was only a small further increase in *AREG* (1.1-fold) and no increase in *VDR* (1.0-fold) expression when compared to EZH2 or BASP1 siRNA alone, with no significant differences observed between either single or double knockdown of EZH2 and BASP1, with this observation made across both the *AREG* and *VDR* genes. These data suggest that BASP1 and EZH2 likely act together on the same pathway to mediate transcriptional repression of *AREG* and *VDR*.

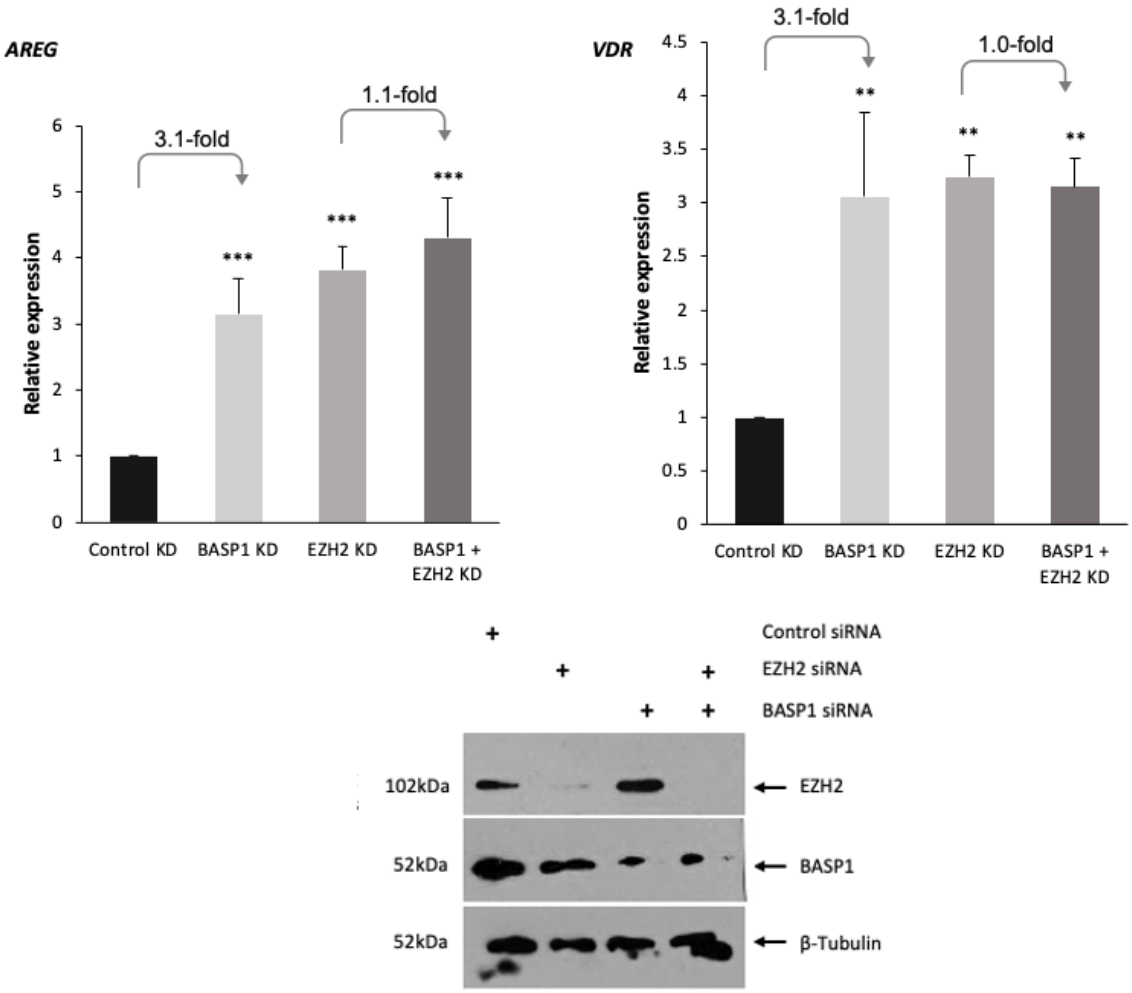

Figure 16. *Relative expression of WT1-target genes following RNA interference in MCF7 cells, with EZH2 siRNA 1.* siRNA-mediated knockdown of BASP1 and EZH2 in MCF7 cells caused a significant increase in relative expression of the WT1-target genes *AREG* and *VDR*, when compared to control siRNA relative expression. Error bars are the standard deviation, where n=3 for experiments for both genes. P-values were obtained from a one-way ANOVA with Tukey's post-hoc test, where *** means p<0.001, ** means p<0.01 and * means p<0.05. P-values were all 0.001 for BASP1 KD, EZH2 KD and BASP1 + EZH2 KD at the *AREG* gene, when compared to control KD levels. Whereas p-values were 0.003, 0.004 and 0.005, respectively, for *VDR.* When results were compared between the BASP1 KD, EZH2 KD and BASP1 + EZH2 KD groups, no significant differences were detected at either promoter (0.31 (*AREG*) and 0.99 (*VDR*) for BASP1 KD compared to EZH2 KD, 0.05 (*AREG*) and 0.94 (*VDR*) for BASP1 KD to BASP1 + EZH2 KD, and 0.55 (*AREG*) and 0.99 (*VDR*) for EZH2 KD to BASP1 + EZH2 KD).
Below, whole-cell extracts were prepared following siRNA transfection and an immunoblot was performed. The immunoblot was probed with either an EZH2 (top), BASP1 (middle) and β-tubulin (bottom) antibody.

3.7.2 EZH2 siRNA 2 produced comparable results for EZH2 at WT1-target gene promoters

Similar experiments using a second siRNA targeting EZH2 knockdown produced comparable results to those seen in Figure 16. Thus, demonstrating that knockdown of EZH2 abolishes BASP1-mediated repression of WT1-target genes (Figure 17).

Figure 17 demonstrates a significant increase in expression of the *AREG* promoter during knockdown of endogenous BASP1 (3.1 ± 0.51) (one-way ANOVA with Tukey's test; p=0.001; n=3) compared to baseline *AREG* expression, with the same trend observed at the *VDR* promoter (2.6

± 0.69) (one-way ANOVA with Tukey's test; p=0.016; n=3). EZH2-targeted knockdown also produced similar results at both the *AREG* (2.4 ± 0.59) (one-way ANOVA with Tukey's test; p=0.014; n=3) and *VDR* (3.1 ± 0.42) (one-way ANOVA with Tukey's test; p=0.004; n=3) promoters, when compared to the control baseline level of expression. Consequently, these data confirm the role of EZH2 as a transcriptional repressor of the WT1-target genes *AREG* and *VDR*. When the cells were double transfected with siRNAs targeting BASP1 and EZH2, again only a small increase in both *AREG* (1.1-fold) and *VDR* (1.2-fold) expression was observed, when compared to EZH2 siRNA alone, with no significant differences observed between either single or double knockdown of EZH2 and BASP1, as witnessed across both the *AREG* and *VDR* genes. Once again, these data indicate that BASP1 and EZH2 likely work collectively through the same epigenetic pathway. It should be noted that immunoblotting revealed a more modest level of EZH2 knockdown by the second siRNA compared to that observed with the first siRNA.

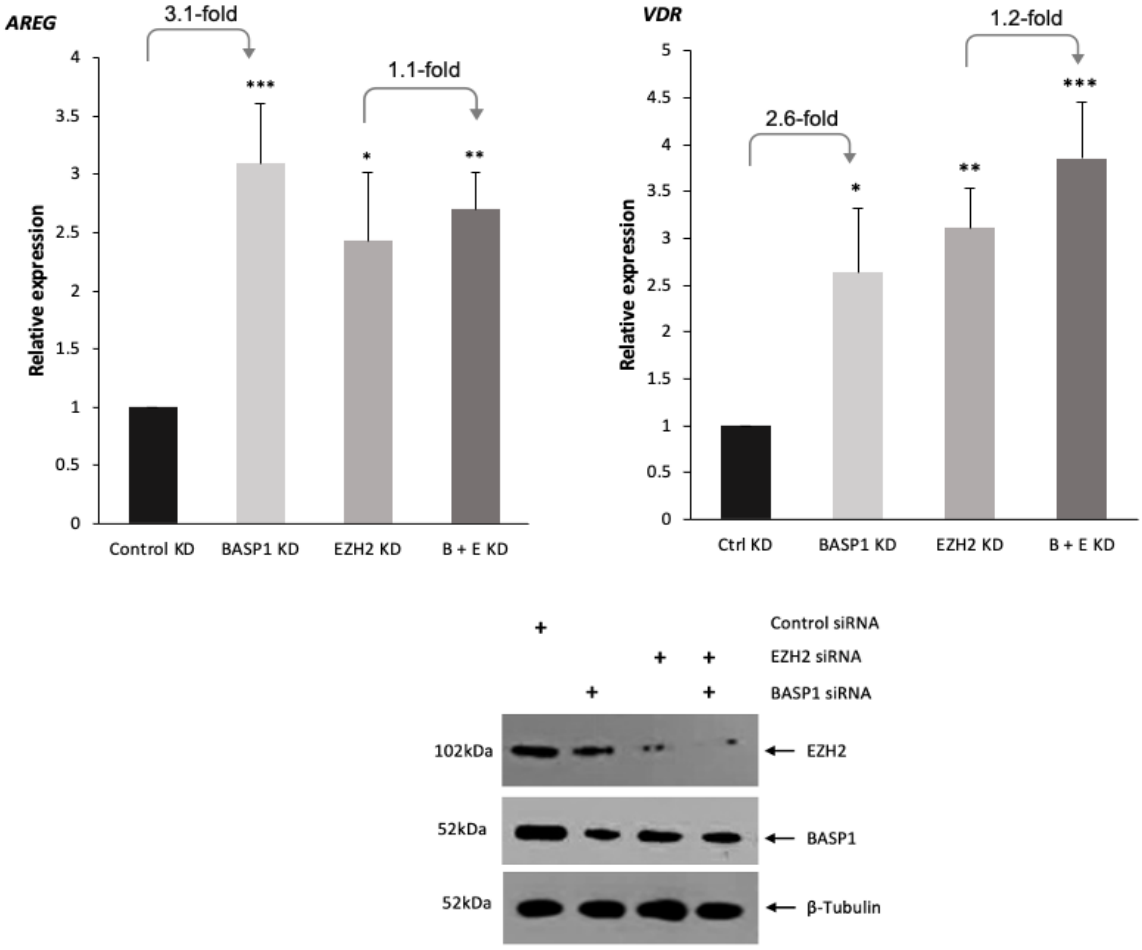

Figure 17. *Relative expression of WT1-target genes following RNA interference in MCF7 cells, with EZH2 siRNA 2.* The genes BASP1 and EZH2 were knocked down in MCF7 cells, causing a significant increase in relative expression of the WT1-target genes *AREG* and *VDR*, when compared to control siRNA relative expression. Error bars are the standard deviation, where n=3 for experiments for both genes. P-values were obtained from a one-way ANOVA with Tukey's post-hoc test, where *** means p<0.001, ** means p<0.01 and * means p<0.05. P-values were 0.001 for BASP1 KD, 0.01 for EZH2 KD and 0.005 for BASP1 + EZH2 KD at the *AREG* gene, when compared to control KD levels. Whereas p-values were 0.016, 0.004 and 0.001, respectively, for *VDR.* When results were compared between the BASP1 KD, EZH2 KD and BASP1 + EZH2 KD groups, no significant differences were detected (0.29 (*AREG*) and 0.67 (*VDR*) for BASP1 KD compared to EZH2 KD, 0.68 (*AREG*) and 0.07 (*VDR*) for BASP1 KD to BASP1 + EZH2 KD, and 0.86 (*AREG*) and 0.32 (*VDR*) for EZH2 KD to BASP1 + EZH2 KD).
Below, whole-cell extracts were prepared following siRNA transfection and an immunoblot was performed. The immunoblot was probed with either an EZH2 (top), BASP1 (middle) and β-tubulin (bottom) antibody.

3.8 EZH2 mediates H3K27me3 deposition at WT1-target genes

The above RNAi experiments suggested that BASP1 likely functions in concert with EZH2 to repress transcription of WT1-target genes. To investigate whether the deposition of trimethylation marks at H3K27 at WT1-target gene promoters was EZH2-dependent, MCF7 cells were transfected with siRNA targeting the knockdown of either EZH2 or BASP1, independently or combined. The cells were used in a ChIP experiment to assess whether BASP1-dependent H3K27me3 marks were depleted upon knockdown of EZH2 (Figure 18).

The results displayed in Figure 18 showed a significant decrease in H3K27me3 mark deposition after knockdown of BASP1 and EZH2, both independently and combined, when compared to the baseline H3K27me3 level seen at WT1-target genes in MCF7 cells transfected with only control siRNA. A 2.6-fold decrease in H3K27me3 enrichment was observed during the knockdown of BASP1 at the *AREG* gene promoter (from 3.23 ± 0.37 to 1.25 ± 0.18) (unpaired t-test; p=0.001; n=3), whilst this was a 2.2-fold enrichment decrease at the *ETS-1* gene promoter (from 4.12 ± 0.37 to 0.88 ± 0.32) (unpaired t-test; p=0.0003; n=3). A similar trend was observed during EZH2 knockdown, which saw a 3.1-fold significant decrease in H3K27me3 enrichment at the *AREG* promoter (1.04 ± 0.63) (unpaired t-test; p=0.0003; n=3), and a 3.0-fold decrease at the *ETS-1* promoter (1.30 ± 0.41) (unpaired t-test; p=0.0009; n=3). Finally, a combination of BASP1 and EZH2 knockdown resulted in a further 4.0-fold significant decrease in H3K27me3 marks (0.80 ± 0.40) (unpaired t-test; p=0.0016; n=3) at the *AREG* promoter. This was also observed at the *ETS-1* promoter (3.3-fold change; 1.30 ± 0.62) (unpaired t-test; p=0.0027; n=3).

This data indicates that BASP1 and EZH2 work in conjunction to trimethylate H3K27 at the two WT1-target genes shown here. The data shows no significant difference between H3K27me3 mark deposition during BASP1 and EZH2 knockdown independently, compared to H3K27me3 mark enrichment during double BASP1 and EZH2 knockdown at the promoters. This again suggests that BASP1 and EZH2 work along the same epigenetic pathway to mediate the trimethylation of H3K27.

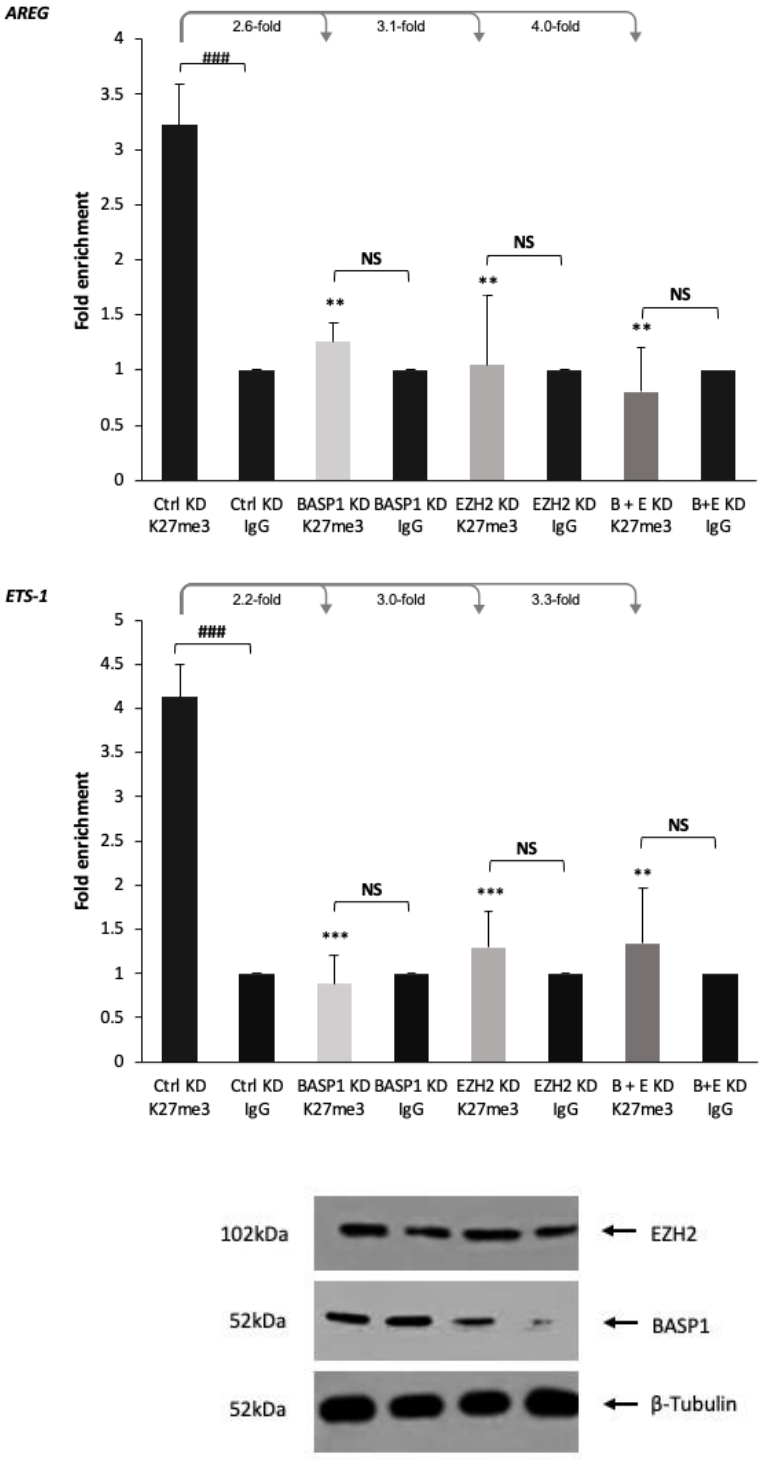

Figure 18. *Fold enrichment of H3K27me3 marks at WT1-target gene promoters during knockdown of BASP1/EZH2 in MCF7 cells.*

MCF7 cells were transfected with appropriate siRNA targeting BASP1 and EZH2, either independently or combined. These cells were used in ChIP experiments. A significant decrease in H3K27me3 fold enrichment at the WT1-target genes *AREG* and *ETS-1* was observed when compared to control baseline level. Error bars are the standard deviation, where n=3 for experiments at both genes. P-values were obtained from an unpaired Student's t-test, where *** means $p<0.001$ and ** means $p<0.01$ when compared to the control KD K27me3 level. ### means $p<0.001$ and NS means non-significant when values were compared within the bracketed area. P-values (*) were 0.0012, 0.0069 and 0.0016 for BASP1 KD, EZH2 KD and BASP1 + EZH2 KD, respectively, at the *AREG* gene compared to control levels; whilst the p-values (#) were 0.0005, 0.067, 0.91 and 0.44 for control KD, BASP1 KD, EZH2 KD and BASP1 + EZH2 KD compared to IgG. P-values (*) were 0.0003, 0.0009 and 0.0027, for BASP1 KD, EZH2 KD and BASP1 + EZH2 KD respectively compared to control knockdown of K27me3 for *ETS-1*; whilst the p-values (#) were 0.0001, 0.78, 0.28 and 0.39 for control KD, BASP1 KD, EZH2 KD and BASP1 + EZH2 KD compared to their respective IgG level.

Whole-cell extracts were prepared following siRNA transfection and ran on an immunoblot. The immunoblot was probed with either EZH2 (top), BASP1 (middle) and β-tubulin (bottom) antibody.

3.9 Analysis of potential interaction between PRC2 components and BASP1

The results presented above suggest that BASP1 works in concert with PRC2 to direct the trimethylation of H3K27. Immunoprecipitation (IP) experiments were used to uncover whether the WT1/BASP1 complex and PRC2 interact. Past studies in the laboratory failed to confirm an interaction between EZH2 and BASP1 using co-immunoprecipitation (co-IP) experiments prepared from nuclear extract samples. In this study, numerous different approaches were taken to optimise the experimental protocol to determine if there is an interaction between BASP1 and either EZH2 or SUZ12.

SUZ12 IPs were probed with BASP1 or the HA-tag antibody in attempt to show an interaction. Whole cell extract was prepared from B-K562 cells and used in an immunoprecipitation experiment with either SUZ12 antibodies or a control rabbit antibody (Figure 19A). The immunoprecipitates were resolved by SDS-PAGE alongside control input B-K562 nuclear extract and then probed with HA-tag antibodies. HA-tagged BASP1 was not detected in the SUZ12 immunoprecipitate.

The same experimental procedure was followed in Figure 19B, but the immunoblot was instead probed with a rabbit BASP1 antibody. Again, BASP1 was not detected in the SUZ12 immunoprecipitate. It is interesting to note the faster migrating band observed in the SUZ12 IP lane. It was questioned whether this was in fact a co-immunoprecipitation which had resolved aberrantly during electrophoresis due to the action of the magnetic beads used in the immunoprecipitation preparation. This idea was ruled out by Figure 19C, in which the SUZ12 IP was ran alongside a SUZ12 IP prepared in the absence of whole cell extract. The same faster-migrating band was seen in the absence of whole cell extract, indicating that the band is likely to be the SUZ12 antibody heavy chain.

Following unsuccessful attempts at co-immunoprecipitating SUZ12 with BASP1, a co-immunoprecipitation with EZH2 was performed. Here, B-K562 whole cell extract was prepared, and a co-IP experiment was attempted with either EZH2 antibodies or a control rabbit antibody which was probed with BASP1 antibody (Figure 19D). Figure 19D shows that an interaction between BASP1 and EZH2 was not successfully detected when using BASP1-K562 whole cell extract. Thus, as this study failed to demonstrate an interaction between BASP1 and PRC2 in B-K562 cells, it is unclear whether the PRC2 is recruited into the WT1/BASP1 complex or whether the action of the PRC2 in trimethylation of H3K27 at WT1-target genes promoters is triggered by a different event.

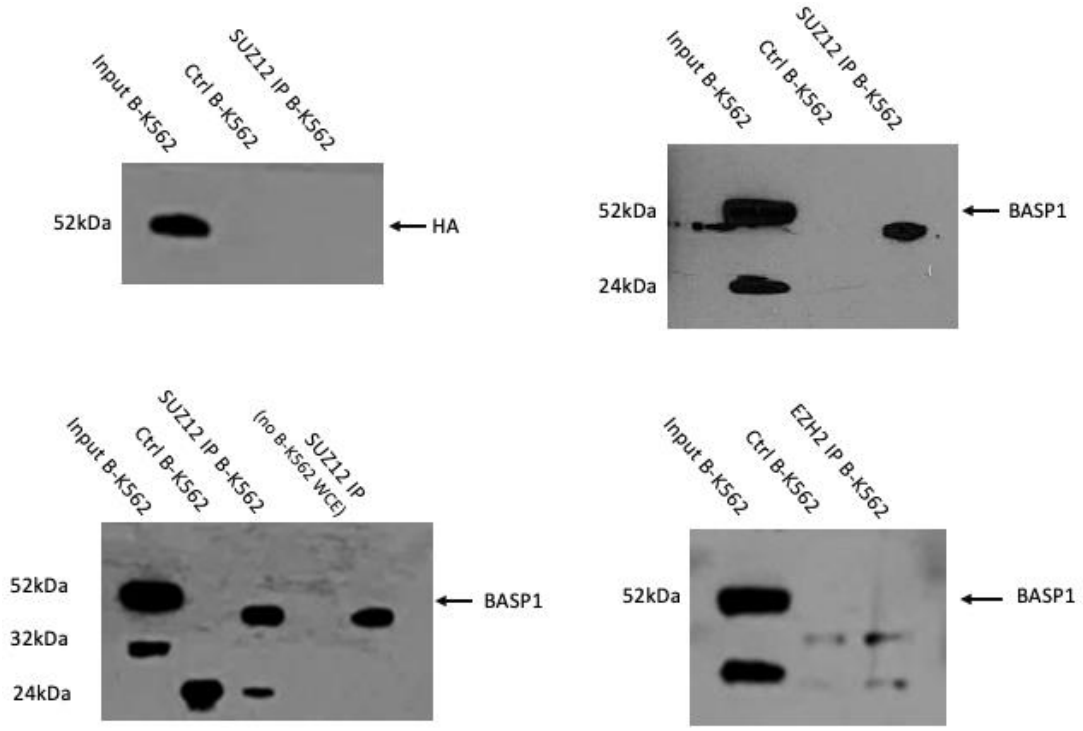

Figure 19. *Immunoblot analyses of SUZ12/EZH2 IP with BASP1/HA-tag probe in BASP1-K562 cells.*
A) A Western blot experiment was performed and probed with a BASP1 antibody. The data showed a band at 52kDa in the BASP1-K562 input lane. No band was observed in the negative control lane, and a band running slightly lower than 52kDa was seen in the SUZ12 IP BASP1-K562 lane.
B) Western blot probed with HA-tag antibody. A band at 52kDa was seen in the input BASP1-K562 lane, whereas no bands were seen in the control IP or SUZ12 IP lanes.
C) A Western blot analysis probed with BASP1 showed a band at 52kDa in the input BASP1-K562 lane. A non-specific band was observed at 24kDa in the control IP lane. The SUZ12 IP BASP1-K562 lane and SUZ12 IP with no BASP1-K562 WCE both showed a band running slightly lower than 52kDa.
D) A Western blot experiment was probed with a BASP1 antibody. The data showed a band at 52kDa in the BASP1-K562 input lane. No band was observed in the negative control lane or in the EZH2 IP BASP1-K562 lane.

4. Discussion

This study explored the role of the PRC2 in BASP1-mediated transcriptional repression of WT1-target genes. This is an extension of the work performed by Dey (2019) and Johnson (2019) in K562 and MCF7 cells. These two previous studies investigated the potential role of EZH2 in depositing H3K27me3 marks at histone tails using ChIP experiments and inhibitor assays. The present study aimed to confirm and extend previous work, including other interaction partners and whether PRC2 recruitment to WT1-target gene promoters has direct functional relevance.

4.1 Characterisation of stable cell lines

Immunoblotting techniques were used to investigate the expression levels of BASP1, EZH2 and SUZ12 in K562 and MCF7 cell lines. It was demonstrated that both BASP1-K562 and G2A-K562 cells expressed high levels of BASP1, whereas V-K562 cells did not express this protein. This finding was important when moving onto ChIP experiments, as it confirmed the V-K562 cells as a suitable control. Despite this, immunoblotting alone cannot confirm that the G2A-K562 cells express the mutant BASP1. However, other studies in the laboratory at the same time using RNA-seq have confirmed that the G2A-K562 cells express the BASP1-G2A mutant derivative (Alexander Moorhouse, personal communication).

All the K562 cell line derivatives were observed to express similar levels of EZH2 and SUZ12. Consequently, the fundamental difference between these two cell lines is the presence or absence of BASP1. Any changes observed in EZH2/SUZ12 recruitment to gene promoters in ChIP experiments between the different cell types suggests a BASP1-mediated mechanism.

MCF7 cells were shown to endogenously express both BASP1 and EZH2. This was important to allow for targeted knockdown of the appropriate protein independently during RNA interference. Studies using the MCF7 cells confirmed results collected using K562 cells, whilst also extending the relevance of the findings into the repressive function of endogenously expressed BASP1.

4.2 BASP1 mediates PRC2 recruitment to WT1-target gene promoters.

A significant increase in H3K27me3 deposition at the WT1-target gene promoters *AREG, ETS-1* and *VDR* was demonstrated in the presence of BASP1 compared to control cells that lack BASP1. This confirms previous experimental data from the lab (Dey, 2019; Johnson, 2019), which taken together suggests that the mechanism by which H3K27me3 marks are deposited at the promoters of WT1-target genes is stimulated by BASP1. Yet, further ChIP experiments were necessary to investigate which factors were shown to be significantly enriched at WT1-target genes in BASP1-K562 cells.

Data collected in the current study supports previous research that EZH2 presence is significantly enriched at WT1-target gene promoters in BASP1-expressing cells. Although this finding used a different EZH2 antibody to demonstrate BASP1-associated EZH2 recruitment, it is not conclusive evidence that the intact PRC2 complex is recruited. Further research was required to confirm the recruitment of the intact PRC2 at the promoters of WT1-target genes in the presence of BASP1.

ChIP experiments showed that SUZ12 was recruited along with EZH2 to the promoter region of WT1-target genes. This finding provides evidence which supports the hypothesis that the canonical PRC2 complex is recruited to promoter regions of WT1-target genes in a BASP1-dependent manner. Thus, it is possible that a mechanism involving both the WT1/BASP1 complex and PRC2 can cumulatively deposit H3K27me3 marks, leading to transcriptional repression. In addition, the data adds to previous knowledge that EZH2 lacks stability to work as a methyltransferase enzyme independently of SUZ12; and thus, the intact PRC2, also containing EED, is likely recruited to regulate this epigenetic mechanism.

Furthermore, the WT1/BASP1 complex and PRC2 share roles in establishing and maintaining cellular differentiation. Therefore, it is possible that these two complexes work synergistically to promote differentiation through the repression of WT1-target genes. Section 1.4 previously discussed both *in vitro* and *in vivo* experimental details which associated the WT1-BASP1 complex with cellular differentiation in the leukaemic cell line K562 and in taste receptor cells; and in cellular reprogramming in iPSCs using the OSKM cocktail. Similar studies have been undertaken in linking the PRC2 to extensive epigenetic reprogramming in mouse germ cells (Prokopuk et al., 2017).

Consequently, the shared role of the WT1/BASP1 complex and PRC2 in differentiation is consistent with their cooperation at WT1-target genes.

4.3 BASP1-mediated recruitment of PRC2 is independent of BASP1-myristoylation

The use of G2A-K562 mutant cells, in which glycine-2 of BASP1 is mutated to alanine and thereby prevents N-terminal myristoylation, showed that EZH2 and SUZ12 recruitment by BASP1 is lipidation-independent. This finding supports previous data which suggests that BASP1 functions via both lipid-dependent and lipid-independent mechanisms when acting as a co-repressor of WT1 (Dey, 2019). Thus, it can be construed that PRC2 recruitment is not reliant on the BASP1-PIP_2 or BASP1-cholesterol interactions. Although both EZH2 and SUZ12 showed significant lipid-independent recruitment across all three genes, the level of EZH2 recruitment at the *AREG* and *VDR* promoters in G2A-K562 cells were not as distinct as previous data collected in the lab (Dey, 2019) or the data collected from the SUZ12 ChIPs. The SUZ12 ChIP data in this study suggest the significant presence of the PRC2 in a lipid-independent manner, and thus this implies that the EZH2 ChIPs lack robustness, rather than the mechanism of EZH2 recruitment being a less lipid-independent mechanism than previously hypothesised.

The data suggest that the recruitment of the PRC2 to WT1-target gene promoters does not occur within the nuclear matrix but rather within the peripheral nucleoplasm. Past research in the lab showed that both myristoylated and non-myristoylated forms of BASP1 protein localise to the chromatin fractions within the nucleus, but only myristoylated-BASP1 is able to interact with the nuclear matrix, which includes the inner nuclear membrane (INM) (Dey, 2019). Hence, it does not appear necessary for factors associated with the deposition of BASP1-mediated repressive histone modifications to interact with INM components, such as emerin. Yet, it is important to confirm the exact localisation of the PRC2 at WT1-target gene promoters, and its potential interaction with non-INM components. Heterochromatin is often located at the nuclear periphery (Fišerová et al., 2017; Holla et al., 2020), and as a result the PRC2 has a well-defined role here too, as demonstrated in the downregulation of the *Msx1* target genes, which are important in myoblast differentiation (Wang et al., 2011). Past studies have also displayed how YY1, another PRC2 interaction partner, interacts with PRC2 at the nuclear periphery to regulate development and differentiation (Harr et al., 2015). Hence, it seems plausible that BASP1 could act via a similar mechanism. It is noteworthy that both BASP1 (Santiago et al., 2021) and PRC2 (Harr et al., 2015) have been shown to interact with YY1 to regulate differentiation events. Despite these findings, questions surround the significance of the lipid-independent mechanism by which BASP1 recruits factors associated with the addition of repressive components.

Past studies have demonstrated how mimicking serine-6 phosphorylation of BASP1 by inducing a S6D mutation can introduce a negative charge which destabilises the myristoyl group's ability to interact with other hydrophobic regions, which may influence membrane attachment (Toska et al., 2012). *In vivo* studies have proposed that PKC phosphorylates S6 of BASP1 (Mosevitsky et al., 1997). In the phosphorylated state of BASP1, it is likely that only lipid-independent mechanisms of BASP1 action will be possible; and thus, this provides potentially another level of complexity to the intricate mechanism as BASP1 may be regulated through phosphorylation events. It is suggested that there would be a defect in transcriptional repression by BASP1 phosphorylation; and therefore, this may act as a switch to turn the repression function off. From the data collected in this study alongside past studies (Dey, 2019), it is possible to predict that BASP1 S6D still recruits PRC2 and thus, H3K27me3 deposition would still occur. Yet, this would need to be tested. It is also necessary to confirm that disruption of the myristoyl group occurs *in vivo* in a phosphorylation state rather than in merely a phosphomimic state which past studies have used.

4.3.1 Potential bivalency at WT1-target gene promoters

Bivalency at promoters is a concept in which chromatin adopts both the active and inactive histone tail modifications, for example the activation mark H3K4me3 and repressive mark H3K27me3, on the same nucleosome. As first described in embryonic stem cells (Bernstein et al., 2006), bivalency facilitates a poised stance for the expression of developmental genes, and since also has been described in iPSCs (Guenther et al., 2010) and adult stem cells (Cui et al., 2009).

Thus, the phosphorylation event at serine 6 on BASP1 disrupts lipid-dependent mechanisms due to the absence of the myristoylated tail, whereas lipid-independent mechanisms are still possible. Thus, H3K27me3 marks could be deposited on histones at WT1-target genes promoters, whilst the active marks H3K4me3 are still present. Therefore, post-translational modification of BASP1 provides a mechanism by which both marks are present, rendering WT1-target gene promoters poised for rapid transcriptional regulation.

The action of the PRC2 is intricately linked with the status of poised bivalent promoters for gene expression due to its role in H3K27me3 deposition (Ku et al., 2008). Despite this, the mechanism by which the PRC2 is recruited to bivalent promoters to aid H3K27me3 deposition is currently unclear. It is possible that the relationship between PRC2 and the WT1/BASP1 complex could play a role in regulating the bivalency at WT1-target gene promoters; especially as the WT1/BASP1 complex has been demonstrated to recruit factors involved in the removal of the active mark H3K4me3.

It is currently unclear whether the H3K27me3 and H3K4me3 histone marks observed at WT1-target gene promoters in the absence of BASP1-myristoylation are present on the same nucleosome. This is because the resolution of the ChIP assays performed in this study was not of a suitable standard. Rather, a more applicable approach to understand whether these marks typical of bivalency are present on the same nucleosome would be to use a re-ChIP assay, which allows for the sequential use of two different antibodies detecting each of the chromatin modifications. It would also be important to ensure thorough optimisation of the ChIP protocol to ensure uniform DNA fragmentation at ~100bp to confirm that single nucleosomes are analysed.

Although the ChIP data shows that the PRC2 is recruited to the WT1-target gene promoters, the technique does not indicate whether this recruitment has a functional relevance or whether it is coincidental. Experiments performed later in the project worked to uncover a role for PRC2 in trimethylation of H3K27 and attempted to unveil a mechanism for this interaction.

4.4 The WT1/BASP1 complex and PRC2 work synergistically to trimethylate H3K27

ChIP and RNA interference analysis demonstrated a relationship between the WT1/BASP1 complex and the PRC2 at WT1-target gene promoters. The experiments showed an important role for EZH2 in BASP1-mediated transcriptional repression of WT1-target genes, with knockdown of EZH2 eliciting a significant increase in *AREG* and *VDR* gene expression. Double knockdown of both proteins produced results consistent with the hypothesised molecular mechanism, in which both BASP1 and EZH2 work in concert to repress transcription. The same conclusion could be drawn from the H3K27me3 ChIP data following siRNA-targeted knockdown of BASP1/EZH2 in MCF7 cells. These data clearly demonstrated the role of EZH2 in BASP1-mediated H3K27me3 mark deposition. The similar level of H3K27me3 reduction during both single and double BASP1/EZH2 knockdown suggests that these proteins work together along the same molecular

pathway to invoke transcriptional repression via the deposition of H3K27me3 marks on WT1-target gene promoters. In accompaniment, the data showed no significant difference between H3K27me3 levels during BASP1/EZH2 knockdown and IgG levels. This suggests that the interaction between the WT1/BASP1 complex and PRC2 largely mediates the deposition of H3K27me3 marks at the WT1-target genes investigated. This finding is consistent with previous work associating the PRC2 with H3K27me3 deposition across heterochromatin, and the previous data in the laboratory linking BASP1 with placement of H3K27 trimethylation at WT1-target genes (Dey, 2019). While the data shows a mechanistic association between the BASP1 and PRC2 complexes, the specific events involved in the recruitment of the PRC2 complex by BASP1 are not clear. One possible mechanism would involve direct binding in which BASP1 directly recruits the PRC2 into a macro-complex. Another possible mechanism could involve a BASP1-mediated alteration in the epigenetic environment at the promoters, which may provide a platform for the recruitment of the PRC2 via an independent mechanism. Both possible mechanisms are outlined in Figure 20.

4.4.1 Potential for a direct binding mechanism

Immunoprecipitation (IP) experiments were used to determine if BASP1 associates with the PRC2 complex in nuclear or cytoplasmic extracts. Yet, the co-IP experiments produced inconclusive results surrounding an interaction event between BASP1 and core components of the PRC2. Multiple attempts were made to visualise an interaction between BASP1 and the PRC2, however all failed, including many of the positive controls. This suggests a possibility that there was a problem with the co-IP experiment. Both whole cell extracts and nuclear extracts were used in the co-IP, as well as different blocking buffers (Tris-based and PBS-based), and different antibodies were trialled in the co-IP and Western blot protocols (for example, a monoclonal mouse EZH2 antibody and a polyclonal rabbit EZH2); all with very limited success. It may be useful for this technique to be re-attempted to first detect a positive control, followed by a co-IP.

Whilst it cannot be concluded that the two complexes do not interact, it seems likely that the mechanism takes a more intricate and complex approach to invoke transcriptional repression through trimethylation of H3K27. Thus, the inability to co-immunoprecipitate SUZ12/EZH2 with BASP1 antibodies suggests that Figure 20B may be a more realistic epigenetic mechanism in this instance.

It is important to acknowledge that whilst the co-IP data failed to show positive results, BASP1 could still interact with PRC2. A past study has shown an interaction between WT1 and EZH2/SUZ12 using co-IP experiments (Xu et al., 2011). It is possible that this interaction was mediated via BASP1, although the role of BASP1 as a co-repressor of WT1 and thus acting as an intermediatory compound within this interaction was not investigated in that study. However, this leaves questions surrounding the negative co-IP results gathered in the current study. One explanation could be that the binding site on BASP1 for PRC2 is concealed by the interaction with

the antibodies used for the IP. Although this is a possibility, it is unlikely that all three of the antibodies used (BASP1, EZH2 and SUZ12) occluded any interaction surface between BASP1 and PRC2 complex. Another explanation could be that perhaps the nature of the BASP1/PRC2 interaction is low affinity or transient, and therefore the binding interaction is lost during the mechanical and chemical stresses of the IP experiment (Bracken, 2006; Ezhkova et al., 2009).

It will be important to use other approaches to explore the association of BASP1 with PRC2 and H3K27 trimethylation. For example, immunofluorescence could be used to determine if BASP1 and PRC2 co-localise in the nuclei of cells. Not only will this visualise any potential co-localisation, but it will also show the location of the complexes in the nucleus. As already discussed, previous evidence indicates that the WT1/BASP1 complex is associated with the nuclear periphery where it is in complex with the inner nuclear membrane protein, emerin (Dey, 2019). Super-resolution microscopy will allow for higher precision analysis of co-localisation, yet neither technique confirms a direct interaction. Instead, it is possible to use surface plasmon resonance technology to investigate an interaction mechanism.

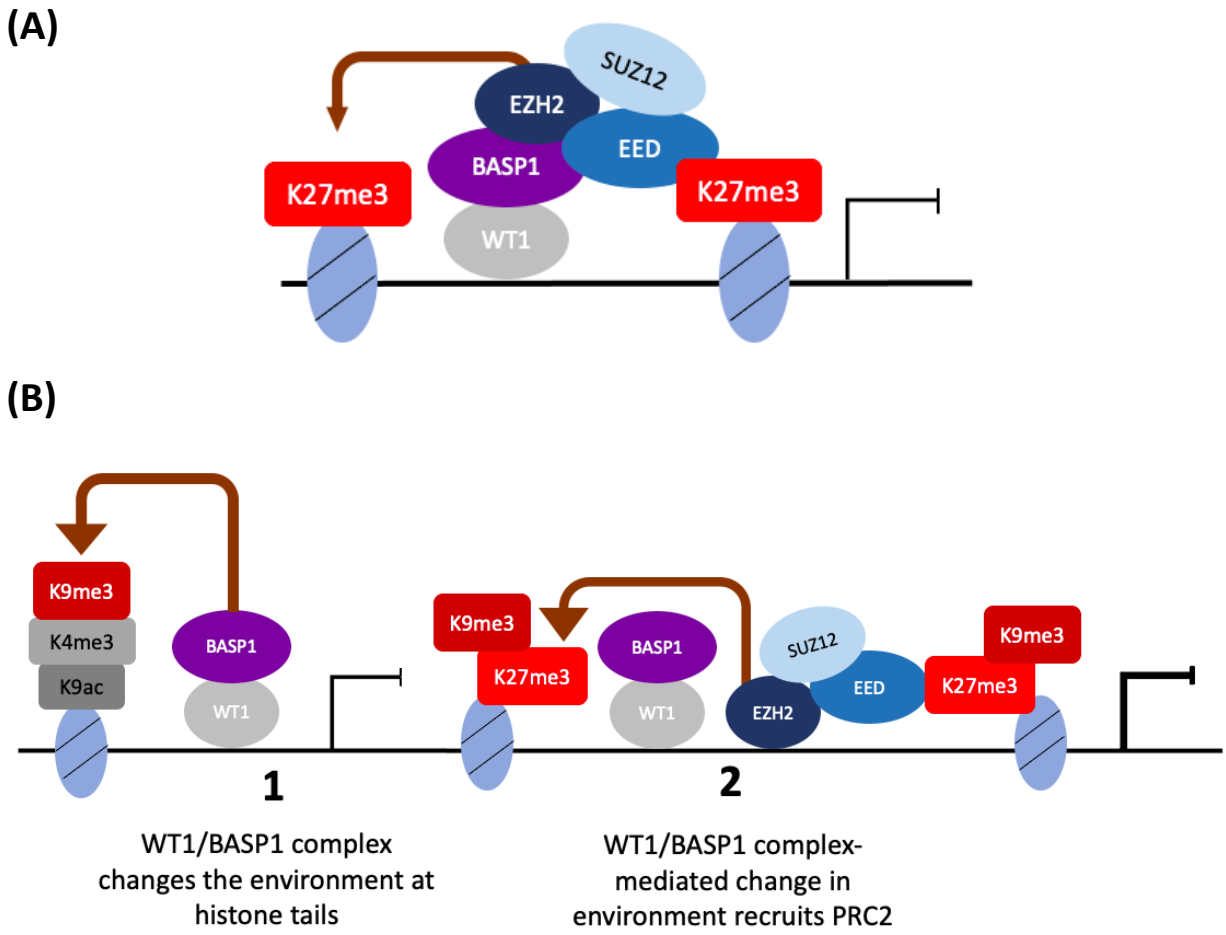

Figure 20. *Two proposed mechanisms of PRC2 recruitment to the WT1/BASP1 complex.*
(A) A potential mechanism involves the direct recruitment of the PRC2 to the WT1/BASP1 complex to add the H3K27me3 marks. EZH2 catalyses the deposition, whilst EED reads previously deposited H3K27me3 marks to continue a positive feedback loop, and SUZ12 works to recruit other necessary factors into the complex.
(B) An alternative mechanism involves the indirect recruitment of the PRC2 following a WT1/BASP1 complex-mediated alternation in the environment at the histone tail (1). From here, the WT1/BASP1 complex-mediated change in chromatin environment recruits the PRC2 for the deposition of H3K27me3 marks.

4.4.2 Proposed alternative mechanisms of PRC2 recruitment

Though past studies have depicted interaction events between the PRC2 and transcription factors, they have been unable to alleviate a mechanism surrounding PRC2 recruitment involving a direct interaction. For example, the transcription factor YY1 interacts with PRC2 at the nuclear periphery for roles in development, yet the mechanism by which PRC2 is recruited to the area is unclear (Harr et al., 2015).

Research has uncovered how previously placed histone modifications can increase the affinity for PRC2 binding. The PCL subunit, a non-core component of PRC2, can interact with H3K36me3, an active mark seen within heterochromatin (Chantalat et al., 2011), and thus recruit PRC2 to the genome (Cai et al., 2013). It is therefore plausible that a similar mechanism occurs at WT1-target gene promoters. Previous ChIP data showed the presence of H3K36me3 marks at many WT1-target gene promoters (Essafi et al., 2011; Dey, 2019), although this fold enrichment was smaller compared to other histone modification marks. H3K36me3 marks are typically found at a higher concentration within the gene body (Sims and Reinberg, 2009), and it is therefore expected that levels are lower within the promoter region. As a consequence, it is possible that the PRC2 is recruited to WT1-target gene promoters through an interaction mediated by PCL-H3K36me3. However, as these marks are less commonly associated with WT1-target genes, perhaps the PRC2 is recruited to WT1-target gene promoters through a more commonly associated histone modification. It is possible that this mechanism is very similar to that outlined above, in which a BASP1-mediated change in the epigenetic landscape could increase the affinity for PRC2. This hypothesised mechanism is depicted in Figure 20B.

Mounting evidence indicates that long non-coding RNAs (lncRNAs) can interact with chromatin-modifying enzyme complexes, including the PRC2. For example, the lncRNA *Xist* targets and interacts with PRC2, recruiting the PRC2 to trimethylate H3K27 on the X-chromosome, leading to transcriptional repression (Zhao et al., 2008). It is possible that a similar mechanism exists during the recruitment of the PRC2 to WT1-target gene promoters, yet further experiments are required to test this hypothesis. Past studies have extensively linked the KTS+ WT1 variant with RNA interactions (Caricasole et al., 1996), and therefore perhaps an intricate mechanism exists in which WT1 interacts with a lncRNA at the WT1-target gene, and this in-turn recruits other histone-modifying complexes, including the BASP1 complex and the PRC2.

Another potential mechanism is associated with the canonical PRC1. Section 1.5.1 discusses a potential interplay and positive feedback loop between PRC1 and PRC2, in which the action of both complexes is essential for polycomb-mediated repression. Recent work used a genome-wide association study to demonstrate the rapid displacement of PRC2 activity and loss of H3K27me3 deposition when the PRC1 is non-functional (Tamburri et al., 2020). It was proposed that the ubiquitination of H2AK119 by the PRC1 stabilises PcG complexes on histone tails. Thus, it is possible that deposition of H2AK119 ubiquitination marks by PRC1 at WT1-target gene promoters is a prerequisite for H3K27me3 deposition by PRC2, and as a result perhaps the core components

of the PRC1 interact with BASP1 in order to alter the environment and consequently encouraging PRC2 recruitment. As a result, future ChIP experiments should explore whether H2AK119 ubiquitination marks are present at WT1-target gene promoters, and from this, investigations should take place into whether either of the core components of the PRC1, the E3 ligases RING1A/B, interact with BASP1.

4.4.3 A possible mechanism for WT1/BASP1 complex coalescence with PRC2 at WT1-target genes

Liquid-liquid phase separation (LLPS) has attracted recent attention as a mechanism of nuclear organisation, which describes how biological macromolecules can form membrane-less compartments through hydrophobicity and other factors (Hyman et al., 2014; Mir et al., 2019; Krainer et al., 2021). Moreover, it offers an explanation on how regions of heterochromatin can gather at the nuclear periphery; thus, providing a mechanism for the formation of distinct local high-concentration environments, which increase the probability of specific biochemical interactions. LLPS is influenced by hydrophobic interactions, and consequently recent research has suggested a role for myristoylated proteins in driving and modulating this state (Zhang et al., 2021). As a direct result of this finding, it could be hypothesised that the myristoylation of BASP1 is intrinsically associated with specific phase separated bodies. Within a single phase-separated body, multiple molecules can function synergistically at a single gene in accompaniment with other proteins without the requirement of a direct interaction, in a robust but plastic and reversible manner. Hence, it is possible that myristoylated BASP1 stabilises the phase-separated body through hydrophobic interactions, allowing for other molecules associated with the WT1/BASP1-complex to coalesce into the same phase-separated body, which is all stabilised through a cholesterol-mediated interaction (Loats et al., 2021).

Recent research has demonstrated that EZH2 can be myristoylated at its N-terminal glycine; and from this is able to undergo LLPS to compartmentalise a common EZH2-substate, STAT3 (Zhang et al., 2021). Hence, it seems plausible that myristoylated-EZH2 could be recruited into the same phase-separated body as myristoylated-BASP1, yet via independent mechanisms. This could aid in understanding how the proteins are both recruited the WT1-target gene promoters but were not shown to interact. Nonetheless, there is argument that the two proteins being within the same phase-separated body would bring about positive IP experiments. It is noteworthy that the NP-40 detergent used during the IP protocol could disrupt lipid-dependent complexes, and thus it is unlikely that complexes within lipid droplets would co-IP. In addition, it is important to acknowledge that the nature of LLPS seems to be spatially and temporally transient. Therefore, it is possible that myristoylated-BASP1 is not present in the droplet at the same time as myristoylated-EZH2. Further research regarding BASP1-mediated phase-separated bodies is necessary to investigate this hypothesis and further understand the significance of the BASP1-mediated lipid-independent

recruitment of PRC2 and any potential interplay between myristoylated forms of both BASP1 and EZH2.

This potential mechanism of coalescence is consistent with the idea that the myristoylation of BASP1 may mediate bivalency of WT1-target gene promoters. During bivalency, the addition of repressive histone marks is a lipid-independent process. However, as this process is absent of BASP1-myristoylation, the formation of a phase-separated body would be negated. Consequently, how the necessary factors involved in repressive mark deposition are brought into close proximity remains unanswered. Nevertheless, instead, it is possible that the EZH2-myristoylation fulfils this role and thus this mediates the formation of a phase-separated body. Here, a phase-separated body formed by myristoylated-EZH2 would recruit unmyristoylated-BASP1, as well as other factors involved in deposition of repressive marks at WT1-target gene promoters, into close proximity. Therefore, this provides a mechanism by which the factors are still recruited into close proximity to add H3K27me3 histone marks at bivalent WT1-target gene promoters, in the absence of myristoylated-BASP1. Such a mechanism would also prevent the removal of H3K4me3, which is necessary for the establishment and maintenance of bivalency at WT1-target gene promoters.

4.6 Significance of this study and its wider impact

The findings from this study aid in further understanding of how the PRC2 is involved in deposition of trimethyl marks at H3K27 to transcriptionally repress WT1-target gene promoters, and how the complex is associated with the WT1/BASP1 complex. By enhancing our understanding of the WT1/BASP1/PRC2 association, future studies can focus on determining how this mechanism may be commonly aberrant in cancer states. Most literature in the field outlines EZH2's role as an oncogenic factor (Lu et al., 2010; Li and Zhang, 2013; Fu et al., 2015), however its role in inducing transcriptional repression through an interaction mechanism with the WT1/BASP1 complex suggests that it might also have a potential role as a tumour suppressor. In the long-term, this may prove useful for the development of novel cancer therapeutics, such as small molecular compounds. For example, dependent on how the mechanism turns aberrant in cancer, a potential therapeutic could be an agonist for EED which maintains the H3K27me3 deposition positive feedback loop, ensuring that transcriptional repression of WT1-target genes still occurs.

Not only could these findings be useful clinically in the development of cancer therapeutics, but they provide new insights surrounding bivalency at WT1-target gene promoters. A suggested mechanism involves the phosphorylation of serine-6 on BASP1 may act as a molecular switch for myristoylation, and thus this may have a role in determining which histone marks are present in the epigenetic landscape at WT1-target genes. Current research has not determined a mechanism of how bivalent promoters form, and hence analysis of how BASP1 interfaces with PRC2 will shed some new light in this area. This will uncover further information surrounding mechanisms of embryonic development and stem cell differentiation.

4.7 Future directions

Future experiments should focus on how the PRC2 recruitment to WT1-target gene promoters is mediated by the WT1/BASP1 complex. This would involve further studies into whether this mechanism is direct or indirect. It would be interesting to use fluorescence microscopy to visualise the potential co-localisation of the WT1/BASP1 complex and PRC2 within the nucleus, although this technique will not conclude whether the interaction is direct or indirect. Further investigations using super-resolution microscopy will add more precision to this co-localisation. Alongside this, the use of surface plasmon resonance (SPR) technology could be useful to detect whether BASP1 and PRC2 complex interact transiently *in vitro*, whilst the use of FRET may shed light on this interaction *in vivo.* The use of all four of these techniques would reveal any BASP1/PRC2 co-localisation (fluorescent microscopy and super-resolution microscopy) and whether this is a direct or indirect interaction (SPR and FRET).

Depending on the outcome of these experiments, it may prove useful to alleviate more of the mechanistic detail surrounding how the PRC2 could be indirectly recruited to the promoters. There is a distinct lack of conclusive research into PRC2 recruitment, and therefore it may be necessary to investigate the role that lncRNAs or the PRC1 may play here. Research would also benefit from investigations into whether the mechanism of PRC2 recruitment is influenced by BASP1-mediated placement of other histone modifications. For example, RNAi against HDAC1 would prevent H3K9 deacetylation, followed by ChIP to check if H3K27 trimethylation is prevented.

As a follow-up investigation, research should work to uncover whether the mechanism operates *in vivo*. An important model system could use the Cre-LoxP^{ER} system in a taste receptor cell mouse model, which allows spatio-temporal control of BASP1 expression (Gao et al., 2014). This model will show whether EZH2 and SUZ12 are recruited to WT1-target genes in the presence or absence of BASP1. Current studies from the Medler lab have shown that H3K27me3 marks are significantly reduced during BASP1 knockout *in vivo* (Stefan Roberts, personal communication). Consequently, it seems highly likely that the PRC2 is also recruited *in vivo.*

As mentioned above, various factors have been reported to associate with the PRC2 complex. Research should include understanding which non-essential factors SUZ12 recruits into the complex. It seems likely that this would include AEBP2, which enhances methyltransferase activity (O'Meara and Simon, 2012), and RbAp46/48, histone chaperone proteins which establish and maintain the chromatin structure (Lejon et al., 2011). In addition, if it is demonstrated that recruitment of the PRC2 to WT1-target gene promoters is mediated by PRC1, then it is expected that the non-core component JARID2 would be present within the PRC2. As a whole, this will improve our understanding of the WT1/BASP1/PRC2 complex and its importance in maintaining repressive chromatin states.

The results collected from the RNA interference experiments demonstrated a functional relevance of EZH2 at WT1-target genes, using two separate EZH2 siRNAs. However, only cells transfected with EZH2 siRNA 1 were used in the final H3K27me3 ChIP. Therefore, it is important to perform the same experiment using EZH2 siRNA 2 to verify the results which displayed a decrease in H3K27me3 deposition in the absence of EZH2 at WT1-target gene promoters. Moreover, it is also important that similar RNA interference experiments are performed using SUZ12 knockdown, allowing for confirmation that the intact PRC2 is critical in BASP1-mediated repression, or whether the presence of SUZ12 at promoters is in fact coincidental. As a consequence, this will provide further insight of the factors recruited by BASP1, and how these can act together as a transcriptional repressor complex. It may also be interesting to explore whether K562 cells provide similar results. This would validate results using both endogenously and ectopically expressed BASP1. During this experiment, only EZH2 would need to be knocked down, with changes in BASP1 expression explored between the BASP1-K562 and V-K562 cells.

As already discussed, re-ChIP should be used to confirm that H3K27me3 and H3K4me3 marks at WT1-target gene promoters are on the same nucleosome. This may reveal more information regarding the role of BASP1 in establishing bivalency at WT1-target gene promoters.

4.8 Conclusion

These future directions will provide further insight into the mechanism of transcriptional repression by BASP1. This study shows that BASP1 and PRC2 complex work synergistically to trimethylate H3K27 at WT1-target gene promoters. It is likely that this contributes to development and differentiation mechanisms and continued investigations into the significance of lipid-independency may have important implications in the poising of bivalent promoters. Further exploration of the interaction between the WT1/BASP1 complex and the PRC2 will also shed light on potential cancer mechanisms and thus aid in the development of clinically useful therapeutics.

VI. References

Almassalha, L.M., Tiwari, A., Ruhoff, P.T., Stypula-Cyrus, Y., Cherkezyan, L., Matsuda, H., Dela Cruz, M.A., Chandler, J.E., White, C., Maneval, C., Subramanian, H., Szleifer, I., Roy, H.K. and Backman, V. 2017. The Global Relationship between Chromatin Physical Topology, Fractal Structure, and Gene Expression. *Scientific Reports*. **7**(1), p.41061.

Amin, E.M., Oltean, S., Hua, J., Gammons, M.V.R., Hamdollah-Zadeh, M., Welsh, G.I., Cheung, M.-K., Ni, L., Kase, S., Rennel, E.S., Symonds, K.E., Nowak, D.G., Royer-Pokora, B., Saleem, M.A., Hagiwara, M., Schumacher, V.A., Harper, S.J., Hinton, D.R., Bates, D.O. and Ladomery, M.R. 2011. WT1 Mutants Reveal SRPK1 to Be a Downstream Angiogenesis Target by Altering VEGF Splicing. *Cancer Cell*. **20**(6), pp.768–780.

Bandiera, R., Vidal, V.P.I., Motamedi, F.J., Clarkson, M., Sahut-Barnola, I., von Gise, A., Pu, W.T., Hohenstein, P., Martinez, A. and Schedl, A. 2013. WT1 maintains adrenal-gonadal primordium identity and marks a population of AGP-like progenitors within the adrenal gland. *Developmental cell*. **27**(1), pp.5–18.

Bansal, H., Seifert, T., Bachier, C., Rao, M., Tomlinson, G., Iyer, S.P. and Bansal, S. 2012. The transcription factor Wilms tumor 1 confers resistance in myeloid leukemia cells against the proapoptotic therapeutic agent TRAIL (tumor necrosis factor α-related apoptosis-inducing ligand) by regulating the antiapoptotic protein Bcl-xL. *The Journal of biological chemistry*. **287**(39), pp.32875–32880.

Bardeesy, N. and Pelletier, J. 1998. Overlapping RNA and DNA binding domains of the wt1 tumor suppressor gene product. *Nucleic acids research*. **26**(7), pp.1784–1792.

Barski, A., Cuddapah, S., Cui, K., Roh, T.-Y., Schones, D.E., Wang, Z., Wei, G., Chepelev, I. and Zhao, K. 2007. High-resolution profiling of histone methylations in the human genome. *Cell*. **129**(4), pp.823–837.

Belali, T., Wodi, C., Clark, B., Cheung, M.-K., Craig, T.J., Wheway, G., Wagner, N., Wagner, K.-D., Roberts, S., Porazinski, S. and Ladomery, M. 2020. WT1 activates transcription of the splice factor kinase SRPK1 gene in PC3 and K562 cancer cells in the absence of corepressor BASP1. *Biochimica et Biophysica Acta (BBA) - Gene Regulatory Mechanisms*. **1863**(12), p.194642.

Bernstein, B.E., Mikkelsen, T.S., Xie, X., Kamal, M., Huebert, D.J., Cuff, J., Fry, B., Meissner, A., Wernig, M., Plath, K., Jaenisch, R., Wagschal, A., Feil, R., Schreiber, S.L. and Lander, E.S. 2006. A Bivalent Chromatin Structure Marks Key Developmental Genes in Embryonic Stem Cells. *Cell*. **125**(2), pp.315–326.

Blackledge, N.P., Rose, N.R. and Klose, R.J. 2015. Targeting Polycomb systems to regulate gene expression: modifications to a complex story. *Nature reviews. Molecular cell biology*. **16**(11), pp.643–649.

Blanchard, J.W., Xie, J., El-Mecharrafie, N., Gross, S., Lee, S., Lerner, R.A. and Baldwin, K.K. 2017. Replacing reprogramming factors with antibodies selected from combinatorial antibody libraries. *Nature Biotechnology*. **35**(10), pp.960–968.

Boland, M.J., Hazen, J.L., Nazor, K.L., Rodriguez, A.R., Gifford, W., Martin, G., Kupriyanov, S. and Baldwin, K.K. 2009. Adult mice generated from induced pluripotent stem cells. *Nature*.

461(7260), pp.91–94.

Bor, Y. 2006. The Wilms' tumor 1 (WT1) gene (+KTS isoform) functions with a CTE to enhance translation from an unspliced RNA with a retained intron. *Genes & Development*. **20**(12), pp.1597–1608.

Boros, J., Arnoult, N., Stroobant, V., Collet, J.-F. and Decottignies, A. 2014. Polycomb repressive complex 2 and H3K27me3 cooperate with H3K9 methylation to maintain heterochromatin protein 1α at chromatin. *Molecular and cellular biology*. **34**(19), pp.3662–3674.

Bracken, A.P. 2006. Genome-wide mapping of Polycomb target genes unravels their roles in cell fate transitions. *Genes & Development*. **20**(9), pp.1123–1136.

Cai, L., Rothbart, S.B., Lu, R., Xu, B., Chen, W.-Y., Tripathy, A., Rockowitz, S., Zheng, D., Patel, D.J., Allis, C.D., Strahl, B.D., Song, J. and Wang, G.G. 2013. An H3K36 methylation-engaging Tudor motif of polycomb-like proteins mediates PRC2 complex targeting. *Molecular cell*. **49**(3), pp.571–582.

Call, K.M., Glaser, T., Ito, C.Y., Buckler, A.J., Pelletier, J., Haber, D.A., Rose, E.A., Kral, A., Yeger, H. and Lewis, W.H. 1990. Isolation and characterization of a zinc finger polypeptide gene at the human chromosome 11 Wilms' tumor locus. *Cell*. **60**(3), pp.509–520.

Cano, E., Carmona, R. and Muñoz-Chápuli, R. 2013. Wt1-expressing progenitors contribute to multiple tissues in the developing lung. *American Journal of Physiology-Lung Cellular and Molecular Physiology*. **305**(4), pp.L322–L332.

Caricasole, A., Duarte, A., Larsson, S.H., Hastie, N.D., Little, M., Holmes, G., Todorov, I. and Ward, A. 1996. RNA binding by the Wilms tumor suppressor zinc finger proteins. *Proceedings of the National Academy of Sciences of the United States of America*. **93**(15), pp.7562–7566.

Carpenter, B., Hill, K.J., Charalambous, M., Wagner, K.J., Lahiri, D., James, D.I., Andersen, J.S., Schumacher, V., Royer-Pokora, B., Mann, M., Ward, A. and Roberts, S.G.E. 2004. BASP1 Is a Transcriptional Cosuppressor for the Wilms{\textquoteright} Tumor Suppressor Protein WT1. *Molecular and Cellular Biology*. **24**(2), pp.537–549.

Carré, G.-A., Siggers, P., Xipolita, M., Brindle, P., Lutz, B., Wells, S. and Greenfield, A. 2018. Loss of p300 and CBP disrupts histone acetylation at the mouse Sry promoter and causes XY gonadal sex reversal. *Human molecular genetics*. **27**(1), pp.190–198.

Carter, J.H., Deddens, J.A., Mueller, G., Lewis, T.G., Dooley, M.K., Robillard, M.C., Frydl, M., Duvall, L., Pemberton, J.O. and Douglass, L.E. 2018. Transcription factors WT1 and p53 combined: a prognostic biomarker in ovarian cancer. *British Journal of Cancer*. **119**(4), pp.462–470.

Chantalat, S., Depaux, A., Héry, P., Barral, S., Thuret, J.-Y., Dimitrov, S. and Gérard, M. 2011. Histone H3 trimethylation at lysine 36 is associated with constitutive and facultative heterochromatin. *Genome research*. **21**(9), pp.1426–1437.

Chau, Y.-Y., Brownstein, D., Mjoseng, H., Lee, W.-C., Buza-Vidas, N., Nerlov, C., Jacobsen, S.E., Perry, P., Berry, R., Thornburn, A., Sexton, D., Morton, N., Hohenstein, P., Freyer, E., Samuel, K., van't Hof, R. and Hastie, N. 2011. Acute Multiple Organ Failure in Adult Mice Deleted for the Developmental Regulator Wt1 A. O. M. Wilkie, ed. *PLoS Genetics*. **7**(12), p.e1002404.

Cho, J., Chang, H., Kwon, S.C., Kim, B., Kim, Y., Choe, J., Ha, M., Kim, Y.K. and Kim, V.N. 2012.

LIN28A Is a Suppressor of ER-Associated Translation in Embryonic Stem Cells. *Cell*. **151**(4), pp.765–777.

Ciferri, C., Lander, G.C., Maiolica, A., Herzog, F., Aebersold, R. and Nogales, E. 2012. Molecular architecture of human polycomb repressive complex 2. *eLife*. **1**.

Clapier, C.R., Iwasa, J., Cairns, B.R. and Peterson, C.L. 2017. Mechanisms of action and regulation of ATP-dependent chromatin-remodelling complexes. *Nature Reviews Molecular Cell Biology*. **18**(7), pp.407–422.

Cooper, S., Grijzenhout, A., Underwood, E., Ancelin, K., Zhang, T., Nesterova, T.B., Anil-Kirmizitas, B., Bassett, A., Kooistra, S.M., Agger, K., Helin, K., Heard, E. and Brockdorff, N. 2016. Jarid2 binds mono-ubiquitylated H2A lysine 119 to mediate crosstalk between Polycomb complexes PRC1 and PRC2. *Nature communications*. **7**, p.13661.

Cui, K., Zang, C., Roh, T.-Y., Schones, D.E., Childs, R.W., Peng, W. and Zhao, K. 2009. Chromatin Signatures in Multipotent Human Hematopoietic Stem Cells Indicate the Fate of Bivalent Genes during Differentiation. *Cell Stem Cell*. **4**(1), pp.80–93.

Deevy, O. and Bracken, A.P. 2019. PRC2 functions in development and congenital disorders. *Development*. **146**(19), p.dev181354.

Dey, A.E. 2019. Investigating the role of BASP1 lipidation in WT1/BASP1 mediated gene regulation. PhD thesis, University of Bristol.

Dong, L., Pietsch, S. and Englert, C. 2015. Towards an understanding of kidney diseases associated with WT1 mutations. *Kidney International*. **88**(4), pp.684–690.

Englert, C., Hou, X., Maheswaran, S., Bennett, P., Ngwu, C., Re, G.G., Garvin, A.J., Rosner, M.R. and Haber, D.A. 1995. WT1 suppresses synthesis of the epidermal growth factor receptor and induces apoptosis. *The EMBO journal*. **14**(19), pp.4662–4675.

Essafi, A., Webb, A., Berry, R.L., Slight, J., Burn, S.F., Spraggon, L., Velecela, V., Martinez-Estrada, O.M., Wiltshire, J.H., Roberts, S.G.E., Brownstein, D., Davies, J.A., Hastie, N.D. and Hohenstein, P. 2011. A Wt1-Controlled Chromatin Switching Mechanism Underpins Tissue-Specific Wnt4 Activation and Repression. *Developmental Cell*. **21**(3), pp.559–574.

Ezhkova, E., Pasolli, H.A., Parker, J.S., Stokes, N., Su, I., Hannon, G., Tarakhovsky, A. and Fuchs, E. 2009. Ezh2 orchestrates gene expression for the stepwise differentiation of tissue-specific stem cells. *Cell*. **136**(6), pp.1122–1135.

Ferrari, K.J., Scelfo, A., Jammula, S., Cuomo, A., Barozzi, I., Stützer, A., Fischle, W., Bonaldi, T. and Pasini, D. 2014. Polycomb-dependent H3K27me1 and H3K27me2 regulate active transcription and enhancer fidelity. *Molecular cell*. **53**(1), pp.49–62.

Fišerová, J., Efenberková, M., Sieger, T., Maninová, M., Uhlířová, J. and Hozák, P. 2017. Chromatin organization at the nuclear periphery as revealed by image analysis of structured illumination microscopy data. *Journal of Cell Science*.

Fu, Y., Chen, J., Pang, B., Li, C., Zhao, J. and Shen, K. 2015. EZH2-Induced H3K27me3 is Associated with Epigenetic Repression of the ARHI Tumor-Suppressor Gene in Ovarian Cancer. *Cell Biochemistry and Biophysics*. **71**(1), pp.105–112.

Gao, Y., Dutta Banik, D., Muna, M.M., Roberts, S.G. and Medler, K.F. 2019. The WT1–BASP1

complex is required to maintain the differentiated state of taste receptor cells. *Life Science Alliance*. **2**(3), p.e201800287.

Gao, Y., Toska, E., Denmon, D., Roberts, S.G.E. and Medler, K.F. 2014. WT1 regulates the development of the posterior taste field. *Development*. **141**(11), pp.2271–2278.

Goodfellow, S.J., Rebello, M.R., Toska, E., Zeef, L.A.H., Rudd, S.G., Medler, K.F. and Roberts, S.G.E. 2011. WT1 and its transcriptional cofactor BASP1 redirect the differentiation pathway of an established blood cell line. *Biochemical Journal*. **435**(1), pp.113–125.

Green, L.M., Wagner, K.J., Campbell, H.A., Addison, K. and Roberts, S.G.E. 2009. Dynamic interaction between WT1 and BASP1 in transcriptional regulation during differentiation. *Nucleic acids research*. **37**(2), pp.431–440.

Griner, E.M. and Kazanietz, M.G. 2007. Protein kinase C and other diacylglycerol effectors in cancer. *Nature reviews. Cancer*. **7**(4), pp.281–294.

Guaragna, M.S., Ribeiro de Andrade, J.G., de Freitas Carli, B., Belangero, V.M.S., Maciel-Guerra, A.T., Guerra-Júnior, G. and de Mello, M.P. 2017. WT1 Haploinsufficiency Supports Milder Renal Manifestation in Two Patients with Denys-Drash Syndrome. *Sexual development : genetics, molecular biology, evolution, endocrinology, embryology, and pathology of sex determination and differentiation*. **11**(1), pp.34–39.

Guenther, M.G., Frampton, G.M., Soldner, F., Hockemeyer, D., Mitalipova, M., Jaenisch, R. and Young, R.A. 2010. Chromatin Structure and Gene Expression Programs of Human Embryonic and Induced Pluripotent Stem Cells. *Cell Stem Cell*. **7**(2), pp.249–257.

Guo, R.-S., Yu, Y., Chen, J., Chen, Y.-Y., Shen, N. and Qiu, M. 2016. Restoration of Brain Acid Soluble Protein 1 Inhibits Proliferation and Migration of Thyroid Cancer Cells. *Chinese Medical Journal*. **129**(12), pp.1439–1446.

Hammes, A., Guo, J.K., Lutsch, G., Leheste, J.R., Landrock, D., Ziegler, U., Gubler, M.C. and Schedl, A. 2001. Two splice variants of the Wilms' tumor 1 gene have distinct functions during sex determination and nephron formation. *Cell*. **106**(3), pp.319–329.

Han, Y., San-Marina, S., Liu, J. and Minden, M.D. 2004. Transcriptional activation of c-myc proto-oncogene by WT1 protein. *Oncogene*. **23**(41), pp.6933–6941.

Harr, J.C., Luperchio, T.R., Wong, X., Cohen, E., Wheelan, S.J. and Reddy, K.L. 2015. Directed targeting of chromatin to the nuclear lamina is mediated by chromatin state and A-type lamins. *Journal of Cell Biology*. **208**(1), pp.33–52.

Hartl, M., Nist, A., Khan, M.I., Valovka, T. and Bister, K. 2009. Inhibition of Myc-induced cell transformation by brain acid-soluble protein 1 (BASP1). *Proceedings of the National Academy of Sciences*. **106**(14), pp.5604–5609.

Hartl, M., Puglisi, K., Nist, A., Raffeiner, P. and Bister, K. 2020. The brain acid-soluble protein 1 (BASP1) interferes with the oncogenic capacity of MYC and its binding to calmodulin. *Molecular Oncology*. **14**(3), pp.625–644.

Højfeldt, J.W., Hedehus, L., Laugesen, A., Tatar, T., Wiehle, L. and Helin, K. 2019. Non-core Subunits of the PRC2 Complex Are Collectively Required for Its Target-Site Specificity. *Molecular Cell*. **76**(3), pp.423-436.e3.

Holla, S., Dhakshnamoorthy, J., Folco, H.D., Balachandran, V., Xiao, H., Sun, L.-L., Wheeler, D., Zofall, M. and Grewal, S.I.S. 2020. Positioning Heterochromatin at the Nuclear Periphery Suppresses Histone Turnover to Promote Epigenetic Inheritance. *Cell*. **180**(1), pp.150-164.e15.

Hyman, A.A., Weber, C.A. and Jülicher, F. 2014. Liquid-Liquid Phase Separation in Biology. *Annual Review of Cell and Developmental Biology*. **30**(1), pp.39–58.

Jain, S.U., Do, T.J., Lund, P.J., Rashoff, A.Q., Diehl, K.L., Cieslik, M., Bajic, A., Juretic, N., Deshmukh, S., Venneti, S., Muir, T.W., Garcia, B.A., Jabado, N. and Lewis, P.W. 2019. PFA ependymoma-associated protein EZHIP inhibits PRC2 activity through a H3 K27M-like mechanism. *Nature Communications*. **10**(1), p.2146.

Jiao, L. and Liu, X. 2015. Structural basis of histone H3K27 trimethylation by an active polycomb repressive complex 2. *Science (New York, N.Y.)*. **350**(6258), p.aac4383.

Johnson, M. 2019. Investigating the role of EZH2 in the WT1/BASP1 repressive complex. Master's thesis, University of Bristol.

Jomgeow, T., Oji, Y., Tsuji, N., Ikeda, Y., Ito, K., Tsuda, A., Nakazawa, T., Tatsumi, N., Sakaguchi, N., Takashima, S., Shirakata, T., Nishida, S., Hosen, N., Kawakami, M., Tsuboi, A., Oka, Y., Itoh, K. and Sugiyama, H. 2006. Wilms' tumor gene WT1 17AA(-)/KTS(-) isoform induces morphological changes and promotes cell migration and invasion in vitro. *Cancer Science*. **97**(4), pp.259–270.

Kaehler, K.C., Politz, O., Henderson, D., Ulbrich, H.-F., Hauschild, A., Mund, C. and Egberts, F. 2015. Novel DNA methylation markers with potential prognostic relevance in advanced malignant melanoma identified using COBRA assays. *Melanoma Research*. **25**(3), pp.225–231.

Karakas, T., Miething, C.C., Maurer, U., Weidmann, E., Ackermann, H., Hoelzer, D. and Bergmann, L. 2002. The coexpression of the apoptosis-related genes bcl-2 and wt1 in predicting survival in adult acute myeloid leukemia. *Leukemia*. **16**(5), pp.846–854.

Kennedy, D., Ramsdale, T., Mattick, J. and Little, M. 1996. An RNA recognition motif in Wilms' tumour protein (WT1) revealed by structural modelling. *Nature genetics*. **12**(3), pp.329–331.

Kent, J., Coriat, A.M., Sharpe, P.T., Hastie, N.D. and van Heyningen, V. 1995. The evolution of WT1 sequence and expression pattern in the vertebrates. *Oncogene*. **11**(9), pp.1781–1792.

Krainer, G., Welsh, T.J., Joseph, J.A., Espinosa, J.R., Wittmann, S., de Csilléry, E., Sridhar, A., Toprakcioglu, Z., Gudiškytė, G., Czekalska, M.A., Arter, W.E., Guillén-Boixet, J., Franzmann, T.M., Qamar, S., George-Hyslop, P.S., Hyman, A.A., Collepardo-Guevara, R., Alberti, S. and Knowles, T.P.J. 2021. Reentrant liquid condensate phase of proteins is stabilized by hydrophobic and non-ionic interactions. *Nature Communications*. **12**(1), p.1085.

Kreidberg, J.A., Sariola, H., Loring, J.M., Maeda, M., Pelletier, J., Housman, D. and Jaenisch, R. 1993. WT-1 is required for early kidney development. *Cell*. **74**(4), pp.679–691.

Ku, M., Koche, R.P., Rheinbay, E., Mendenhall, E.M., Endoh, M., Mikkelsen, T.S., Presser, A., Nusbaum, C., Xie, X., Chi, A.S., Adli, M., Kasif, S., Ptaszek, L.M., Cowan, C.A., Lander, E.S., Koseki, H. and Bernstein, B.E. 2008. Genomewide Analysis of PRC1 and PRC2 Occupancy Identifies Two Classes of Bivalent Domains. *PLOS Genetics*. **4**(10), p.e1000242.

Laity, J.H., Dyson, H.J. and Wright, P.E. 2000. Molecular basis for modulation of biological function by

alternate splicing of the Wilms{\textquoteright} tumor suppressor protein. *Proceedings of the National Academy of Sciences*. **97**(22), pp.11932–11935.

Laugesen, A. and Helin, K. 2014. Chromatin repressive complexes in stem cells, development, and cancer. *Cell stem cell*. **14**(6), pp.735–751.

Laugesen, A., Højfeldt, J.W. and Helin, K. 2016. Role of the Polycomb Repressive Complex 2 (PRC2) in Transcriptional Regulation and Cancer. *Cold Spring Harbor perspectives in medicine*. **6**(9), p.a026575.

Lavarone, E., Barbieri, C.M. and Pasini, D. 2019. Dissecting the role of H3K27 acetylation and methylation in PRC2 mediated control of cellular identity. *Nature Communications*. **10**(1), p.1679.

Lee, S.B., Huang, K., Palmer, R., Truong, V.B., Herzlinger, D., Kolquist, K.A., Wong, J., Paulding, C., Yoon, S.K., Gerald, W., Oliner, J.D. and Haber, D.A. 1999. The Wilms tumor suppressor WT1 encodes a transcriptional activator of amphiregulin. *Cell*. **98**(5), pp.663–673.

Lee, T.H. and Pelletier, J. 2001. Functional characterization of WT1 binding sites within the human vitamin D receptor gene promoter. *Physiological genomics*. **7**(2), pp.187–200.

Lejon, S., Thong, S.Y., Murthy, A., AlQarni, S., Murzina, N. V, Blobel, G.A., Laue, E.D. and Mackay, J.P. 2011. Insights into association of the NuRD complex with FOG-1 from the crystal structure of an RbAp48·FOG-1 complex. *The Journal of biological chemistry*. **286**(2), pp.1196–1203.

Li, B., Yan, J., Phyu, T., Fan, S., Chung, T.-H., Mustafa, N., Lin, B., Wang, L., Eichhorn, P.J.A., Goh, B.-C., Ng, S.-B., Kappei, D. and Chng, W.-J. 2019. MELK mediates the stability of EZH2 through site-specific phosphorylation in extranodal natural killer/T-cell lymphoma. *Blood*. **134**(23), pp.2046–2058.

Li, H. and Zhang, R. 2013. Role of EZH2 in Epithelial Ovarian Cancer: From Biological Insights to Therapeutic Target. *Frontiers in Oncology*. **3**.

Li, L., Meng, Q., Li, G. and Zhao, L. 2020. BASP1 Suppresses Cell Growth and Metastasis through Inhibiting Wnt/β-Catenin Pathway in Gastric Cancer I. G. Zizzari, ed. *BioMed Research International*. **2020**, pp.1–9.

Little, M. and Wells, C. 1997. A clinical overview of WT1 gene mutations. *Human mutation*. **9**(3), pp.209–225.

Liu, J., Vidi, P.-A., Lelièvre, S.A. and Irudayaraj, J.M.K. 2015. Nanoscale histone localization in live cells reveals reduced chromatin mobility in response to DNA damage. *Journal of Cell Science*. **128**(3), pp.599–604.

Loats, A.E., Carrera, S., Fleming, A.F., Roberts, A.R.E., Sherrard, A., Toska, E., Moorhouse, A.J., Medler, K.F. and Roberts, S.G.E. 2021. Cholesterol is required for transcriptional repression by BASP1. *Proceedings of the National Academy of Sciences*. **118**(29).

Loeb, D.M., Evron, E., Patel, C.B., Sharma, P.M., Niranjan, B., Buluwela, L., Weitzman, S.A., Korz, D. and Sukumar, S. 2001. Wilms' tumor suppressor gene (WT1) is expressed in primary breast tumors despite tumor-specific promoter methylation. *Cancer research*. **61**(3), pp.921–925.

Lozzio, C.B. and Lozzio, B.B. 1975. Human chronic myelogenous leukemia cell-line with positive Philadelphia chromosome. *Blood*. **45**(3), pp.321–334.

Lu, C., Han, H.D., Mangala, L.S., Ali-Fehmi, R., Newton, C.S., Ozbun, L., Armaiz-Pena, G.N., Hu, W., Stone, R.L., Munkarah, A., Ravoori, M.K., Shahzad, M.M.K., Lee, J.-W., Mora, E., Langley, R.R., Carroll, A.R., Matsuo, K., Spannuth, W.A., Schmandt, R., Jennings, N.B., Goodman, B.W., Jaffe, R.B., Nick, A.M., Kim, H.S., Guven, E.O., Chen, Y.-H., Li, L.-Y., Hsu, M.-C., Coleman, R.L., Calin, G.A., Denkbas, E.B., Lim, J.Y., Lee, J.-S., Kundra, V., Birrer, M.J., Hung, M.-C., Lopez-Berestein, G. and Sood, A.K. 2010. Regulation of Tumor Angiogenesis by EZH2. *Cancer Cell*. **18**(2), pp.185–197.

Maekawa, S., Maekawa, M., Hattori, S. and Nakamura, S. 1993. Purification and molecular cloning of a novel acidic calmodulin binding protein from rat brain. *Journal of Biological Chemistry*. **268**(18), pp.13703–13709.

Maheswaran, S., Englert, C., Bennett, P., Heinrich, G. and Haber, D.A. 1995. The WT1 gene product stabilizes p53 and inhibits p53-mediated apoptosis. *Genes & development*. **9**(17), pp.2143–2156.

Maheswaran, S., Park, S., Bernard, A., Morris, J.F., Rauscher, F.J. 3rd, Hill, D.E. and Haber, D.A. 1993. Physical and functional interaction between WT1 and p53 proteins. *Proceedings of the National Academy of Sciences of the United States of America*. **90**(11), pp.5100–5104.

Marsh, L.A., Carrera, S., Shandilya, J., Heesom, K.J., Davidson, A.D., Medler, K.F. and Roberts, S.G. 2017. BASP1 interacts with oestrogen receptor α and modifies the tamoxifen response. *Cell Death & Disease*. **8**(5), pp.e2771–e2771.

Mayo, M.W., Wang, C.Y., Drouin, S.S., Madrid, L. V, Marshall, A.F., Reed, J.C., Weissman, B.E. and Baldwin, A.S. 1999. WT1 modulates apoptosis by transcriptionally upregulating the bcl-2 proto-oncogene. *The EMBO journal*. **18**(14), pp.3990–4003.

McCarty, G., Awad, O. and Loeb, D.M. 2011. WT1 protein directly regulates expression of vascular endothelial growth factor and is a mediator of tumor response to hypoxia. *The Journal of biological chemistry*. **286**(51), pp.43634–43643.

McMaster, M.L., Gessler, M., Stanbridge, E.J. and Weissman, B.E. 1995. WT1 expression alters tumorigenicity of the G401 kidney-derived cell line. *Cell growth & differentiation : the molecular biology journal of the American Association for Cancer Research*. **6**(12), pp.1609–1617.

Menke, A.L., Shvarts, A., Riteco, N., van Ham, R.C., van der Eb, A.J. and Jochemsen, A.G. 1997. Wilms' tumor 1-KTS isoforms induce p53-independent apoptosis that can be partially rescued by expression of the epidermal growth factor receptor or the insulin receptor. *Cancer research*. **57**(7), pp.1353–1363.

Mir, M., Bickmore, W., Furlong, E.E.M. and Narlikar, G. 2019. Chromatin topology, condensates and gene regulation: shifting paradigms or just a phase? *Development*. **146**(19), p.dev182766.

Miyoshi, Y., Ando, A., Egawa, C., Taguchi, T., Tamaki, Y., Tamaki, H., Sugiyama, H. and Noguchi, S. 2002. High expression of Wilms' tumor suppressor gene predicts poor prognosis in breast cancer patients. *Clinical cancer research : an official journal of the American Association for Cancer Research*. **8**(5), pp.1167–1171.

Moffett, P., Bruening, W., Nakagama, H., Bardeesy, N., Housman, D., Housman, D.E. and Pelletier, J. 1995. Antagonism of WT1 activity by protein self-association. *Proceedings of the National*

Academy of Sciences of the United States of America. **92**(24), pp.11105–11109.

Morrison, D.J., English, M.A. and Licht, J.D. 2005. WT1 induces apoptosis through transcriptional regulation of the proapoptotic Bcl-2 family member Bak. *Cancer research*. **65**(18), pp.8174–8182.

Mosevitsky, M. and Silicheva, I. 2011. Subcellular and regional location of 'brain' proteins BASP1 and MARCKS in kidney and testis. *Acta histochemica*. **113**(1), pp.13–18.

Mosevitsky, M.I. 2005. Nerve Ending "Signal" Proteins GAP-43, MARCKS, and BASP1 *In*:, pp.245–325. Available from: https://linkinghub.elsevier.com/retrieve/pii/S007476960545007X.

Mosevitsky, M.I., Capony, J.P., GYu, S., Novitskaya, V.A., AYu, P. and Zakharov, V. V 1997. The BASP1 family of myristoylated proteins abundant in axonal termini. Primary structure analysis and physico-chemical properties. *Biochimie*. **79**(6), pp.373–384.

Nakagama, H., Heinrich, G., Pelletier, J. and Housman, D.E. 1995. Sequence and structural requirements for high-affinity DNA binding by the WT1 gene product. *Molecular and cellular biology*. **15**(3), pp.1489–1498.

Nakagawa, S., Okabe, H., Sakamoto, Y., Hayashi, H., Hashimoto, D., Yokoyama, N., Sakamoto, K., Kuroki, H., Mima, K., Nitta, H., Imai, K., Chikamoto, A., Watanabe, M., Beppu, T. and Baba, H. 2013. Enhancer of zeste homolog 2 (EZH2) promotes progression of cholangiocarcinoma cells by regulating cell cycle and apoptosis. *Annals of surgical oncology*. **20 Suppl 3**, pp.S667-75.

Natoli, T.A., McDonald, A., Alberta, J.A., Taglienti, M.E., Housman, D.E. and Kreidberg, J.A. 2002. A Mammal-Specific Exon of WT1 Is Not Required for Development or Fertility. *Molecular and Cellular Biology*. **22**(12), pp.4433–4438.

O'Meara, M.M. and Simon, J.A. 2012. Inner workings and regulatory inputs that control Polycomb repressive complex 2. *Chromosoma*. **121**(3), pp.221–234.

Oji, Y., Miyoshi, S., Maeda, H., Hayashi, S., Tamaki, H., Nakatsuka, S.-I., Yao, M., Takahashi, E., Nakano, Y., Hirabayashi, H., Shintani, Y., Oka, Y., Tsuboi, A., Hosen, N., Asada, M., Fujioka, T., Murakami, M., Kanato, K., Motomura, M., Kim, E.H., Kawakami, M., Ikegame, K., Ogawa, H., Aozasa, K., Kawase, I. and Sugiyama, H. 2002. Overexpression of the Wilms' tumor gene WT1 in de novo lung cancers. *International journal of cancer*. **100**(3), pp.297–303.

Oji, Y., Miyoshi, Y., Kiyotoh, E., Koga, S., Nakano, Y., Ando, A., Hosen, N., Tsuboi, A., Kawakami, M., Ikegame, K., Oka, Y., Ogawa, H., Noguchi, S. and Sugiyama, H. 2004. Absence of mutations in the Wilms' tumor gene WT1 in primary breast cancer. *Japanese journal of clinical oncology*. **34**(2), pp.74–77.

Oji, Y., Yamamoto, H., Nomura, M., Nakano, Y., Ikeba, A., Nakatsuka, S., Abeno, S., Kiyotoh, E., Jomgeow, T., Sekimoto, M., Nezu, R., Yoshikawa, Y., Inoue, Y., Hosen, N., Kawakami, M., Tsuboi, A., Oka, Y., Ogawa, H., Souda, S., Aozasa, K., Monden, M. and Sugiyama, H. 2003. Overexpression of the Wilms' tumor gene WT1 in colorectal adenocarcinoma. *Cancer science*. **94**(8), pp.712–717.

Oksuz, O., Narendra, V., Lee, C.-H., Descostes, N., LeRoy, G., Raviram, R., Blumenberg, L., Karch, K., Rocha, P.P., Garcia, B.A., Skok, J.A. and Reinberg, D. 2018. Capturing the Onset of PRC2-Mediated Repressive Domain Formation. *Molecular cell*. **70**(6), pp.1149-1162.e5.

Owen, C., Fitzgibbon, J. and Paschka, P. 2010. The clinical relevance of Wilms Tumour 1 (WT1) gene mutations in acute leukaemia. *Hematological oncology*. **28**(1), pp.13–19.

Pasini, D., Bracken, A.P., Hansen, J.B., Capillo, M. and Helin, K. 2007. The polycomb group protein Suz12 is required for embryonic stem cell differentiation. *Molecular and cellular biology*. **27**(10), pp.3769–3779.

Paterni, I., Granchi, C., Katzenellenbogen, J.A. and Minutolo, F. 2014. Estrogen receptors alpha (ERα) and beta (ERβ): subtype-selective ligands and clinical potential. *Steroids*. **90**, pp.13–29.

Peters, A.H.F.M., Kubicek, S., Mechtler, K., O'Sullivan, R.J., Derijck, A.A.H.A., Perez-Burgos, L., Kohlmaier, A., Opravil, S., Tachibana, M., Shinkai, Y., Martens, J.H.A. and Jenuwein, T. 2003. Partitioning and plasticity of repressive histone methylation states in mammalian chromatin. *Molecular cell*. **12**(6), pp.1577–1589.

Ponzio, G., Rezzonico, R., Bourget, I., Allan, R., Nottet, N., Popa, A., Magnone, V., Rios, G., Mari, B. and Barbry, P. 2017. A new long noncoding RNA (lncRNA) is induced in cutaneous squamous cell carcinoma and down-regulates several anticancer and cell differentiation genes in mouse. *Journal of Biological Chemistry*. **292**(30), pp.12483–12495.

Prokopuk, L., Stringer, J.M., Hogg, K., Elgass, K.D. and Western, P.S. 2017. PRC2 is required for extensive reorganization of H3K27me3 during epigenetic reprogramming in mouse fetal germ cells. *Epigenetics & Chromatin*. **10**(1), p.7.

Qi, X., Zhang, F., Wu, H., Liu, J., Zong, B., Xu, C. and Jiang, J. 2015. Wilms' tumor 1 (WT1) expression and prognosis in solid cancer patients: a systematic review and meta-analysis. *Scientific reports*. **5**, p.8924.

Raffeiner, P., Schraffl, A., Schwarz, T., Röck, R., Ledolter, K., Hartl, M., Konrat, R., Stefan, E. and Bister, K. 2017. Calcium-dependent binding of Myc to calmodulin. *Oncotarget*. **8**(2), pp.3327–3343.

Rechtsteiner, A., Costello, M.E., Egelhofer, T.A., Garrigues, J.M., Strome, S. and Petrella, L.N. 2019. Repression of Germline Genes in Caenorhabditis elegans Somatic Tissues by H3K9 Dimethylation of Their Promoters. *Genetics*. **212**(1), pp.125–140.

Reddy, J.C., Morris, J.C., Wang, J., English, M.A., Haber, D.A., Shi, Y. and Licht, J.D. 1995. WT1-mediated transcriptional activation is inhibited by dominant negative mutant proteins. *The Journal of biological chemistry*. **270**(18), pp.10878–10884.

Rusk, N. 2017. Antibodies trigger reprogramming. *Nature Methods*. **14**(11), p.1035.

Santiago, F.S., Li, Y., Zhong, L., Raftery, M.J., Lins, L. and Khachigian, L.M. 2021. Truncated YY1 interacts with BASP1 through a 339KLK341 motif in YY1 and suppresses vascular smooth muscle cell growth and intimal hyperplasia after vascular injury. *Cardiovascular research*.

Simpson, L.A., Burwell, E.A., Thompson, K.A., Shahnaz, S., Chen, A.R. and Loeb, D.M. 2006. The antiapoptotic gene A1/BFL1 is a WT1 target gene that mediates granulocytic differentiation and resistance to chemotherapy. *Blood*. **107**(12), pp.4695–4702.

Sims, R.J. and Reinberg, D. 2009. Processing the H3K36me3 signature. *Nature Genetics*. **41**(3), pp.270–271.

van Steensel, B. and Belmont, A.S. 2017. Lamina-Associated Domains: Links with Chromosome

Architecture, Heterochromatin, and Gene Repression. *Cell*. **169**(5), pp.780–791.

Stoll, R., Lee, B.M., Debler, E.W., Laity, J.H., Wilson, I.A., Dyson, H.J. and Wright, P.E. 2007. Structure of the Wilms Tumor Suppressor Protein Zinc Finger Domain Bound to DNA. *Journal of Molecular Biology*. **372**(5), pp.1227–1245.

Stypula-Cyrus, Y., Damania, D., Kunte, D.P., Cruz, M. Dela, Subramanian, H., Roy, H.K. and Backman, V. 2013. HDAC Up-Regulation in Early Colon Field Carcinogenesis Is Involved in Cell Tumorigenicity through Regulation of Chromatin Structure. *PLOS ONE*. **8**(5), p.e64600.

Takasaki, A., Hayashi, N., Matsubara, M., Yamauchi, E. and Taniguchi, H. 1999. Identification of the calmodulin-binding domain of neuron-specific protein kinase C substrate protein CAP-22/NAP-22. Direct involvement of protein myristoylation in calmodulin-target protein interaction. *The Journal of biological chemistry*. **274**(17), pp.11848–11853.

Tamburri, S., Lavarone, E., Fernández-Pérez, D., Conway, E., Zanotti, M., Manganaro, D. and Pasini, D. 2020. Histone H2AK119 Mono-Ubiquitination Is Essential for Polycomb-Mediated Transcriptional Repression. *Molecular Cell*. **77**(4), pp.840-856.e5.

Toska, E., Campbell, H.A., Shandilya, J., Goodfellow, S.J., Shore, P., Medler, K.F. and Roberts, S.G.E. 2012. Repression of Transcription by WT1-BASP1 Requires the Myristoylation of BASP1 and the PIP2-Dependent Recruitment of Histone Deacetylase. *Cell Reports*. **2**(3), pp.462–469.

Toska, E. and Roberts, S.G.E. 2014. Mechanisms of transcriptional regulation by WT1 (Wilms' tumour 1). *Biochemical Journal*. **461**(1), pp.15–32.

Toska, E., Shandilya, J., Goodfellow, S.J., Medler, K.F. and Roberts, S.G.E. 2014. Prohibitin is required for transcriptional repression by the WT1–BASP1 complex. *Oncogene*. **33**(43), pp.5100–5108.

Ullmark, T., Montano, G. and Gullberg, U. 2018. DNA and RNA binding by the Wilms' tumour gene 1 (WT1) protein +KTS and −KTS isoforms—From initial observations to recent global genomic analyses. *European Journal of Haematology*. **100**(3), pp.229–240.

Valovka, T., Schönfeld, M., Raffeiner, P., Breuker, K., Dunzendorfer-Matt, T., Hartl, M. and Bister, K. 2013. Transcriptional control of DNA replication licensing by Myc. *Scientific Reports*. **3**(1), p.3444.

Voigt, P., Tee, W.-W. and Reinberg, D. 2013. A double take on bivalent promoters. *Genes & Development*. **27**(12), pp.1318–1338.

Wagner, N., Michiels, J.F., Schedl, A. and Wagner, K.-D. 2008. The Wilms' tumour suppressor WT1 is involved in endothelial cell proliferation and migration: expression in tumour vessels in vivo. *Oncogene*. **27**(26), pp.3662–3672.

Wagner, N., Wagner, K.-D., Hammes, A., Kirschner, K.M., Vidal, V.P., Schedl, A. and Scholz, H. 2005. A splice variant of the Wilms{\textquoteright} tumour suppressor Wt1 is required for normal development of the olfactory system. *Development*. **132**(6), pp.1327–1336.

Wali, R.K., Momi, N., Dela Cruz, M., Calderwood, A.H., Stypula-Cyrus, Y., Almassalha, L., Chhaparia, A., Weber, C.R., Radosevich, A., Tiwari, A.K., Latif, B., Backman, V. and Roy, H.K. 2016. Higher Order Chromatin Modulator Cohesin SA1 Is an Early Biomarker for Colon Carcinogenesis: Race-Specific Implications. *Cancer prevention research (Philadelphia, Pa.)*. **9**(11), pp.844–854.

Wang, D., Horton, J.R., Zheng, Y., Blumenthal, R.M., Zhang, X. and Cheng, X. 2018. Role for first zinc finger of WT1 in DNA sequence specificity: Denys-Drash syndrome-associated WT1 mutant in ZF1 enhances affinity for a subset of WT1 binding sites. *Nucleic acids research*. **46**(8), pp.3864–3877.

Wang, H., Wang, L., Erdjument-Bromage, H., Vidal, M., Tempst, P., Jones, R.S. and Zhang, Y. 2004. Role of histone H2A ubiquitination in Polycomb silencing. *Nature*. **431**(7010), pp.873–878.

Wang, J., Kumar, R.M., Biggs, V.J., Lee, H., Chen, Y., Kagey, M.H., Young, R.A. and Abate-Shen, C. 2011. The Msx1 Homeoprotein Recruits Polycomb to the Nuclear Periphery during Development. *Developmental cell*. **21**(3), pp.575–588.

Wang, W., Lee, S.B., Palmer, R., Ellisen, L.W. and Haber, D.A. 2001. A Functional Interaction with CBP Contributes to Transcriptional Activation by the Wilms Tumor Suppressor WT1 *. *Journal of Biological Chemistry*. **276**(20), pp.16810–16816.

Wang, Z.Y., Qiu, Q.Q., Huang, J., Gurrieri, M. and Deuel, T.F. 1995. Products of alternatively spliced transcripts of the Wilms' tumor suppressor gene, wt1, have altered DNA binding specificity and regulate transcription in different ways. *Oncogene*. **10**(3), pp.415–422.

Wiederkehr, A., Staple, J. and Caroni, P. 1997. The motility-associated proteins GAP-43, MARCKS, and CAP-23 share unique targeting and surface activity-inducing properties. *Experimental cell research*. **236**(1), pp.103–116.

Wiles, E.T. and Selker, E.U. 2017. H3K27 methylation: a promiscuous repressive chromatin mark. *Current opinion in genetics & development*. **43**, pp.31–37.

Wu, H., Zeng, H., Dong, A., Li, F., He, H., Senisterra, G., Seitova, A., Duan, S., Brown, P.J., Vedadi, M., Arrowsmith, C.H. and Schapira, M. 2013. Structure of the Catalytic Domain of EZH2 Reveals Conformational Plasticity in Cofactor and Substrate Binding Sites and Explains Oncogenic Mutations. *PLOS ONE*. **8**(12), p.e83737.

Xu, B., Zeng, D., Wu, Y., Zheng, R., Gu, L., Lin, X., Hua, X. and Jin, G.-H. 2011. Tumor suppressor menin represses paired box gene 2 expression via Wilms tumor suppressor protein-polycomb group complex. *The Journal of biological chemistry*. **286**(16), pp.13937–13944.

Xu, C., Wu, C., Xia, Y., Zhong, Z., Liu, X., Xu, J., Cui, F., Chen, B., Røe, O.D., Li, A. and Chen, Y. 2013. WT1 promotes cell proliferation in non-small cell lung cancer cell lines through up-regulating cyclin D1 and p-pRb in vitro and in vivo. *PloS one*. **8**(8), p.e68837.

Xu, W., Ji, J., Xu, Y., Liu, Yawei, Shi, L., Liu, Yi, Lu, X., Zhao, Y., Luo, F., Wang, B., Jiang, R., Zhang, J. and Liu, Q. 2015. MicroRNA-191, by promoting the EMT and increasing CSC-like properties, is involved in neoplastic and metastatic properties of transformed human bronchial epithelial cells. *Molecular Carcinogenesis*. **54**(S1), pp.E148–E161.

Yamagishi, M. and Uchimaru, K. 2017. Targeting EZH2 in cancer therapy. *Current Opinion in Oncology*. **29**(5), pp.375–381.

Yang, L., Han, Y., Saurez Saiz, F. and Minden, M.D. 2007. A tumor suppressor and oncogene: the WT1 story. *Leukemia*. **21**(5), pp.868–876.

Yao, Y., Hu, H., Yang, Y., Zhou, G., Shang, Z., Yang, X., Sun, K., Zhan, S., Yu, Z., Li, P., Pan, G., Sun, L., Zhu, X. and He, S. 2016. Downregulation of Enhancer of Zeste Homolog 2 (EZH2) is

essential for the Induction of Autophagy and Apoptosis in Colorectal Cancer Cells. *Genes*. **7**(10), p.83.

Zhang, J., Zeng, Y., Xing, Y., Li, X., Zhou, L., Hu, L., Chin, Y.E. and Wu, M. 2021. Myristoylation-mediated phase separation of EZH2 compartmentalizes STAT3 to promote lung cancer growth. *Cancer Letters*. **516**, pp.84–98.

Zhang, Y., Xu, C., Ye, Q., Tong, L., Jiang, H., Zhu, X., Huang, L., Lin, W., Fu, H., Wang, J., Persson, P.B., Lai, E.Y. and Mao, J. 2021. Podocyte apoptosis in diabetic nephropathy by BASP1 activation of the p53 pathway via WT1. *Acta Physiologica*.

Zhao, J., Sun, B.K., Erwin, J.A., Song, J.-J. and Lee, J.T. 2008. Polycomb proteins targeted by a short repeat RNA to the mouse X chromosome. *Science (New York, N.Y.)*. **322**(5902), pp.750–756.

Zhou, L., Fu, L., Lv, N., Liu, J., Li, Yan, Chen, X., Xu, Q., Chen, G., Pang, B., Wang, L., Li, Yonghui, Zhang, X. and Yu, L. 2018. Methylation-associated silencing of BASP1 contributes to leukemogenesis in t(8;21) acute myeloid leukemia. *Experimental & Molecular Medicine*. **50**(4), p.44.

Zink, D., Fischer, A.H. and Nickerson, J.A. 2004. Nuclear structure in cancer cells. *Nature Reviews Cancer*. **4**(9), pp.677–687.